Faculty of Natural Science and Technology
Department of Physics

NTNU
Innovation and Creativity

MASTER'S THESIS FOR

STUD. TECHN. HELENE RØDAL

Thesis started:	01.20.2007
Thesis submitted:	06.18.2007

DISCIPLINE: CONDENSED MATTER PHYSICS

Norsk tittel:	*"Et mikroskala studium av elektrorheologi i løsninger med nano-silikater"*
English title:	*"A Microscale Study of Electrorheological Behaviors of Nano-Silicate Suspensions"*

This work has been carried out at NTNU, under the supervision of Professor Jon Otto Fossum

---

Trondheim, June 18th 2007

Jon Otto Fossum

Responsible supervisor

Professor at Department of Physics

Abstract

This paper presents the experimental activities carried out to study the electrorheological behavior of nano-silicate clays in microscale systems. Electrorheological fluids were made of the synthetic clay, Laponite, dissolved in silicone oil, turpentine or distilled water, where the two latter solvents evaporates at ambient temperature. Sample droplets were taken from these samples and placed on an electrode of several parallel, conducting microbands with a spacing of either $1\mu m$ or $10\mu m$. A voltage was applied over a pair of neighboring microbands and the electrorheological response within the sample droplet was observed with different types of optical microscopes.

These experiments have revealed that modified Laponite dissolved in either silicone oil or turpentine have shown signs of the ER-effect when placed on the $10\mu m$ gap electrode. However, the chain formations were unstable due to counteracting effects. To investigate self assembly of particles during evaporation, samples were placed between crossed polarizers. Birefringence was observed for droplets on hydrophobic substrate, but not on hydrophilic substrate. A look for birefringence within the electric field as a confirmation of chain formations did not give positive results. The ER-effect was neither observed for samples placed on the $1\mu m$ gap electrode.

Preface

This master's thesis was carried out during the 10th and last semester of the program for a Master of Science(Sivilingeniør i Fysikk og Matematikk) at the Norwegian University of Science and Technology(NTNU). It was performed at the division of complex materials at the Department of Physics.

The object of this thesis was to study the electrorheological behavior of nanosilicate synthetic clays in microscale systems. The observation was done utilizing different types of optical microscopes. Two types of electrodes, with a spacing of either $1\mu m$ or $10\mu m$, were used as an electric field environment.

The experimental results are separated in two sections. The first section presents the preliminary experiments that were carried out during the fall semester in 2006. These results have already been presented in an unpublished report handed in at the Department of Physics at NTNU on December 20th 2006. The second section is called main experiments, and presents the experimental activities carried out during my work on the diploma in the spring semester in 2007.

With this experimental work, I have gained insight into electrorheology in addition to useful experience in practical laboratory work.

I would like to thank my supervisor Professor Jon Otto Fossum for allowing me to work with this subject and giving me support and guidelines throughout the working period of this thesis. Great gratitude is also sent to Dr. Ahmed Gmira at the Department of Physics at NTNU, who has assisted me with experimental work and helped me gain insight into specific topics of this thesis. I would also like to thank Geir Helgesen and PhD student Eldrid Svåsand at the Physics Department at Institute for Energy Technology(IFE) in Norway, for allowing me to visit them and use their experimental equipment. They have also given me assistance during experimental work at IFE, and participated in useful discussions that have provided me with a greater insight into the topic of this thesis. For that, I am very grateful. My cordial thanks also to the rest of the staff at the Physics Department at IFE for their assistance and warm welcome. Last, but not least, I would like to acknowledge my gratitude to the rest of my fellow master students for helpful discussions and guidelines.

Trondheim, June 18th 2007 Helene Rødal

Contents

Chapter 1

Introduction

The electrorheological(ER) response was discovered by Willis M. Winslow in 1949 [1,2]. He described it as a phenomenon originated from electrically induced fibration of a solute consisting of small particles. Such solutions are called ER-fluids. Subsequent to this discovery, there has been great research on this topic [2–6].

ER-fluids are typically composed of colloidal particles dissolved in an insulating, nonpolar liquid. When this solution is exposed to a strong electric field, the particles interact in such a way that chains are formed and aligned parallel to the electric field. The effect usually occurs within milliseconds, and when the field is turned off, the chains are detached and the ER-fluid is once again isotropic. Thus, the ER-effect is reversible. Macroscopically, the ER-effect cause the ER-fluid to undergo a transition from liquid state to semi-solid state of higher viscosity.

One type of colloidal particles is synthetic clays, which have been given increased experimental attention during the last decades [7]. It has been used as a solid particle constituent in ER-fluids [8], and will play the same role in the ER-fluids used for the experiments presented in this thesis. Two types of the synthetic clay, Laponite, are used here; Laponite RD and a surface modified Laponite named Alkyl quaternary ammonium smectite (and hereafter referred to as modified Laponite). Two main types of solvents are used; silicone oil and turpentine, where the latter is an evaporating solvent at ambient temperature.

An ER-fluid only reveals its characteristic effect when placed in a strong electric field. To apply the electric field, the sample is placed between conducting parallel plates separated by a distance d. An applied voltage, V, over these plates results in an electric field directed from the positive plate to the negative plate, given by:

$$E = \frac{V}{d}$$

Hence, a strong applied electric field requires a high voltage when the distance, d, is held constant.

The main objective of this thesis is to investigate the electrorheological behavior of Laponite particles within a microscale system. Fabricated electrodes with microband spacing in the order of micrometers is utilized as the electric field environment, and the behavior of the ER-fluids is observed by different types of optical microscopes.

The motivation for learning more about ER-fluids is not only a physicist's natural curiosity. ER-fluids are applicable in all types of systems where a large change in viscosity is beneficial. Such a phenomena can be utilized in the industry as a mechanical interface. Examples are clutches, brakes, damping systems, valves and locks [9–11]. It can also be used in haptic[1] systems [13] where mechanical equipment is used to simulate tactile movement. However, before ER-fluids accomplish widespread commercialization there are some challenges to overcome. One of the main challenges is the low yield stress which characterizes the strength of the fibrillated chains [10]. In addition, the working temperature range is not wide enough and the stability of the ER-fluid is poor due to sedimentation [9].

Despite the large amount of published research on the ER-phenomena during the last decades, there have been little or no published research on the ER-behavior of fluids in a micro scale system. The experimental results presented in this thesis may therefore contribute to broaden the information of the behavior of ER-fluids and thus bring ER-fluids closer to widespread commercialization.

[1] Pertains the sense of touch [12].

Chapter 2

Scientific Background

This chapter gives a scientific background of electrorheology, in addition to experimental materials and techniques.

The first section presents a theoretical background of the ER-effect and ER-fluids. The second section presents the structure and behavior of clay, which is used as a solid particle constituent in ER-fluids.

Different experimental aims requires different techniques to gain more information about the sample. In this report, crossed polarizers are utilized with the aim to confirm the presence of the ER-effect. Third section describes the motivation for this.

The fourth and last section gives the theoretical background of droplet evaporation. At least one of the ER-solvents utilized in this thesis, evaporates at ambient temperature, and in order to analyze the particle formation after complete evaporation, one must compare the influence from evaporation effects with the influence from the electric field.

2.1 The Electrorheological Effect

When certain solutions of solid particles are exposed to a strong electric field, the fluid undergoes a phase transition where its rheological behavior changes significantly. Such solutions are termed *electrorheological fluids*(or ER-fluids) and the phase transition is caused by the *electrorheological effect*(or ER-effect) [3].

There are three main types of ER-effects observed in ER-fluids; the positive ER-effect, the negative ER-effect and the photo-electrorheological(PER) effect [3]. The positive ER-effect is signified by increasing rheological properties with applied electric field. The complementary opponent is the negative ER-effect, signified by decreasing rheological properties with applied electric field. The third and last type of ER-effect is the photo-electrorheological(PER) effect, signified by an enhancement of the ER-effect when exposed to ultra violet illumination in addition to the electric field.

In this case, only the positive ER effect is of interest. It is characterized by a transition from liquid state to semi-solid state when exposed to a strong electric field, typically between $0.5 - 2kV/mm$ [2, 3, 9]. It is commonly accepted that the transition of the (positive) ER-fluid occurs due the formation of fibrillated

chains along the electric field direction. This is illustrated in Fig.2.1.

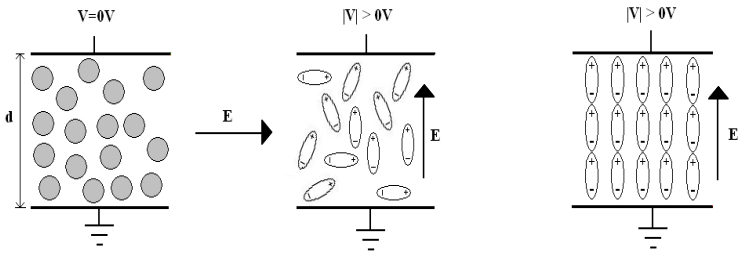

Figure 2.1: *Formation of chains due to dipolar interactions activated by an applied electric field. This illustration is based on Fig.6 (a) in [14].*

The voltage required to activate the ER-effect is called the trigger voltage. When the field is turned off, the ER-fluid may return to its initial liquid state, thus making the transition reversible. In addition to the electric field, the response from the ER-fluid also depend on its ingredients, and these will be described in the following section.

2.1.1 The Three Components

There are three main components of the ER-fluid; the dispersed phase, the dispersing phase and, if necessary, additives to enhance the stability of the ER-effect [3].

The Dispersed Phase

The dispersed phase can be either liquid or solid. Whether or not a material is suited as a dispersed phase in an ER-fluid depends on its unique physical properties. One of these critical properties is its geometric design. The particle size is usually between $0.1\mu m$ and $100\mu m$ and for too small or too large particles, the ER-effect will diminish. For small particles the Brownian motion can dominate over the chain formations, while for large particles it is expected that the ER-effect is weakened due to sedimentation. The shape of the particles also influences the ER-effect because the dielectric properties of the particles depend on their shape. Ellipsoidal particles are expected to give a stronger response than spherical particles due to a stronger induced dipole moment (for ellipsoidal particles). Its electrical properties should include both a very low electric conductivity (less than $10^{-6}S/m$) and a large dielectric constant (> 10 is preferred). Due to the strength of the applied electric field it is also beneficial for the dispersed phase to possess a high breakdown strength.

The Dispersing Phase

The dispersing phase is a non-conductive liquid or oil. Its preferable physical properties are high boiling point, low viscosity, high breakdown strength, low dielectric constant and relatively high density($> 1.2g/ml$). Examples are silicone oil, paraffin and vegetable oil.

Additives

Additives are polar particles adsorbed on to the dispersed particles' surface and act to increase the particle's sedimentation properties and enhance the ER-effect. Examples of additives are water, acid, salt and surfactants.

2.1.2 Origin of the ER-effect

There are different models suggesting an explanation of the physics behind the transition of the ER-fluid. Two of the most common models are the polarization model and the conduction model. The polarization model regards the dielectric mismatch between the solvent and the solute as an essential factor behind the ER-effect [14,15]. An increasing mismatch will lead to a correspondingly greater ER-effect. This model's limitations and lack of precision forced a new model to arrive, namely the conduction model, proposed by Atten [16]. The conduction model focuses on the particle interaction, but the major shortcoming of this model is that it does not consider the micro structural change of the ER-fluid during the transition. Together with other models it is possible to explain a lot of the physical phenomena concerning the ER-effect.

As described in Sec.2.1.1, the properties of the ER-fluid's constituents play a vital part in the ER-effect. Due to these properties, their interaction, under influence of a strong electric field, leads to the ER effect signified by formation of fibrillated chains which are aligned parallel to the electric field.

The ER-fluid contains small, polar particles dissolved in a non-polar, insulating liquid. As a result of its physical properties, the ER-fluid undergoes a transition from a liquid to a rigid, semi-solid state of higher viscosity when exposed to a strong electric field. After activating the electric field, the ER response is usually observed within milliseconds [17]. To achieve maximum viscosity, the time can be longer, and depends on factors such as the electric field strength and the dielectric properties of the fluid. The degree of solidification depends (among others) on the solid volume fraction which can range from 5% to 50% [2]. As a result of the transition, the viscosity can increase by a factor of up to 10^5 [18] but the usual magnification is about 2 to 3 orders [19].

Formation of fibrillated chains within an ER fluid exposed to an electric field is partially due to a great mismatch between the dielectric constants of the solute and the solvent. An external electric field causes the positively charged center of a polarizable particle to be slightly shifted in comparison to its negative opponent, thus forming an electric dipole. The relative dielectric constant of a substance represents its polarizability when exposed to an external electric field. This is shown in Eq.2.1,

$$\begin{aligned} \vec{D} &= \varepsilon_0 \vec{E} + \vec{P} \\ &= \varepsilon_0 \vec{E} + \varepsilon_0 \chi \vec{E} \\ &= \varepsilon_0 \varepsilon_r \vec{E} \end{aligned} \tag{2.1}$$

where $\vec{D}$ is the electric displacement, ε_0 is the vacuum permittivity, ε_r is the relative dielectric constant(or relative permittivity), χ is the electric susceptibility, $\vec{E}$ is the electric field and $\vec{P}$ is the polarization [20].

Hence, a mismatch in the (relative) dielectric constants leads to a corresponding mismatch in polarization. An applied external electric field will thus induce an inhomogeneous internal electric field, and correspondingly an inhomogeneous distribution of dipoles. This can induce a transition from liquid to solid state caused by an inner ordering of the dipoles.

Each particle's motion is determined by the electric field from other dipoles in the vicinity and the external electric field. The dipolar interaction forces are described in Fig.2.2.

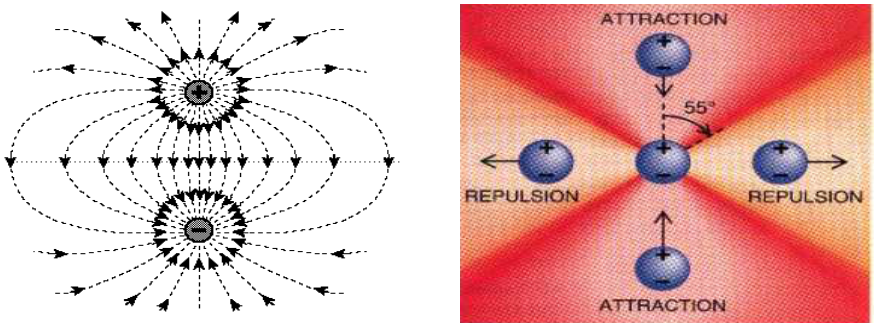

(a) (b)

Figure 2.2: *Field from electric dipoles. (a) The electric field lines from a single dipole [21]. (b) Dipolar interaction forces [22].*

Dipole charge centers of opposite charges are attracted to each other, while those of equal charge are repelled from each other. In addition, the dipoles are repelled from each other in the direction perpendicular to the polarization direction. Dipoles will be aligned parallel to the electric field as shown in Fig.2.3. When accelerated by the electric field, a dipole can move from the repelling region to the attractive region of another dipole and ultimately get trapped in the attractive region. Hence, the attractive force can cause the dipoles to form chains, while the repulsive force causes the chains to align relative to each other. The resulting process is sketched in Fig.2.1.

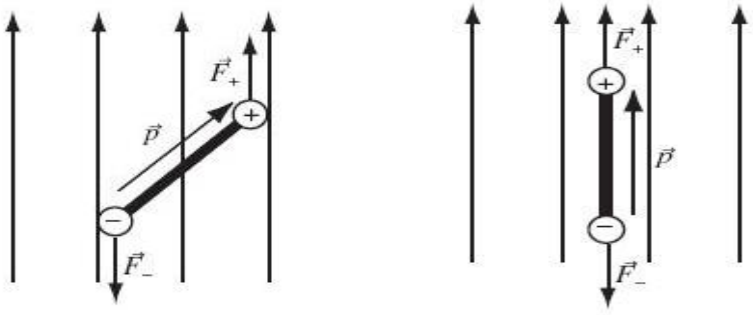

(a) (b)

Figure 2.3: *Electric dipole in an external electric field [23]: (a) The electric field exerts a torque on the dipole. (b)The final equilibrium state of the dipole.*

Since the ER-fluid also consist of a non-polar fluid, the induced dipoles can

move freely within this liquid. The resulting chain formation leads to an increased inner order. As the electric field is increased, the strength of the dipolar interaction forces also increase. When the voltage approaches the trigger voltage, the dipolar interaction forces between the solid particles of the dispersed phase are strong enough to induce chain formation. An increase of the voltage subsequent to the chain formation will lead to a further increase of the interaction forces between the dipoles, thus increasing the strength of each chain. A strong dipolar interaction force holding the chains in position leads to a strong ability to resist a change in position. Macroscopically this means that the samples' ability to resist changes in geometrical shape has increased. This ability is signified by an increase in the viscosity. Hence, an increased electric field eventually leads to a sudden inner ordering of solid particles, which in turn leads to a sudden increase in viscosity. As described earlier in this section, this is the hallmark of the (positive) ER-effect[1].

[1] For a more thorough discussion on the ER-effect it is recommended to read an article from A. P. Gast and C. F. Zukoski [2] in addition to two more recent articles from T. Hao [3, 9].

2.2 Clay

Natural clay is a rather easily accessible material in the nature. It is found in mudstones, shales and soils at almost any place on earth. For thousands of years man has known and used clay as a production material. Among these products are body paints, tools as well as bricks and porcelain [24]. On the other hand, it was not until the mid-1930s that one began a scientific study of clay [25].

Clay is composed primarily of fine-grained minerals such as silica, alumina, possibly magnesia, and water, together with impurities such as alkalies. 'Clay' is a common concept that includes all minerals with a sheetlike crystal structure which allows the sheets to slide past one another [24].

A key parameter in all definitions of clay is the size, but in spite of this there is no generally accepted upper limit of the clay platelet size. Different disciplines use different size limits. For example, in pedology clay is classified as a material whose particles have $< 2\mu m$ in equivalent spherical diameter. In geology and sedimentology this limit is commonly set to $< 4\mu m$, while in colloid science the general limit is $< 1\mu m$ [25]. Since this is a study of colloidal suspensions, we accept the latter limit ($< 1\mu m$).

Clay minerals signifies a class of (hydrated) phyllosilicates or sheet silicates whose unit particle is platelet shaped [8, 25]. These minerals may be natural or synthetic. Each clay platelet is $0.7 - 1\mu m$ thick and its lateral size varies from a few tens of nm to a few μm. Each clay platelet consists of several sheets of either tetrahedral or octahedral structure which are coupled together face to face. The structures of the tetrahedron and octahedron are presented in Fig.2.4.

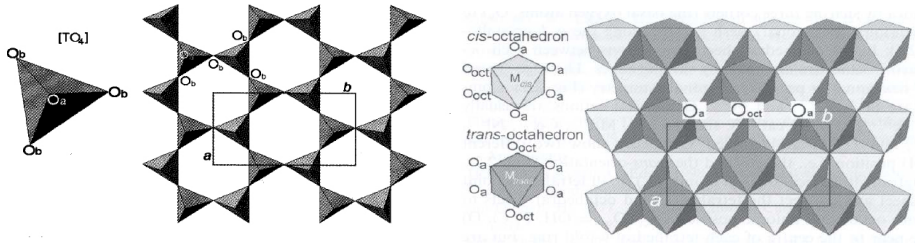

(a) (b)

Figure 2.4: *The tetrahedral and octahedral sheets of the silicate unit cell. Figure (a) illustrates the tetrahedron(left) and the tetrahedral sheet. Figure b) illustrates the octahedron (left) and the octahedral sheet. For both figure (a) and figure (b), $O_{a,b}$ refer to apical and basal oxygen atoms respectively and a and b are unit-cell parameters [25].*

The ratio of tetrahedral sheets to octahedral sheets may be 2:1 or 1:1 as pictured in Fig.2.5. In this thesis only 2:1 clay minerals have been used.

For a 2:1 clay mineral, the octahedral sheet is sandwiched between two opposing tetrahedral sheets where the different sheets are held together by van der Waal forces [24]. Six octahedral sites and eight tetrahedral sites constitute the layer unit cell of the 2:1 clay mineral. If all the six octahedral sites are occupied, the structure is referred to as trioctahedral. When only four of the six

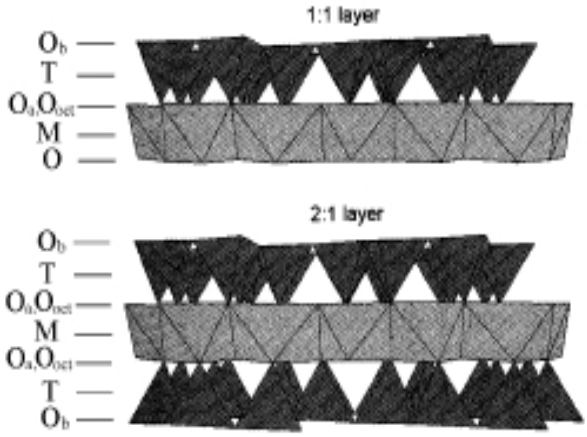

Figure 2.5: *1:1 and 2:1 structure of clay platelets [25].*

octahedral sites are occupied the structure is referred to as dioctahedral [8, 25]. Depending on the composition of the tetrahedral and octahedral sheets, some 2:1 phyllosilicates(e.g. pyrophyllite and talc) are electrically neutral, while others(e.g. smectites and mica) are negatively charged.

In case of negative layer charge, the platelets will be connected by sharing interlayer cations such as Na^+ or K^+ [26]. Due to the interlayer cations, clay platelets are usually stacked together forming aggregates that contain hundreds of platelets. Single layers and clay particles may occur in very dilute dispersions, but for suspensions of higher concentration the clay particles form aggregates. We refer to an assembly of layers as a 'particle', and an assembly of particles as an 'aggregate'.

2.2.1 Smectites

Smectites are particles of colloidal size where the particles are made up stacks of 2:1 phyllosilicate platelets [25]. Each smectite unit-cell has a permanent negative surface charge which varies from $0.4e^-$ to $1.2e^-$ [25].

To balance the negative surface charge, they form stacks of several clay platelets(particles) which share intercalated alkaline or alkaline-earth cations. The intercalated cations may be exchanged with other cations due to the fairly moderate surface charge, and by doing so, the surface of the platelets are modified.

Since the interlayer space between the clay platelets is filled with cations that electrostatically attract water molecules or other polar molecules, water-molecules may penetrate the layers and surround the cations, which cause the smectite particles to swell [27].

The permanent surface charge and the presence of interlayer cations are the main factors that separate the structure of smectites from that of other 2:1 phyllosilicates [25]. Examples of smectites are montmorillionite, hectorite and laponite [8, 25, 26], of which the latter is described in the following section.

Laponite

Laponite is a swelling 2:1 synthetic smectite, and the most widely studied synthetic clay until present time [7]. Its chemical composition is given by $Si_8Mg_{5.45}Li_{0.4}H_4O_{24}Na_{0.7}$ [28].

Each Laponite unit cell is made up of one octahedral magnesia sheet positioned in the middle of two opposed tetrahedral silica sheets. Fig.2.6 illustrates the (crystal) structure of the Laponite unit-cell.

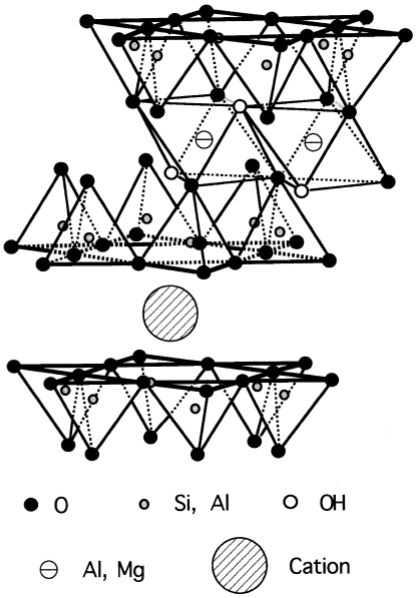

Figure 2.6: *Structure of a single Laponite sheet [29].*

The surface of the Laponite unit-cell has a negative net charge, whereas the edges are slightly positively charged. This is demonstrated in Fig.2.7. Due to substitution of Lithium ions with Magnesium ions, the platelet surface has a negative net charge, whereas the small positive charge at the edges comes from broken bonds [8, 30]. All in all, each unit-cell has a permanent negative net charge of $0.4e^-$ [31] distributed at the surface.

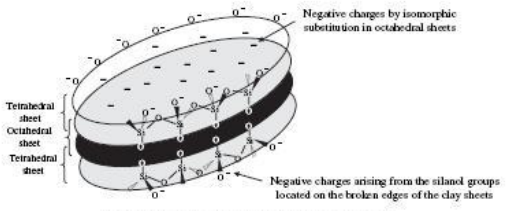

Figure 2.7: *Description of the unit-cell of the Laponite particle [32].*

To balance the negative net charge, stacks of Laponite platelets(i.e. particles) are formed by the sharing of intercalated Na^+ cations. By replacing or

isolating the cations between each Laponite sheet, the physical properties of Laponite particles can be altered.

Modified Laponite

As described in the previous section, the properties of Laponite particles may be altered by replacing or isolating the cations between each Laponite platelet. The type of modified Laponite used here has been surface modified by replacing the cations, and is called Alkyl Quaternary Ammonium Smectite(AQAS).

Quaternary ammonium surfactants are cations, adsorbed on Laponite surfaces through ion exchange [33]. This adsorption only occurs at the face of the Laponite sheet, where the net charge is negative, thus leaving the edges unaltered. Fig.2.8 shows a sketch of the AQAS platelet.

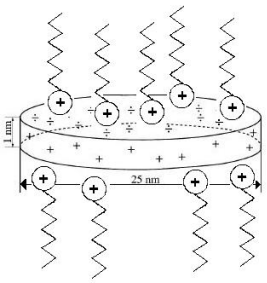

Figure 2.8: *Quaternary ammonium cations are adsorbed on the Laponite platelet surface. This figure is based on Fig.1 in an article by Bakk et al. [34].*

Quaternary ammonium cations have a structure in the form NR_4^+ where each R is an alkyl group. When the original sodium ions are partially or fully replaced by quaternary ammonium ions, the minimum spacing between two Laponite sheets will increase since one sodium atom naturally possess a smaller surface area than a molecule of five atoms such as quaternary ammonium ions.

As the relative distance between each Laponite platelet is increased, the strength of the attractive forces between them will decrease. Therefore, the aggregates of several Laponite sheets will be easier to break down. Hence, the adsorbed quaternary ammonium chains will counteract the tendency to form aggregates of several Laponite platelets. As a result, AQAS particles dissolve easier than Laponite RD particles.

2.3 Polarized Light

In optical microscopy, light is used as the source of information. By using polarized light one can gain formation about the particle configuration within the sample. As an example, the nematic particle arrangement within liquid crystals has been observed by using polarization microscopy [20].

Light can be represented by transverse[2] electromagnetic waves where the electric and magnetic wave vectors mutually fluctuate perpendicular to each other. In electrodynamics, the polarization vector represents the direction of the transverse electric field and describes the direction of oscillation in the plane perpendicular to the propagation direction.

The left part of Fig.2.9 pictures the electric field vector, $\vec{E}$, fluctuating in the xy-plane, the magnetic field vector, $\vec{B}$, fluctuating in the xz-plane and the wave propagating in the x-direction. The right part of Fig.2.9 shows a trace of the electric field vector as it propagates in the x-direction.

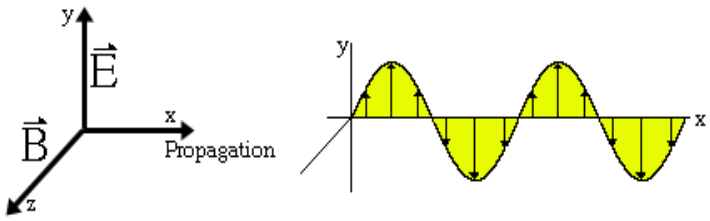

Figure 2.9: *Electromagnetic wave [35].*

Light emitted from the sun, or most other light sources, has no specific direction of fluctuation, i.e. it is polarized in different directions and to different degrees. It is therefore termed as unpolarized [36]. Polarized light can exhibit three main types of polarization; linear polarization, circular polarization and elliptical polarization.

2.3.1 Types of Polarization

When electromagnetic waves fluctuate in one specific plane, they are considered to be linearly polarized [36].

In circular polarization, the **E** vector proceeds in the form of a helix around the axis of propagation, while it retains its magnitude. There are two different types of circular polarization. If the tip of the electric field vector rotates clockwise when looking toward the light source, it is said to be right-circularly polarized. If the rotation is counter clockwise it is said to be left-circularly polarized.

Elliptical polarization is a composite of both linear and circular polarization and the tip of the electric field vector now proceeds in the form of a flattened helix. The vector rotates and changes magnitude at the same time.

[2]The amplitude displacement is perpendicular to the direction of wave propagation.

2.3.2 Creating Polarized Light

There are various occurrences that can produce polarized light and these are listed below [36]:
- scattering,
- reflection,
- transmission,
- selective absorption or
- double refraction.

In the experiments presented in this thesis, polarized light is created by either selective absorption or double refraction. Incoming non-polarized light can be linearly polarized by selective absorption. Since the incoming light has no direction of polarization, it is polarized in all directions with no specific preference. As this ray of light passes through a *Polariod*, the waves with different direction of polarization than the optical axis of the Polaroid will be absorbed. In other words, only waves with polarization direction parallel to the optical axis of the Polaroid are transmitted through it. Thus, the rays that exit the Polaroid are linearly polarized. The Polaroid material is from hereon called a polarizer due to its production of polarized light.

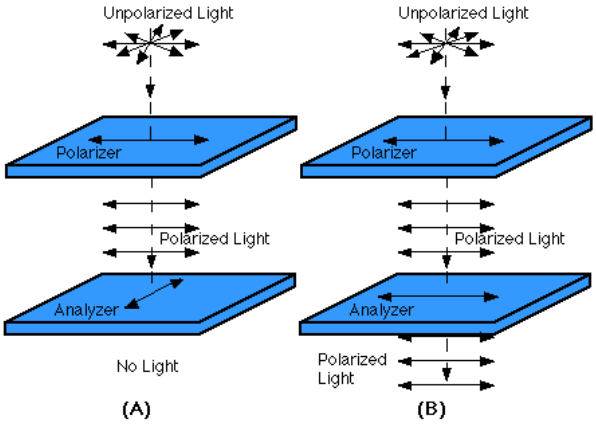

Figure 2.10: *Polarized light: (A)Crossed polarizers lead to zero transmittance of light. (B)Parallel polarizers lead to transmittance of polarized light [37].*

If two polarizers are set up in series and aligned so that their optical axes are parallel, the light that pass through the first polarizer also pass through the second one with the same resulting polarization. However, if the polarizers are aligned with perpendicular optical axes, i.e. crossed, no light can pass through both of the polarizers because the polarized light from the first is extinguished by the second. This is illustrated in Fig.2.10. As the angle is increased from 0° to 90°, the amount of light transmitted through both of the polarizers decreases from maximum to minimum. By placing a third polarizer between two crossed polarizers and aligning the optical axis of this polarizer at an angle $> 0°$ relative to the other two, some of the light will be transmitted through all three polarizers.

In other words, if a material, positioned between two crossed polarizers, changes the polarization of the incoming linear polarized light there will be some transmittance of light through the last polarizer. Hence, one can determine the presence of a polarizing material between crossed polarizers by the transmittance of light through them.

A birefringent material is another element that produces polarized light [36, 38]. Such materials demonstrate double refraction [35], i.e. they have two indices of refraction, which leads to the incoming wave being separated into two rays. A difference in index of refraction results in a difference in velocity, because the velocity, v, of the wave within a material with refractive index n, is given as

$$n = \frac{c}{v}$$

where c is the velocity of light in vacuum [39].

A difference in velocity leads to a phase difference which depends on the thickness of the material through which it is transmitted. As they exit the birefringent material and recombine, the state of polarization has changed due to the phase difference.

Anisotropic materials are birefringent, which means that placing an anisotropic material between crossed polarizers will lead to a transmittance of light. Pictures of birefringent materials placed between crossed polarizers show distinguished areas with different colors depending on the length and orientation of the birefringent material [35].

In this case, one search for chain formations, which is an anisotropic distribution of particles. Thus, by placing the sample between crossed polarizers it is possible to detect optical anisotropy [40].

2.4 The Physics of Evaporating Droplets

Evaporated, sessile droplets containing solid constituents tend to leave a dense ring-shaped deposition along the edge of the stain [41]. Such an effect can be either advantageous or undesirable depending on the specific area of application. In both cases, the physics of drying solutes is of great interest in many industrial and scientific processes in order to control the droplet evaporation process to give the desired outcome.

For example, paint manufacturers seek an evenly dispersed color which remains so during drying and use different additives to ensure this [41]. In the electronics industry, dense nanoparticle suspensions are used to form complex patterns that are subsequently dried to drive off the suspending liquid, and leave the solid constituents deposited for use as electronic devices [42]. Conductors and electrodes are formed by inkjet printing metal nanoparticle inks, which requires an uniform deposited film [42].

During evaporation there are several competing mechanisms that influence the final particle distribution of the dried droplet. Parameters like particle concentration, size and shape, and type of substrate all have an impact on the particle flow during evaporation. The composition of such parameters determines which mechanism that dominates during evaporation, and thus also determines the particle configuration after complete evaporation. Several evaporative mechanisms are described in the following sections.

2.4.1 The Coffee-Stain Effect

It is not an unknown phenomenon that spilled coffee left until dry leaves a stain with a dark edge. A significant dark edge reveals that the coffee particles initially spread uniformly within the fluid, ends up at the periphery of the spilled drop after evaporation is completed. The effect causing the particles to assemble at the periphery of the droplet is called the coffee-stain effect. This effect is not restricted to coffee, but applicable for all sessile droplets with solid constituents that are placed on a rough substrate to ensure contact line pinning [41]. For example, dried soap water droplets or water color marks also have enhanced edges after complete evaporation [41, 43, 44].

Droplets follow one of two evaporating mechanisms: either the contact angle is maintained constant by de-pinning the contact line(e.g. droplet on non-wetting surface [41]) or the contact area is maintained constant by a pinned contact line(e.g. colloidal dispersions on a rough substrate [45]) [46]. Here, the substrate is considered to have a rough surface and only the pinned contact line droplet where the coffee-stain effect is present, is of further interest.

Deegan et.al. proposed two specific conditions that must be fulfilled in order to get ring-shaped patterns: contact line pinning and evaporation mainly at the edge of the droplet [41]. Subsequently, Hu and Larson showed that for simple organic fluids with clean droplet surfaces, the particles are mainly drawn toward the center of the droplet, rather than the edge [47]. This is due to thermal Marangoni flows induced by evaporation. Hence, when ring-shaped patterns are formed in evaporating droplets, both a pinned contact line and suppression of Marangoni flow must be fulfilled.

A pinned contact line of the drying drop results in an outward radial fluid flow from the interior to replenish the liquid removed from the edge [41, 44]. If the droplet contains solid constituents, these will be transported by the replenishing flow from the interior toward the edge of the droplet. As the liquid evaporates, more and more particles will end up at the edge. This is what cause the final ring-shaped pattern which is characteristic for the coffee-stain effect. An illustration of the mechanism behind this effect is demonstrated in Fig.2.11.

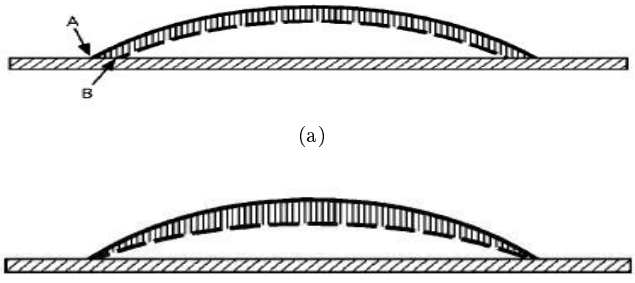

(a)

(b)

Figure 2.11: *Illustration of the origin of the particle assembly at the edges [41]. When the edge of the droplet is not pinned(a), uniform evaporation at the surface of the droplet results in a loss of liquid volume, represented by the hashed line area, and lead to a decrease in height from the solid line to the dashed line, while the edge of the droplet will move from A to B. In case of pinned edges(b), the motion from A to B is prevented by an outflow to replenish the liquid removed from the edge.*

It is known that up to 100% of the solid constituents can end up at the periphery of the droplet [41]. However, in case of rapid evaporation, large particle concentration, slow particle movement or other factors, all particles may not reach the edge before the droplet is dry. Instead, the radial flow toward the periphery of the droplet lead to radial deposits of residual particles.

2.4.2 Self-Assembly of Particles

The deposition of a droplet on a substrate initiates inner circular currents around the center of the droplet. In addition, the particles are transported toward the edge by the replenishing outflow due to evaporative loss. Some of the particles within this flow are deposited at the edge instead of being transported back into the droplet's interior. Due to this circulating outflow, the particles deposited at the edge are aligned in a preferential direction determined by the circular flow. As a result, the edge of the droplet may be divided into four sections as illustrated in Fig.2.12

The broken arrow indicates the direction of the inner circular currents, and the arrows within each of the four sections represent the preferred direction of alignment as a result of the circular outflow. These ordered sections represent different nematic states with corresponding nematic directors. A nematic state is an anisotropic state where the particles exhibit a long-range orientational

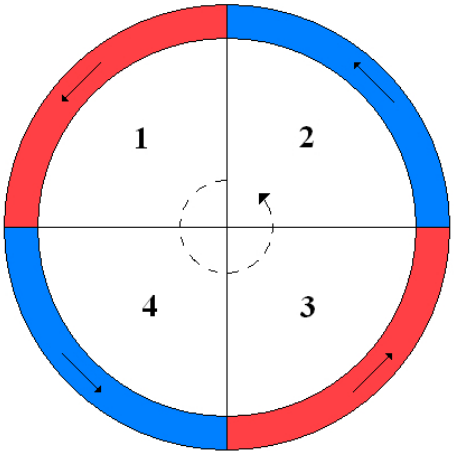

Figure 2.12: *Particle self-assembly at the edge of a dried droplet. Red and blue sections and the edge represent two different nematic states observed when using crossed polarizers. The broken arrow around the center of the circle indicates the direction of the inner circular current induced by deposition of the droplet on the substrate.*

order but no long-range positional order. The preferred orientation is specified by means of a unit vector referred to as the nematic director [20].

There are four sections with different particle alignments, but each of the sections have a corresponding opponent where the preferred direction is parallel but oppositely aligned. In Fig.2.12, particles within section 1 are aligned parallel to those in section 3, and correspondingly those in section 2 are aligned parallel to those in section 4. Thus, there are two pairs of nematic orientations.

Due to anisotropic distribution of the particles within the edge of the evaporated droplet, birefringence may be observed while the dried droplet is placed between crossed polarizers(see Sec.2.3). As shown in Fig.2.12 there are two pairs of nematic orientations, which result in two different colors observed when using crossed polarizers. Since the nematic director in section 1 in Fig.2.12 is parallel to the director in section 3, these will show the same color when placed between crossed polarizers, while sections 2 and 4 will show a different color. Thus, the color distribution will appear as is shown in this figure.

The type of pattern emerging after evaporation depends partly on the concentration of solid particles. If the concentration is too low, it will weaken the effect, while a higher concentration will enhance the effect and result in greater contrasts between the observed colors when using crossed polarizers. Also, the size of the droplet compared to the concentration of particles influence the degree of self-assembly. In case of hydrophilic(wetting) substrates the droplet and its particles are spread over a large surface area, thus creating a reduced effective concentration of particles. As a result the degree of self-assembly is weakened and may vanish. Correspondingly, for droplets evaporated on hydrophobic(non-wetting) substrates, particle self-assembly will be more observable due to a smaller surface area and thus greater effective particle concentration.

Self-assembly of particles within an evaporating droplet have been observed in droplets consisting of for example DNA molecular chains [48] or single walled carbon nanotubes [46][3].

2.4.3 Formation of Crust

Evaporative loss of solvent from the free surface of the deposited droplet leads to a local increase in concentration of solid constituents at the free surface, which in turn lead to the formation of a thin glassy or gelled crust [46]. As a result, the evaporative loss is slowed down, but not completely stopped. When the evaporation proceeds, the loss of solvent leads to a decrease of the enclosed volume, which eventually results in a fracture of the crust, and thus formation of cracks.

[3] For a more thorough discussion on particle self-assembly in evaporating droplets it is recommended to read the master's thesis for Hege S. Bjørnsen [49].

Chapter 3

Materials

The ER-effect occurs as a result of dipole-dipole interactions within a strong electric field (see Sec.2.1). The strength and type of dipole-dipole interaction within the field depends on the composites of the ER-fluid. This chapter presents the material components of the ER-fluid used here, and describes the sample preparation method.

3.1 Solute

The solute is the dispersed phase (see Sec.2.1), represented by synthetic clay particles. Two types of the synthetic clay Laponite were used here, i.e. Laponite RD and modified Laponite(AQAS).

Laponite RD

Laponite RD is a synthetic layered silicate, purchased from Southern Clay Products (a subsidiary of Rockwood specialties) as a white powder. It is insoluble in water and at concentrations of 2% and higher, gels can be produced. For more detailed information I refer to the theory presented in Sec.2.2.1 on page 10 and specifications of the product reproduced in App.D.

Modified Laponite

AQAS is a surface modified synthetic layered silicate, purchased from Southern Clay Products as a white powder. Due to the surface modification it is easier dispersed in solvents than Laponite RD. For more information about AQAS, I refer to the theory presented in Sec.2.2.1 on page 11.

3.2 Solvent

When choosing the type of solvent in the ER-fluid, it is important to take into account that the type of equipment used to examine the sample might vary. The spacing(gap) between the electrode microbands determines the area to be examined. As this area decreases, the equipment used to examine this will vary.

As long as the particles within the electrode gap are observable through an optical microscope, and well defined images of the Laponite particles can be obtained, it is convenient to use silicone oil as a solvent. There are several examples of the ER-effect with samples containing this oil [8,50,51], and possible prospective results are therefore comparable with these.

However, when the size of the electrode gap requires a magnification that exceeds the maximum obtainable magnification of an optical microscope, it is necessary to find different equipments to detect the presence of the ER-effect. This is the case for the electrode of $1\mu m$ gap. For such small electrode gaps it might be beneficial to substitute the optical microscope with an atomic force microscope (AFM). By replacing the optical microscope with an AFM, there are new challenges to overcome concerning the ER-fluid. When examined by an AFM, it is preferred that the examined specimen is solid to avoid particle attachment to the tip of the cantilever. This means that, when using the AFM, the chains should already have been formed and remain so after the electric field is turned off. To achieve this, one can use a solvent that evaporates after the chains have been formed. In this way, the ER-effect is no longer reversible and the chain formations are unable to rearrange after the electric field is deactivated. This solvent must in addition fulfill the necessary requirements needed to form an ER-fluid together with Laponite. As stated in Sec.2.1, the ideal solvent is an insulating fluid of high boiling temperature(T_c), low dielectric constant(ε_r), high density(ρ) and low viscosity(η).

An evaporating solvent named isoparaffin has been used before in an AFM study of magnetic colloidal particles [52]. However, there are also other solvents that might be suitable for this purpose. Among these solvents were ethanol, isopropanol(also named isopropyl alcohol), ethyl acetate and turpentine, all of which have a low electric conductivity(see [53–55] and App.C, respectively). These fluids are listed with their relevant physical properties in Tab.3.1.

Table 3.1: Physical properties of solvents

Fluid	η $(mPa \cdot s)$	T_c $(^\circ C)$	ε_r (-)
Ethanol	1.20 [56]	78 [57,58]	24.3 @25°C [59]
Isopropanol	2.4 [54]	82 [60]	18.6 [54]
Ethyl acetate	0.426 [61]	77.2 [62]	6.0 @25°C [59]
Turpentine	1 @21°C [63,64]	160 [62]	2.2 @20°C [59]
Isoparaffin	1.4 @25°C [65]	–	2.0 @20°C [65]
Silicone Oil	100 @25°C [8]	$\approx$ 300 [66]	2.5 [8]

Compared to silicone oil which has been used in ER-fluids together with Laponite in previous experiments [8], these liquids have lower densities and viscosities in addition to a lower boiling temperature which was the initial criteria. As described in Sec.2.1 it is important for the solute and solvent to have a great mismatch in polarizability, represented by their dielectric constant. Since Laponite particles are polarizable, the solvent should possess a low dielectric constant. Since silicone oil has already displayed ER-properties together with Laponite, it was natural to compare the dielectric constant of the new solute

with the one for silicone oil. Turpentine and isoparaffin both have a low dielectric constant, but due to a fairly large price for isoparaffins, this solvent was declined. Thus, turpentine was chosen as an evaporating solvent for Laponite. It was interesting to see if it was still possible to observe the ER-effect despite the deviations from the ideal solvent. When the optical microscope was used, the solvent could be both turpentine and silicone oil since evaporation was no longer an important criteria.

Turpentine

Turpentine was selected as an evaporating substitute for silicone oil due to its low electric conductivity ($\approx 400pS/m$, see App.C) and low dielectric constant. Mineral turpentine is a solvent that is widely used in the painting industry, and it was purchased from a traditional paint store. It is a colorless liquid with a petroleum solvent odor, and classified as hazardous. Preparation of samples was therefore done under ventilation, and the turpentine container was otherwise stored within a ventilation chamber. When performing experiments, the volume of turpentine was in the order of micro liters, thus it was assumed that ventilation during experiments was unnecessary. Some relevant physical properties of turpentine are listed in Tab.3.1.

Silicone Oil

Silicone oil is a viscous fluid with an electric conductivity of $\approx 10pS/m$ [67] and thus regarded as an insulating fluid. The specific type of silicone oil used here was Rotitherm M150, purchased from Carl ROTH [68].

3.3 Sample Preparation

A digital weight was used to measure the weight of the Laponite sample. The solvent volume was measured in milliliters with a measuring glass that had a maximum measurable volume of $50ml$.

Laponite powder and solvent were mixed together at ambient temperature. After mixing the ingredients the sample was shaken by hand for about two to three minutes. The final step in preparing the sample was one (or more) of the following methods:

- Sedimentation
- Filtration
- Centrifuge
- Ultrasound bath

These methods shared the main purpose of increasing the possibility of including smaller particles within the sample droplet. It was important that the particles within the electric field were small enough due to the size of the gap within the electrode. If the particles were too large, it would be impossible to form chains, and instead they would fill the gap with aggregates. By examining smaller particles it may be possible to induce and verify the ER-effect.

When the sample was left for sedimentation, the largest aggregates sedimented to the bottom of the sample container, leaving the smallest ones in the upper phase, termed as the supernatant phase. The droplet to be examined was taken from this phase, where the concentration of small aggregates was highest.

Another way to ensure that only small particles participated in the sample droplet, was to filtrate the sample. This was done after mixing the ingredients. An electric pump with a filter of $0.2\mu m$ was used. In this way, only the aggregates of size less than $0.2\mu m$ got through the filter. The filtrated sample was also left to sediment, and the supernatant phase was used for examination.

An alternative to filtration was centrifugation. This was done by a centrifuge named centrifuge ISO 9001 B4i from Jouan Quality System. The samples were centrifuged for 15 minutes at 3000 rotations per minute(rpm).

Instead of excluding the larger Laponite aggregates, it was also possible to separate the aggregates into smaller ones. This could be done by placing the sample in an ultrasound bath, where the sample was shaken thoroughly. Such a treatment destroyed some of the bonds between the aggregates, thus leaving smaller aggregates behind. Hence, the average aggregate size was reduced. There were two different ultrasound baths that could be utilized. One was named Bransonic 12 (from KEBO Lab) and the other was named Branson 5510. The sample droplet was taken out by a transfer pipette which was set to a fixed volume between $0.1\mu l$ and $5\mu l$.

Chapter 4

Experimental Equipment

To be able to initialize the ER-effect, the sample must be placed within an electric field of sufficient strength. This was done with an electric field environment represented by an electrode coupled to a DC voltage supply. Further details of these parts are given in the first section.

Next section presents the observation equipment needed to observe the particle movement or position within the electric field. Two types of optical microscopes were used, where one of them was a Zeiss stereo microscope and the other was a microscope named Nikon Optiphot. The last section presents the experimental setup.

4.1 Electric Field Components

Electrodes were used to create the electric field, and consisted of several microbands where the spacing between these was in the order of micrometers. The microband spacing is called a gap. The sample was placed over at least two of these microbands which were coupled to a DC voltage supply. When a voltage was applied over one (or several) of these gaps, an electric field was enabled (see Ch.1).

4.1.1 Electrodes

Two different types of electrodes were purchased from Abtech. One was a model named IAME-co-IME[1] and had a gap of $1\mu m$. The other model was named IAME[2] and had a gap of $10\mu m$. The electrodes were made of gold or platinum conducting microbands on a substrate of hydrophilic(wetting) glass. By applying a voltage over these microbands, the electric field environment was enabled. The two types of electrodes are displayed in Fig.4.1.

During the experimental activities, the connection between the electrodes and their wires evolved. In the early stages, a pair of thin copper wires covered with insulating material were glued to a pair of microbands by using conducting silver paint. The thinnest type of copper wires had a diameter of $0.18mm$.

[1] Independently Addressable Microband Electrode (IAME) in combination with an Interdigitated Microsensor Electrode (IME) [69]

[2] Independently Addressable Microband Electrodes [69]

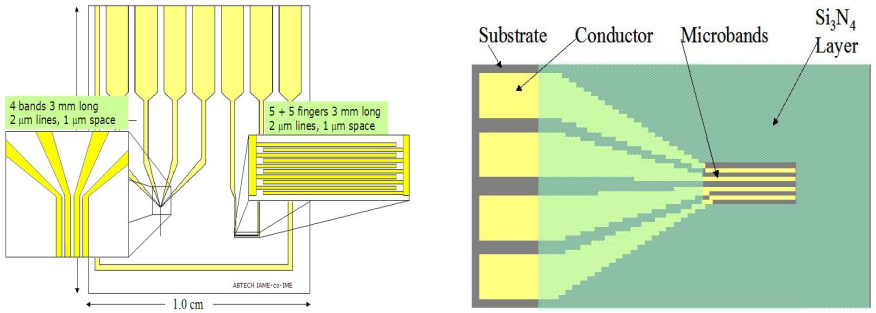

(a) (b)

Figure 4.1: *A sketch of the electrodes [69]. (a)IAME-co-IME electrode with* $1\mu m$ *gap. (b)IAME electrode with* $10\mu m$ *gap.*

An intermediate section connected the thin wires to the power supply. By using such thin wires, the point of connection between the microbands and the wires became very fragile, and the wires often detached. For the $1\mu m$ gap electrodes, thicker wires was not an option due to narrow microbands. However, for the $10\mu m$ gap electrode, thicker copper wires were attached to the microbands with conductive epoxy. By doing so, the electrode could endure a rougher treatment, and acetone or turpentine did not dissolve the epoxy, as it did with the conductive silver paint.

Examples of electrodes coupled to the thinnest wires with silver paint are pictured in Fig.4.2.

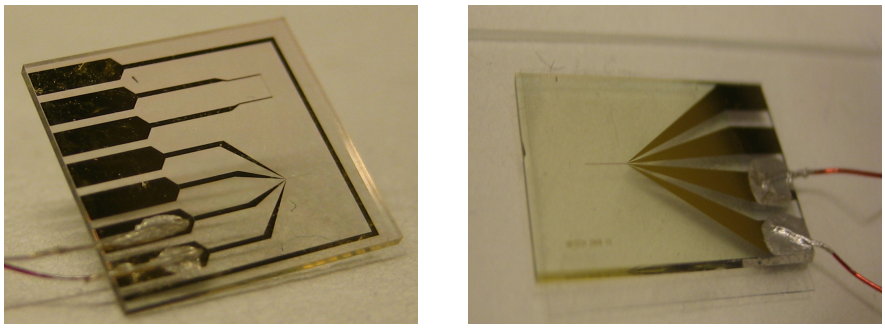

(a) (b)

Figure 4.2: *Both types of electrodes coupled with thin wires by using conducting silver paint: (a)IAME-co-IME, (b)IAME.*

A picture of the $10\mu m$ gap electrode connected to thicker copper wires using epoxy is presented in Fig.4.3. The wires attached to the electrode were connected to the power supply by the setup shown in this picture. A plastic plate with attached wires and holes formed a solid base for the electrode as the wires from the electrode were fastened in these holes. With that, the electrode was connected to the power supply.

Fig.4.3 also pictures a line of conductive silver paint that combine the two lower microbands to one of the microbands with wires. Thus, the two lower

microbands had the same potential as one of the microbands connected to the power supply. With this, one ensured that only the upper gap had an electric field, because the voltage difference between the other two gaps was therefore set to zero.

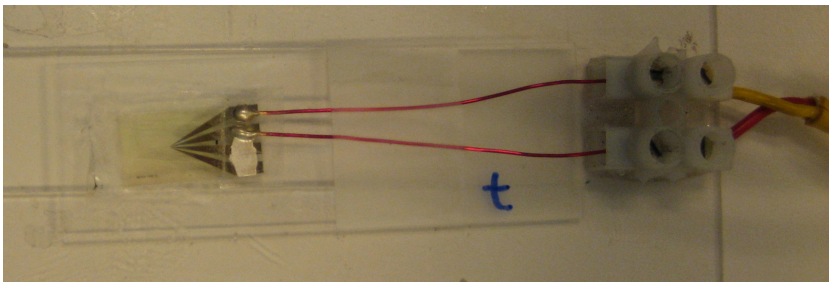

Figure 4.3: *A $10\mu m$ gap electrode connected to two copper wires with conductive epoxy.*

4.1.2 Power Supply

For the $10\mu m$ gap electrode, two main types of power supply were used. One of them was a laboratory DC power supply with a maximum voltage output of $32V$ and a minimum voltage output of about $3V$. The other voltage source was a triple output DC power supply from BK precision, with a similar range of voltage output.

For the electrode with $1\mu m$ gap, it was necessary to have a more accurate voltage output in the low-voltage region. For this purpose, an instrument from National Instruments called DAQ Pad 6020E was utilized. It had a voltage output between $-10V$ and $10V$, and no current output. It was monitored from the computer with a program from National Instruments called Measurement and Automotation.

4.2 Observation Techniques

Two different optical microscopes were utilized when observing the samples. Some of the experiments were carried out at NTNU utilizing the Zeiss optical microscope. However, when the experiments needed a larger magnification or an improved image quality, they were carried out at the Institute of Energy Technology(IFE) utilizing their Nikon Optiphot microscope.

4.2.1 Zeiss Stemi 2000C

Zeiss Stemi 2000C is a stereo microscope that includes a camera port for digital cameras. Instead of observing the sample through the eyepieces one can use a camera to record the experiment, either by capturing single pictures or by recording a video. When observing the ER-effect there were several parts that contributed to the final recorded movie. An extra 2x magnification lens was attached to the microscope and illumination of the sample could be done from

both above and below the sample. A specimen table was used to control the sample's position.

Three different types of cameras were used with the microscope and are pictured in Fig.4.4.

(a) (b) (c)

Figure 4.4: *Three different digital cameras used together with the Zeiss optical microscope: (a)The Hitachi camera, (b) the PixelLink camera and (c) the Q-imaging camera.*

One of them was a Hitachi camera(Fig.4.4(a)) which was connected to the computer through a serial port and a coaxial cable. With the program named National Instruments Vision Assistant 8.0 (implemented in LabView 8.0) it was possible to record a series of single frames. Due to a limited size of computer memory and camera efficiency, it was only possible to record a series of 400 frames, corresponding to a 13 second video, before the computer ended the recording process with an error message. Camera adjustments such as brightness and contrast were performed with a program named KP-D28/D591 Remote Control.

The second type of camera was a PixelLink mega pixel fire wire camera (Fig.4.4(b)). One advantage with this camera was the simple and common recording program named Windows Movie Maker. It had a greater capacity to record longer movies because it was not limited to the number of frames, but to how much free space that was available on the computer. A program named PixelLink Capture was used as a preview program and included some manual settings.

The third type of camera used here, was a Q-imaging (micropublisher) camera (Fig.4.4(c)) connected to the computer with a firewire cable. It was only able to take snapshots, and these were captured and adjusted with the accompanying user interface named Q-capture.

An model from Zeiss named LCD 1500 was utilized as a light source, especially for illumination from below the sample. In this case, the sample was placed on a sample box, and the light was directed down into the box and reflected back up from the box by mirrors. Thus, illumination was redirected up to the sample from beneath.

The Zeiss microscope Stemi 2000C is pictured in fig(4.5).

Figure 4.5: *Zeiss Stemi 2000C microscope with an additional 2x magnification lens attached to it.*

4.2.2 Nikon Optiphot

A second type of optical microscope was utilized for experimental activities. It was a model from Nikon named Optiphot, and is pictured in Fig.4.6.

Like the Zeiss microscope, the Nikon microscope also includes a camera port for attaching a digital camera. Two different cameras were used together with this microscope.

Videos were captured with a 3-CCD(charge-coupled device [71, 72]) JVC color video camera(KY-F55B), with a 0.6x ocular lens. It was attached to the camera port and connected to a JVC video recorder and a TV screen. Single frames were captured with a Q-imaging camera connected to the computer with a USB cable. The image resolution could be up to $2560x1920$ pixels, and image adjustments and captures were performed with the accompanying program named Q-capture.

Illumination of the sample could be done both from above and below the sample. When comparing the magnification of both of the microscopes (Nikon and Zeiss), it was evident that the magnification of the stereo microscope, Stemi 2000C, was less and of lower quality than with the Nikon Optiphot microscope. Experimental videos were recorded to a mini digital video(miniDV) disc, which could be transferred to computer files by using a computer program called ULEAD video studio. Recorded videos from the miniDV could be saved as single frames or as a video file.

Figure 4.6: *Nicon Optiphot microscope [70].*

4.3 Experimental Setup

The electrode was attached to a microscope slide with a (two sided) tape, and placed on the sample board. Illumination of the sample could be done from below or above, or both. The camera was mounted on top of the microscope and connected to the computer. Wires from the electrode were connected to the DC voltage source and a voltage between $0-37V$ was applied over the electrode gap. A sample droplet of a fixed volume was taken from the sample with a transfer pipette and placed on the microbands of the electrode. A typical experimental setup is shown schematically in Fig.4.7, and the final setup is pictured in Fig.4.8.

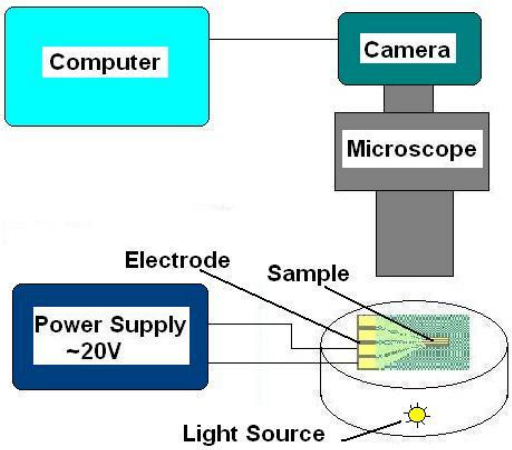

Figure 4.7: *Schematic illustration of the experimental setup. Here, the illumination of the sample comes from underneath, but illumination from above the sample has also been used.*

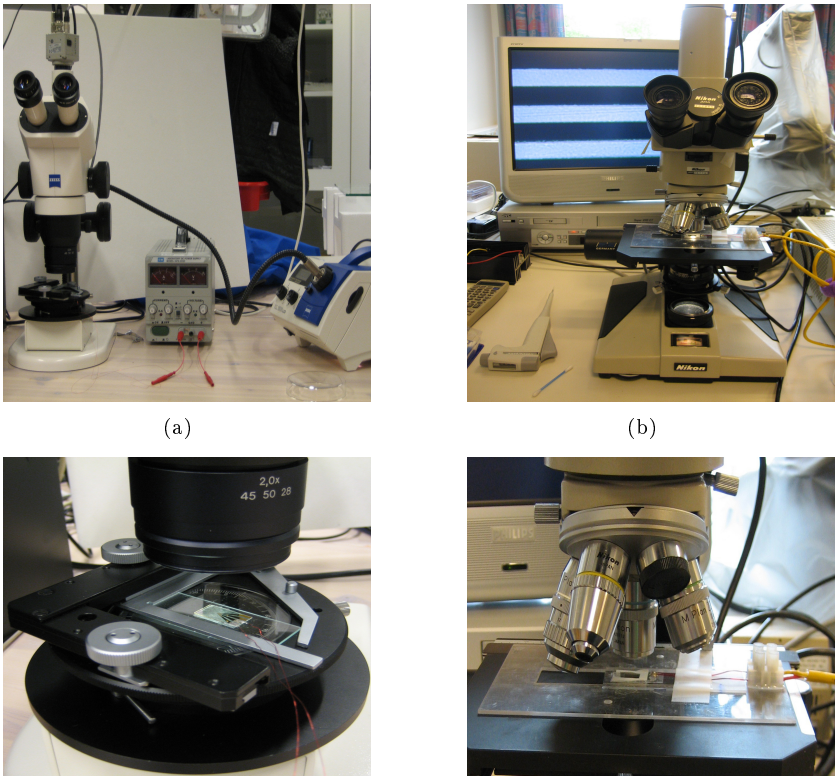

Figure 4.8: *Experimental setup: (a) Zeiss Stemi 2000C microscope and accompanying equipment. (b) Nikon Optiphot microscope and accompanying equipment. (c) The IAME electrode on the specimen table and underneath the 2x magnification lens attached to the Zeiss microscope. (d) The IAME electrode on the specimen table of the Nikon Optiphot microcope.*

Chapter 5

Experiments and Results

Numerous experiments were performed with the aim to observe the ER-effect and explore the micro scale ER-behavior of different samples containing synthetic clay particles. The ER-behavior was observed by optical microscopy while the sample droplet was placed on one of the two electrodes described in Sec.4.1.1. The first section presents the preliminary experiments where only the $10\mu m$ gap electrode was utilized. The samples contained either Laponite RD or modified Laponite dissolved in silicone oil or turpentine. The results from the preliminary experiments were used as guidelines on how to improve the ER-response from the samples and verify the ER-effect. As a result, Laponite RD was no longer a constituent in the samples used in the main experiments, which are described in the last section. Here, both the $10\mu m$ gap electrode and the $1\mu m$ gap electrode were utilized and the samples were observed with one of the two optical microscopes described in Sec.4.2.

5.1 Preliminary Experiments

These experiments were carried out to explore the ER-behavior of different types of ER-fluids[1]. The Zeiss optical microscope was utilized to observe the sample's reaction to the applied electric field. For the electric field environment, only the $10\mu m$ gap electrode was utilized because the magnification of the microscope was too low to observe particle sizes in the order of $\leq 1\mu m$. Two different synthetic clays and two different solvents were used in the experiments presented here, which resulted in four different types of samples with respect to the ingredients. Both the applied voltage and the sample preparation technique was varied in order to map the ER-behavior of the given sample. Interesting experimental observations are presented below.

[1] The preliminary experiments were carried out during the fall semester in 2006 as a preparation for further experimental activities to be carried out in the coming semester, spring 2007. The experiments presented here have been presented earlier in an unpublished report handed in on December 20th, 2006

5.1.1 Observation of the ER-effect

The aim of this experiment was to observe the presence of the ER-behavior in samples of different ingredients. If possible, it was also desired to compare the reactions from the different samples.

In this experiment, four different samples of equal solid particle concentration were made by dissolving $0.1g$ of synthetic clay in $10ml$ of liquid solvent. Thus, the final sample had a portion of $0.01g/ml$ of synthetic clay particles. These four samples consisted of:

- Laponite RD and turpentine
- Modified Laponite and turpentine
- Laponite RD and silicone oil
- Modified Laponite and silicone oil

A $10\mu m$ gap electrode was connected to a DC voltage supply with an output voltage of $20V$, thus creating the electric field environment. Before each experiment, the electrode was cleaned with acetone to remove dust or other contaminating material that could destroy the electrode. A droplet of $0.1\mu l$ was placed over the microbands and a video sequence of 400 frames with the Hitachi camera was initialized. There was no cover glass on top of the sample droplet. After the video capture was started, a DC voltage of $20V$ was applied over the two lower microbands. Each sample was tested three times, leading to 12 videos where there could be indications of the ER-effect. The videos had a resolution of $768x576$ pixels.

Results

There were four types of potential ER-suspensions in this experiment, but only one sample showed an obvious reaction to the applied electric field. The samples where the ER-effect was not observed are presented and discussed in App.B.1.

Modified Laponite dissolved in Turpentine

The one sample that gave an interesting reaction was the sample of turpentine and modified Laponite, and this is shown in Fig.5.1. As the field was applied one noticed a sudden reaction within the sample droplet. The Laponite particles present within the electric field immediately assembled in something that might resemble chains across the microband gap. Subsequently, an increasing amount of particles were trapped and aligned within the electric field. The reaction was the similar for all three tests of this sample.

To be able to verify if there were chain formations present, it would be beneficial with an improved magnification and image quality. The gap of $10\mu m$ was visible, but small, even with maximum magnification. However, this experiment still showed results indicating that turpentine might be suited as a solvent in an ER-fluid.

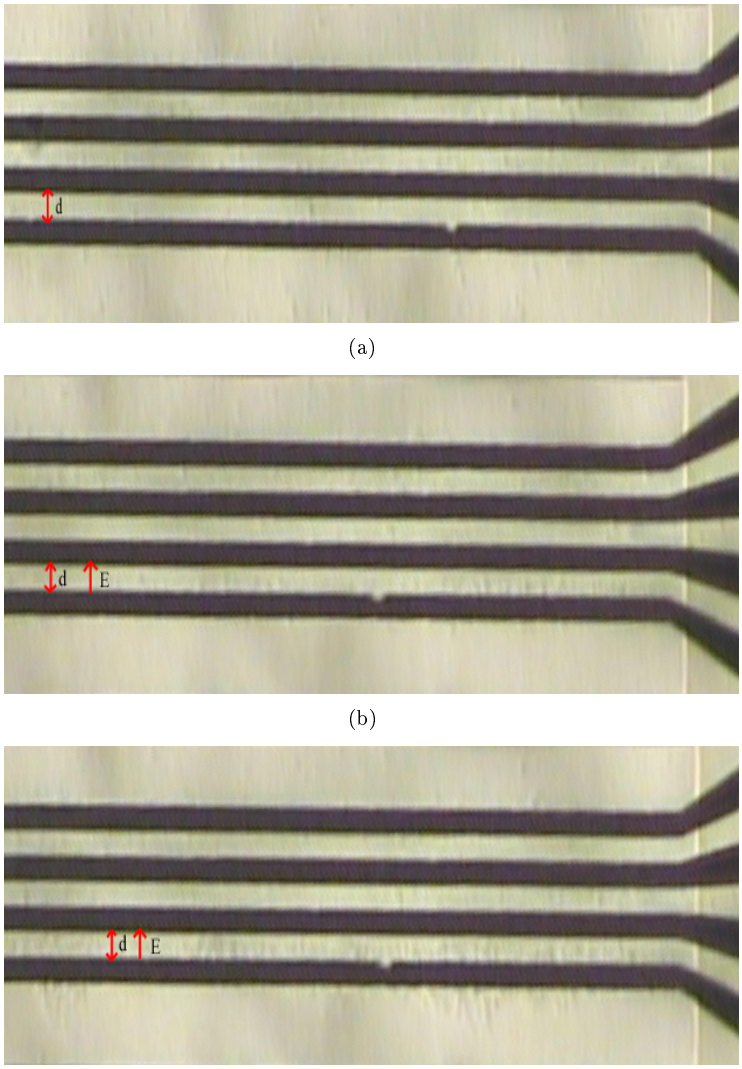

Figure 5.1: $0.1\mu l$ *droplet of modified Laponite and turpentine before (a), immediately after (b) and about* 10 *seconds after (c) the electric field was applied. A voltage of* $20V$ *was applied over the two lowest microbands, which have a spacing of* $d = 10\mu m$*. By comparing these pictures one can see that there might be chain formations within the lowest gap in pictures (b) and (c), i.e there are indications of the ER-effect.*

Brief Summary

A brief summary of the experimental results presented in this section is given below.

- Four sets of samples containing either Laponite RD or modified Laponite dissolved in either silicone oil or turpentine were placed on the $10\mu m$ gap electrode where a voltage of $20V$ was applied over the lower gap. The initial solid particle concentration before sedimentation was $0.01g/ml$.
- None of the samples containing Laponite RD, i.e. neither the ones dissolved in turpentine nor the ones dissolved in silicon oil, showed signs of the ER-effect as the electric field (of $20V/10\mu m$) was applied. This was also the case for the sample containing modified Laponite in silicone oil.
- The sample containing modified Laponite dissolved in turpentine showed indications of the ER-effect and this is depicted in Fig.5.1.
- To be able to confirm the presence of the ER-effect it would be beneficial to have a microscope of better magnification and pictures of better quality.

5.1.2 Trigger Voltage

The trigger voltage is the minimum voltage needed to induce chain formations within the electric field. From the previous section we know that only one sample, i.e. turpentine and modified Laponite, showed a reaction resembling to the ER-effect. Thus, this sample was also used for the trigger voltage experiment. First, the sample of $0.1g$ modified Laponite dissolved in $10ml$ of turpentine was shaken thoroughly by hand to dissolve the larger aggregates at the bottom of the container. Afterward, it was left for sedimentation.
A $10\mu m$ gap electrode was connected to a DC voltage supply with a maximum output voltage of $30V$. The sample droplet of $0.1\mu l$ was extracted from the supernatant phase and placed on top of the four microbands of the electrode. No cover glass was added on top of the sample.

The disadvantage of using turpentine was the limited recording time due to evaporation. It was therefore necessary to increase the voltage fast enough to include as large spectrum of voltage as possible in one movie. In order to let evaporation of turpentine be the only limiting factor on the time of capture, the PixelLink camera was used instead of the Hitachi camera. Hence, the recording time was not limited by the camera but by the evaporation rate. The videos had a resolution of $768x576$ pixels and the voltage was increased from $5V$ to about $30V$ in time intervals of 10 seconds.

Results

Some snapshots from the recorded movie are presented in Fig.5.2.

As can be seen from Fig.5.2, there was accumulation of Laponite particles within the electrode gap.

The particles reacted to the field even at a voltage of about $5V$ (Fig.5.2(a)), but no chain formation was yet observed. At about $15V$, some particles remained within the electrode gap, attaching themselves to one of the charged microbands. When increasing the field further, more and more particles bonded

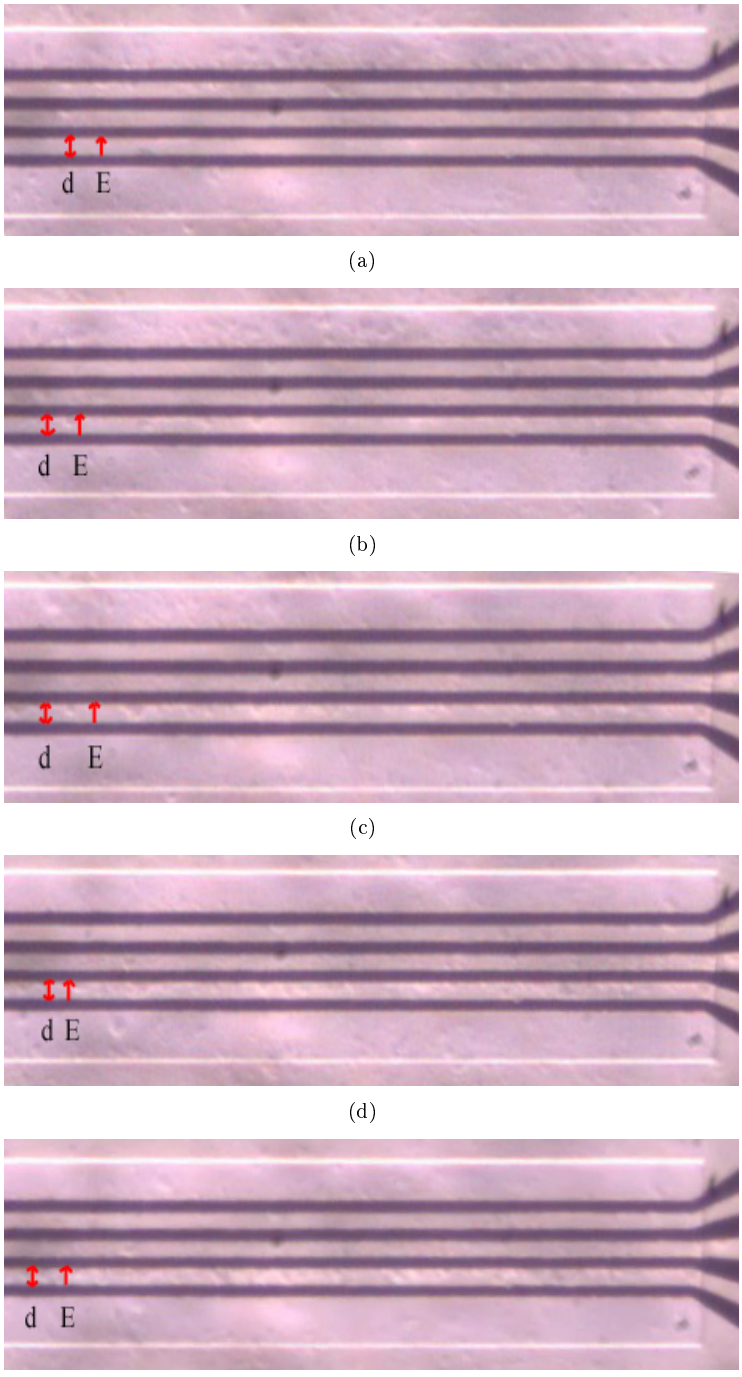

Figure 5.2: *The sample's reaction to an increasing electric field. (a)*$5V$*, (b)*$10V$*, (c)*$15V$*, (d)*$20V$ *and (e)*$> 20V$*. The voltage was applied over the two lowest microbands which have a spacing of* $d = 10\mu m$*. One can see that the Laponite particles assembled within the lowest gap as the applied voltage increased.*

together with other particles within the electrode gap. When exceeding a voltage of $20V$, an increasing amount of particles was ripped away from the electric field gap due to strong circular currents. The voltage was simply too high to allow chain formations.

When observing the ER-behavior of this sample, there are evidently three main effects that counteract chain formations. First, thermal convection, induced by temperature differences within the droplet, led to irregular currents within the droplet. Since the sample was mainly illuminated from below, the temperature would be higher at the electrode/droplet interface than at the free surface of the droplet. This temperature difference led to a heat current that would continue until equilibrium was reached. Since the particles were small, they were easily accelerated and therefore vulnerable to currents such as convection.

Second, the applied electric field induced electrophoretic convection due to the colloidal dipoles within the electric field. This was observed by circular flows around the electric field which increased in velocity as the voltage increased, and often ripped away particles inside the electric field gap on their way.

Finally, turpentine is an evaporative solvent and evaporation effects could also have interfered with the ER-effect (see Sec.2.4).

As observed in the previous experiment with indications of the ER-effect, it was difficult to verify if the observed effect was chain formations or unorganized flocculation of dipoles within the microband gap. The sample should have been prepared in such a way that only small particles were present in the sample droplet. In addition, the amount of particles should be adjusted to a minimum. Hence, the sample preparation should be adjusted to provide a more suitable sample.

Due to unstable chain formations caused by the factors mentioned above, a specific voltage where the particles began to assemble in chains could not be determined.

Brief Summary

A brief summary of the experimental results presented in this section is given below.

- A $0.1\mu l$ droplet from a sample of modified Laponite and turpentine was placed on the $10\mu m$ gap electrode where a voltage, increasing from $5-30V$, was applied over the lower gap.

- The first reaction to the electric field was observed at about $5V$, but it was not until the applied voltage reached $15V$ that particles assembled and partly remained within the lowest gap.

- Effects from induced electrophoretic convection, thermal convection and evaporation resulted in unstable particle formations within the electric field. As the electric field increased more and more particles were trapped within the lowest gap, but a large portion of these were also ripped away from the gap by electrophoretic convection recognized by strong circular currents around the gap.

- Due to these counteracting effects it was difficult to determine a specific value of the trigger voltage. In addition, the presence of the ER-effect was not easily detectable due to low picture magnification and large particles.

- The sample preparation method should be changed so that the amount and size of particles within the sample droplet is reduced to a minimum that still allows fibrillated chains to be formed within the electric field gap.

5.1.3 Testing Sample Preparation Techniques

Previous experimental sessions, presented in Sec.5.1.1 and Sec.5.1.2, have shown indications of the ER-effect where the particle size evidently was too large. It would be beneficial with a sample where the amount of particles was minimized to prevent filling the gap with aggregates. Thus, different sample preparation methods were tested to explore their influence on the particle size.

In Sec.5.1.1 it was noted that none of the samples with silicone oil gave an observable ER-response. It was also interesting to see that no samples with Laponite RD gave an ER-response. Maybe the fraction of solid material to liquid was the reason, or perhaps the sample should have been prepared differently.

A set of four different concentrations of Laponite RD in silicone oil were examined. The samples were centrifuged at $3000rpm$ in $15min$ before use, and the droplet of interest was taken from the supernatant phase, as before. The initial concentrations were $0.005g/ml, 0.01g/ml, 0.02g/ml$ and $0.03g/ml$.

The two samples with the lowest concentration ($0.005g/ml$ and $0.01g/ml$) were prepared and examined before preparing the two samples of higher concentration. The two samples of highest concentration were based on the two samples of lower concentration. The sample of $0.005g/ml$ of Laponite RD consisted of $0.1g$ of Laponite and $20ml$ of liquid. By adding $0.3g$ of Laponite RD to this solution there was a total of $0.4g$ Laponite RD in $20ml$ of liquid, resulting in a fraction of $0.02g/ml$ of solid particles. For the initial sample of $0.01g/ml$ it was added $0.4g$ of Laponite RD after examination, giving a total of $0.6g$ of Laponite RD in $20ml$ of liquid. This resulted in a solid particle fraction of $0.03g/ml$. After mixing the ingredients, the new samples were put in the centrifuge again.

A total volume of $0.2\mu l$ had been removed from the initial sample used in two sets of experiments. This was regarded as negligible compared to the total volume of the sample. The uncertainty of the weight and the volume measuring cup was considered to be more significant than this fraction of volume extraction. Thus, the initial solid volume fraction was regarded as reliable. The process was repeated for turpentine and Laponite RD. However, only two different volume concentrations were used; $0.005g/ml$ and $0.02g/ml$, because the initial sample of $0.01g/ml$ seemed to be contaminated. Foam arose on top of the solution after shaking it.

For all the experiments described in this section a voltage of $20V$ was applied over the two lowest microbands which had a spacing of $10\mu m$. By using the Zeiss optical microscope and a connected PixelLink camera, the particle movements within the sample was recorded. The videos had a resolution of $768x576$ pixels.

Results

None of the samples showed signs of the ER-effect. Apparently the amount of particles within the supernatant phase was too low to induce chain formations, or the particle size was reduced to the point where they were no longer observable with the Zeiss optical microscope. Further details of the experimental results are given in App.B.2 and a brief summary of these results is given in the following Section.

Brief Summary

A brief summary of the experimental results presented in this section is given below.

- Samples of silicone oil and Laponite RD were prepared with concentrations between $0.005g/ml$ and $0.03g/ml$ and either filtrated with a $0.2\mu m$ filter, or centrifuged at a speed of $3000rpm$ in $15min$. When a voltage of $20V$ was applied, no ER-effect was observed due to too low particle concentration within the supernatant phase, or too small particles to be observed with the Zeiss optical microscope.

- Samples of turpentine and Laponite RD have been prepared with concentrations of $0.005g/ml$ and $0.02g/ml$ and either filtrated or centrifuged like the silicone oil samples. Also here, no ER-effect was observed when the voltage of $20V$ was applied which probably was an effect of too low particle concentrations within the supernatant phase, or particles too small to be observed with the Zeiss optical microscope.

- A sample of $0.01g/ml$ of modified Laponite in turpentine was first centrifuged, and after examination filtrated. When the voltage of $20V$ was applied no ER-effect was observed. As for the other samples, this was probably due to too low particle concentrations within the supernatant phase, or particles too small to be observed with the Zeiss optical microscope.

- None of the samples in these experiments showed signs of the ER-effect. The sample preparation method was not improved by the actions carried out here. If centrifugation is chosen, the speed and time could be reduced to prevent all the particles from ending up in the sedimentary phase. If filtration is chosen, the sample should be stirred for a long time to dissolve larger aggregates and thus increase the amount of particles present in the sample after filtration.

5.2 Main Experiments

Based on the results obtained in the preliminary experiments, alterations were performed with the aim to improve the overall performance of the ER-fluid and the observability of the expected ER-effect.

Solvents and solutes of the ER-fluid remained the same as described in Ch.3 except for Laponite RD. As mentioned in Sec.5.1.1, Laponite RD showed poor electrorheological properties together with either silicone oil or turpentine. Hence, Laponite RD was no longer of critical interest. The ingredients of the ER-fluid was from hereon modified Laponite dissolved in either turpentine or silicone oil, and the electrorheological properties of these two types of ER-fluids are described and discussed further in this section.

The experimental equipment differed somewhat from what was used in the preliminary experiments, and is described in Ch.4.

One of the main requirements discovered during the preliminary experiments, was an improved picture quality with a greater magnification. The ER-effect had most likely occurred with the turpentine and modified Laponite sample, but more detailed information needed to be extracted from the pictures(and videos) in order to confirm or disprove the ER-effect. One option was to add an extra lens to the stereo microscope, Zeiss Stemi 2000C. However, a stereo microscope was not suited for greater magnifications than what was used during the preliminary experiments[2]. Thus, it was necessary to search for new types of optical microscopes with a satisfying magnification.

Subsequently, it was decided to utilize an optical microscope named Nikon Optiphot with possibilities for significantly greater magnifications[3]. Further details of the Nikon Optiphot Microscope and accompanying equipment are given in Sec.4.2.2.

Another requirement stated in Sec.5.1, was a sample with a convenient concentration of small enough Laponite particles. With this in mind, the sample preparation method took a new direction. Filtration, centrifugation or plain sedimentation all led to a sample of too low quality, thus all of these methods were replaced by an ultrasound bath. By placing the sample in an ultrasound bath, the aggregates will break down into smaller aggregates, which leads to a decrease in the average particle size. Further details are given in Sec.3.3.

The experiments presented in the following sections include these experimental changes described above.

5.2.1 Trigger Voltage with Turpentine Samples

Two different sample concentrations with modified Laponite and turpentine were made and are listed below.

- T_1: $0.105g$ modified Laponite in $10ml$ turpentine($0.01g/ml$).
- T_2: $0.048g$ modified Laponite in $10ml$ turpentine($0.005g/ml$).

[2]This conclusion was made after discussing the situation with professionals from Edmund Optics [73].

[3]The Nikon Optiphot microscope was owned by the Physics Department at the Institute for Energy Technology(IFE) at Kjeller, Norway, and experimental activities utilizing this microscope were performed at this place.

Both samples were placed in an ultrasound bath for about one hour after mixing the ingredients, and for about 15 minutes before each experimental session. A sample droplet with a volume between $2.5\mu l$ and $5\mu l$ was taken from the supernatant phase with a transferpipette and placed on a $10\mu m$ gap electrode. By using the Nikon Optiphot microscope, described in Sec.4.2.2, it was possible to achieve a better magnification and image quality than what was possible with the Zeiss microscope used in the preliminary experiments, presented in Sec.5.1. A 3-CCD JVC video camera was connected to the microscope to record the particle configuration within the sample droplet. The camera is described in Sec.4.2.2. The videos had a resolution of $720x576$ pixels. Results and discussions are presented below.

Results

A DC voltage of either $V < 10V$, $V = 10V$, $V = 15V$, $V = 20V$ or $V > 20V$ was applied over two microbands in the $10\mu m$ gap electrode. The sample droplet was placed on the microbands in this electrode.

Fig.5.3 presents the response from the T_1 sample when a voltage of $10V$ was applied over the upper microband gap. The applied electric field accelerated the Laponite particles, but no chain formations or aggregation could be observed, i.e. there was no observable ER-effect within the sample. This is shown by comparing Fig.5.3(a) and (b).

The same type of experiment was performed with sample T_2, which also gave a negative result i.e. no observable ER-effect. Fig.5.4 displays the sample T_2 after a voltage of $10V$ was applied. No flocculation or chain formation was observed.

In addition, a voltage of $8V$ was applied over both of these samples, all giving the same negative response as in the case of $10V$ applied voltage which is shown here. Apparently, an applied voltage of $10V$ or lower would not create a strong enough electric field to induce chain formations.

Afterward, a voltage of $15V$ was applied over the same type of electrode with either of the two turpentine samples and induced a response resembling the ER-effect. The response from sample T_1 and T_2 is shown in Fig.5.5 and Fig.5.6, respectively.

When observing the experimental videos which the pictures in Fig.5.5 and Fig.5.6 were taken from, it was evident that induced electrophoretic convection and thermal convection made the chain formations unstable. These videos are presented in App.A file 1 and file 2 for sample T_1 and T_2, respectively.

The consequence of convection within the sample droplet can also be observed by comparing Fig.5.5(b) and (c). Evidently, the chain formations in one of the figures were destroyed and replaced by a new set of chains located elsewhere. Thus, chain formations were alternately formed and destroyed.

In the final experimental session of this type, both of the turpentine samples were exposed to an applied voltage of $20V$ to see if chain formations were possible at such a strong electric field. As described in Sec.5.1.1, when applying a voltage of $20V$ over the sample with modified Laponite and turpentine, there were signs of chain formations within the electric field. Now, the sample was prepared differently, and the trigger voltage might thereby be different due to a change in the inner structure of the sample.

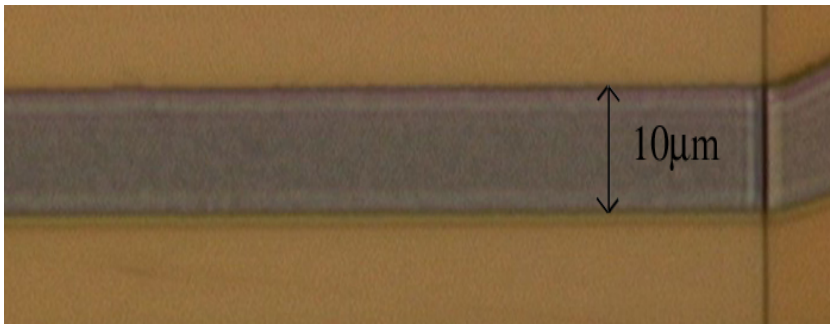

(a)

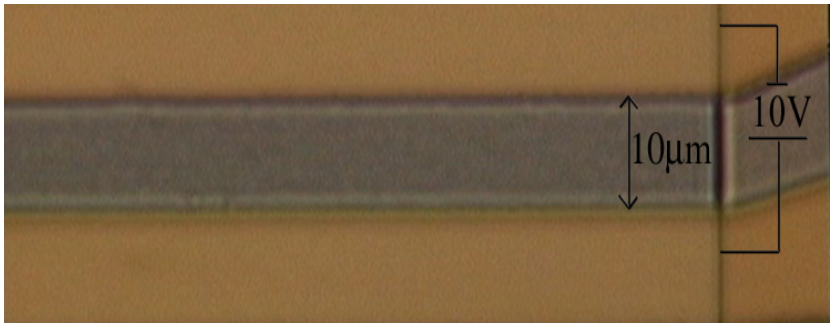

(b)

Figure 5.3: *Droplet of* $\approx 2.5\mu l$ *from the supernatant phase of sample* T_1*, placed over the microbands of a* $10\mu m$ *gap electrode. Picture (a) shows the sample before the voltage was applied, and picture (b) shows the sample after the voltage of* $10V$ *was applied. These pictures show no indications of an ER-effect.*

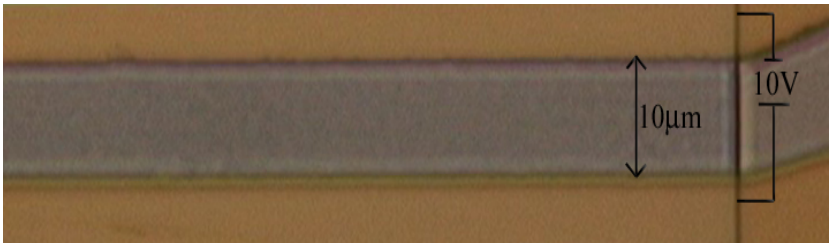

Figure 5.4: *Droplet of* $\approx 2.5\mu l$ *from the supernatant phase of sample* T_2*, placed over the microbands of a* $10\mu m$ *gap electrode. The applied voltage was* $10V$*, which gave no observable ER-effect.*

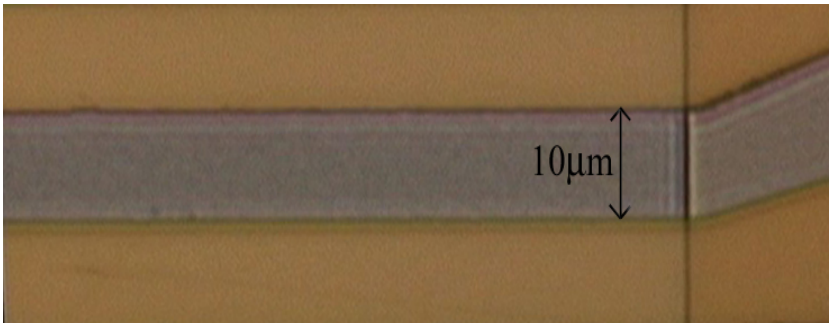

(a)

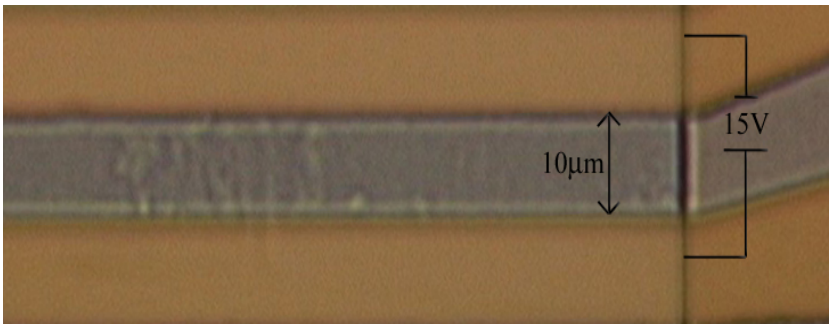

(b)

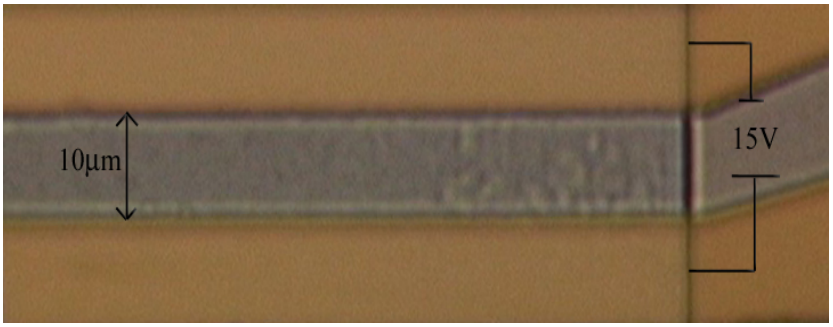

(c)

Figure 5.5: *Droplet of* $\approx 2.5\mu l$ *from the supernatant phase of sample* T_1*, placed over the microbands of a* $10\mu m$ *gap electrode. Picture (a) shows the sample before the voltage was applied, and pictures (b) and (c) shows the sample after the voltage of* $15V$ *was applied. Pictures (b) and (c) gives indications of the presence of the ER-effect, although the chains were not stable due to electrophoretic convection.*

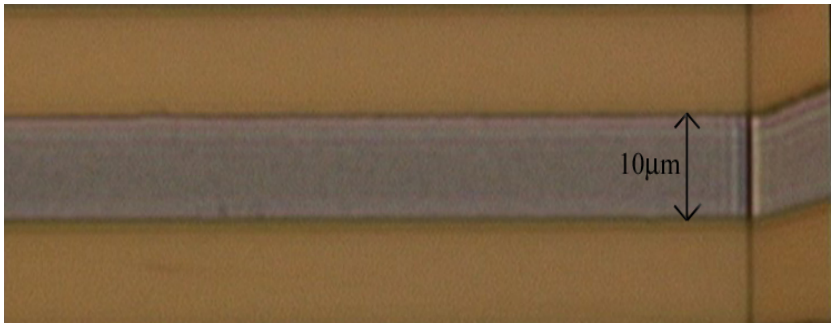

(a)

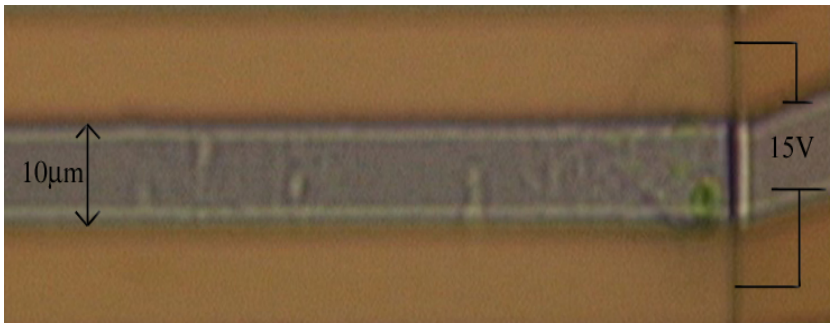

(b)

Figure 5.6: *Droplet of* $\approx 2.5\mu l$ *from the supernatant phase of sample* T_2*, placed over the microbands of a* $10\mu m$ *gap electrode. Picture (a) shows the sample before the voltage was applied, and picture (b) shows the sample after the voltage of* $15V$ *was applied. There are indications of an ER-effect here, but some of the Laponite particles were only gathered together as large aggregates such as the one with the green spot in picture (b) positioned in the right end of the gap.*

The results from the new set of experiments with samples T_1 and T_2 are pictured in Fig.5.7 and Fig.5.8, respectively.

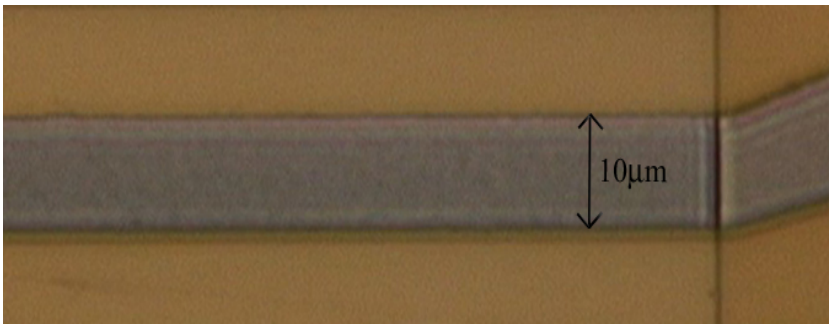

(a)

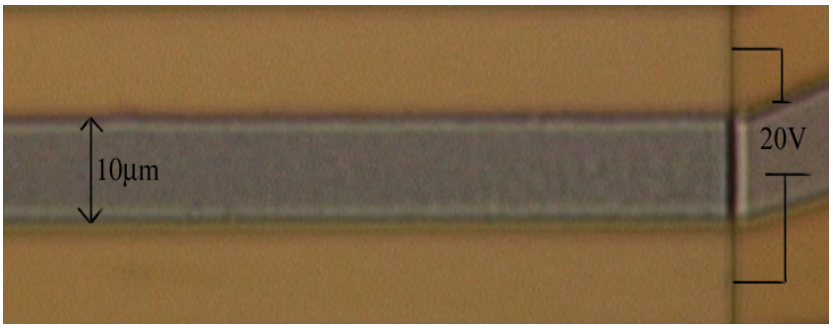

(b)

Figure 5.7: *Droplet of* $\approx 2.5\mu l$ *from the supernatant phase of sample* T_1*, placed over the microbands of a* $10\mu m$ *gap electrode. Picture (a) shows the sample before the voltage was applied, and picture (b) shows the sample after the voltage of* $20V$ *was applied. There are no indications of the ER-effect here.*

As opposed to the preliminary experiments with modified Laponite and turpentine, described in Sec.5.1.1, the samples displayed no signs of chain formations in this experiment. The main difference between these two experiments was the sample preparation method. In Sec.5.1.1 the sample was simply left for sedimentation before the experiments, while these samples were put in an ultrasound bath to destroy the aggregates, and subsequently left for sedimentation before the experiment. By placing the sample in an ultrasound bath, the average size of the Laponite aggregates was smaller than before the ultrasound bath treatment, and this might alter the trigger voltage.

It is known that for too small or too large particles, the ER-effect will be diminished, as presented in Sec.2.1.1. In this case, it might be that the particles were so small that Brownian motion dominated and prohibited the presence of the ER-effect. This Brownian motion was probably also amplified by a high ambient temperature between $25°C$ and $27°C$, which was higher than for the preliminary experiments.

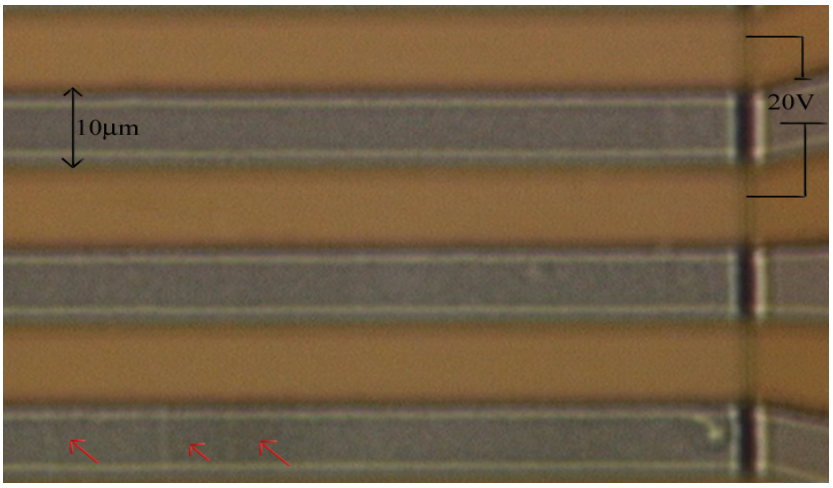

Figure 5.8: *Droplet of* $\approx 2.5\mu l$ *from the supernatant phase of sample* T_2*, placed over the microbands of a* $10\mu m$ *gap electrode. A voltage of* $20V$ *was applied over the upper gap and no indications of the ER-effect was observed. The red arrows in the lower gap points toward strong current flows due to the strong electric field.*

However, due to strong circular currents around the electric field gap, it was evident that a strong induced electrophoretic convection hindered the formation of chains. Thus, for this sample the ER-effect seemed to be unattainable at such high voltages.

In another attempt to reproduce these results, the T_1 and T_2 samples were yet again placed in the ultrasound bath for about 15 minutes. A $2.5\mu l$ droplet from the supernatant phase of sample T_1 was placed on the same electrode ($10\mu m$ gap) and a constant voltage of either $10V$, $15V$ or $20V$ was applied over the upper gap. The samples gave no indications of chain formations regardless of the electric field strength. Due to induced electrophoretic convection and small particles, chain formations were unattainable.

In the case of an applied voltage of $20V$ or $10V$, the results were not unexpected due to the already negative results described above. Previous experimental sessions have showed indications of chain formations at a voltage of $15V$, as pictured in Fig.5.5, and this was also expected to be observed here. However, the T_1 sample did not give a different response at $15V$ than at $10V$ or $20V$. Fig.5.9 shows the particle configuration within the droplet from sample T_1 after being exposed to a strong electric field created by an applied voltage of $15V$. Strong currents due to induced electrophoretic convection evidently prohibited the presence of the ER-effect. The corresponding video of the experiment is presented in file 3 in App.A.

The Laponite aggregates may have become too small to display the ER-effect, or the trigger voltage might be changed due to a reduction in average particle size. Therefore, both sample T_1 and T_2 were shaken and left for sedimentation for at least 24 hours without being placed in the ultrasound bath before next experimental session.

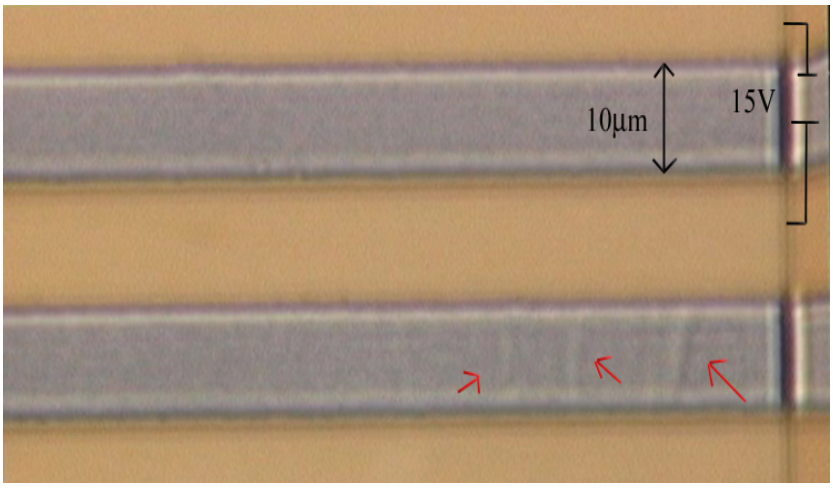

Figure 5.9: *Droplet of* $\approx 2.5\mu l$ *from the supernatant phase of sample* T_1*, placed over the microbands of a* $10\mu m$ *gap electrode. A voltage of* $15V$ *was applied over the upper gap and no indications of an ER-effect was observed. The red arrows in the lower gap points toward strong current flows as a result of induced electrophoretic convection.*

Afterward, a $5\mu l$ droplet from the sedimentary phase of sample T_1 was placed on the $10\mu m$ gap electrode and a voltage with increasing strength from $V_0 = 0V$ to $V_{max} = 27V$ was applied over the upper gap.

Fig.5.10 displays the particle configurations after the electric field was applied. Both large aggregates and smaller particles were present within the electric field, and the particle configuration of the small particles resembled chain formations.

Sample T_2 also gave indications of the ER-effect. In this case, a $5\mu l$ droplet was taken from the supernatant phase to decrease the size of the particles. It was placed on the $10\mu m$ gap electrode and an increasing voltage from $V_0 = 0V$ to $V_{max} = 27V$ was applied over the upper gap. It was not until the applied voltage reached V_{max} that signs of chain formations was observed, and these are shown in Fig.5.11. Lower voltages gave no indications of an ER-effect.

As explained in Sec.5.1, convection is the term used for fluid motions induced by factors such as a temperature difference or an electric or magnetic field. In this case one can observe both electrophoretic convection and thermal convection. The first is induced by the electric field, while the latter is induced by temperature differences within the droplet.

In case of illumination mainly from below the sample, as here, the inner temperature of the droplet will vary, thus leading to heat flows and convection.

In addition, the evaporation of the droplet is also expected to contribute to the temporary destruction of chains or aggregates.

To prevent or minimize such counteracting effects as convection and evaporation, a cover glass could be placed on top of the sample droplet during the experiment. In this way, the droplet would be squeezed between the cover glass and the electrode's substrate and microbands, resulting in a two dimensionally formed sample droplet. This would reduce the extension of the current flows

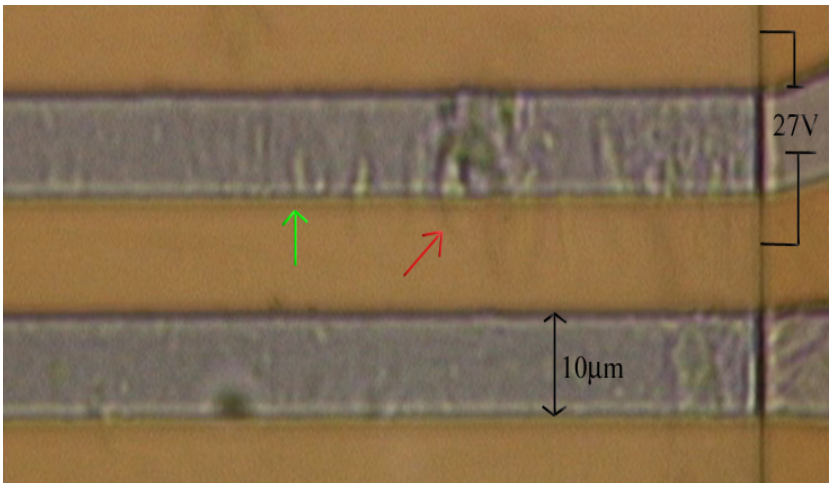

Figure 5.10: *Droplet of* $5\mu l$ *from the sedimentary phase of sample* T_1*, placed over the microbands of a* $10\mu m$ *gap electrode. A voltage of* $V_{max} = 27V$ *was applied over the upper gap. The red arrow in the upper gap points toward large Laponite aggregates while the green arrow points toward indications of chain formations with smaller particles.*

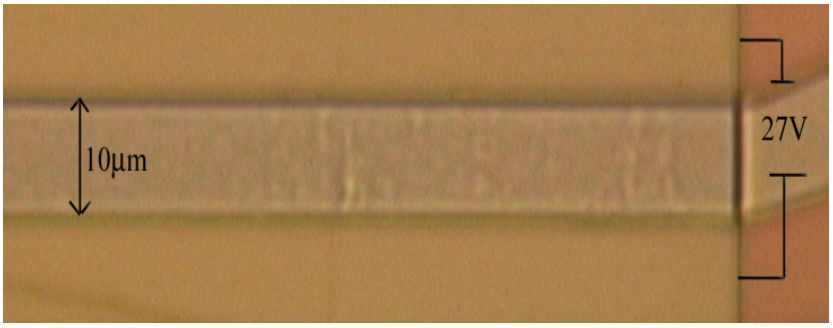

Figure 5.11: *Droplet of* $5\mu l$ *from the supernatant phase of sample* T_2*, placed over the microbands of a* $10\mu m$ *gap electrode. A voltage of* $V_{max} = 27V$ *is applied over the upper gap. There are indications of the ER-effect here.*

and might reduce the damage on the chains done by convection.

By adding a cover glass on top of the droplet, the evaporation process should also be slowed down due to a reduction in free surface area.

The volume of the sample droplet, which was about $2.5\mu l$, might also be too large. A smaller droplet would naturally be of smaller size, which in turn would lead to a smaller temperature difference within the droplet. As a result, the heat currents would be weakened and thus thermal convection would have a less influence on the particle motion.

Brief Summary

A brief summary of the experimental results presented in this section is given below.

- When placed in an ultrasound bath for approximately one hour in addition to a $15min$ ultrasound bath treatment before the first experimental activities, both of the turpentine samples, T_1 and T_2, showed indications of chain formations at an applied voltage of $15V$. The chain formations were temporarily formed and destroyed due to convection and evaporation effects. Fig.5.5 on page 42 and Fig.5.6 on page 43 displays the observed indications of chain formations.

- The same samples showed no sign of chain formations at voltages of $10V$ nor lower, and neither at $20V$ nor higher. This was evident by observing the particle formations presented in Fig.5.3 on page 41, Fig.5.4 on page 41, Fig.5.7 on page 44 and Fig.5.8 on page 45.

- Further ultrasound bath treatments seemed to make these results less reproducible. Subsequent to these indications of the ER-effect, it was difficult to induce chain formations at the previously mentioned voltages. At $V = 10V$ or less, and at $V = 20V$ or higher, the lack of chain formations did not contradict the previous results, but at $V = 15V$, which previously gave positive results, there was no longer signs of the ER-effect. It might be that the particles had become too small and hence the trigger voltage might have been changed. Only strong current flows induced by the electric field was observed and these can be seen in Fig.5.9 on page 46.

- Afterward, both of the turpentine samples were shaken thoroughly and left for sedimentation for over 24 hours. They were no longer placed in the ultrasound bath before the experimental sessions. Samples from the sedimentary phase of T_1 showed signs of chain formations with the smaller particles at $V = 27V$. Samples from the supernatant phase of T_2 also displayed signs of chain formations at $V = 27V$. This is depicted in Fig.5.10 on page 47 and Fig.5.11 on page 47, respectively.

- Based on the previous experiments it appears that for such micro scale systems, the ER-effect depends among others strongly on the particle size which also is the case for the trigger voltage. In addition, if there were chain formations within the electric field, these were made unstable by convection and evaporation effects. Chains were alternately formed and destroyed.

5.2.2 Trigger Voltage with Silicone Oil Samples

In the preliminary experiments there were no signs of chain formations within the samples of silicone oil. By utilizing the Nikon Optiphot microscope, the particle motion was observed in greater detail than with the Zeiss optical microscope. Hence, it might be possible to map the ER-properties of modified Laponite dissolved in silicone oil.

Two different samples of modified Laponite dissolved in silicone oil were prepared with the same concentration as the turpentine samples used in Sec.5.2.1. These are listed below.

- S_1: $0.100g$ modified Laponite in $10ml$ silicone oil$(0.01g/ml)$
- S_2: $0.050g$ modified Laponite in $10ml$ silicone oil$(0.005g/ml)$

Both samples were placed in an ultrasound bath for one hour after mixing the ingredients, and for another hour before each experimental session. A sample droplet with a volume between $2.5\mu l$ and $5\mu l$ was taken from the supernatant phase with a transferpipette and placed on a $10\mu m$ gap electrode. To observe the particle movement and configuration within the electric field, the Nikon Optiphot microscope was used together with the connected 3-CCD JVC camera. The captured videos had a resolution of $720x576$ pixels. Results and discussions are presented below.

Results

When using the new equipment described above, it was now apparent that silicone oil samples might also display the ER-effect together with modified Laponite in microscale systems. This section presents snapshots from several recorded videos that showed indications of the presence of the ER-effect, and also illustrates counteracting effects that must be diminished if the samples, S_1 and S_2, were to exhibit a stable ER-effect.

The first example of chain formations was seen within a $5\mu l$ droplet from the supernatant phase of sample S_2 placed over the microbands of the $10\mu m$ gap electrode. A DC voltage increasing from $0V$ to $15.7V$ was applied over the upper gap, which attracted the Laponite particles. As opposed to the preliminary experiments with no observable ER-effect, this video showed signs of chain formations though the chains consisted of larger aggregates than for the turpentine samples presented in Sec.5.2.1. The first sign of chains were seen at a voltage of $10V$, and as the voltage increased one could see several configurations similar to chains within the upper gap. The experimental video is shown in file 4 in App.A, and snapshots from this video are pictured in Fig.5.12(a).

When the time increased, more Laponite particles assembled within the electric field. Some of them were small particles, but there were also larger particles present which only filled the gap, as shown in Fig.5.12(b).

Since the sample droplet consisted of several large Laponite aggregates, the electrode gap would eventually be filled with these instead of chains. The particle formations similar to chains presented in Fig.5.12(a) represented a temporary state induced by the electric field. However, this temporary state was destroyed by the additional large Laponite aggregates that eventually ended up in the gap.

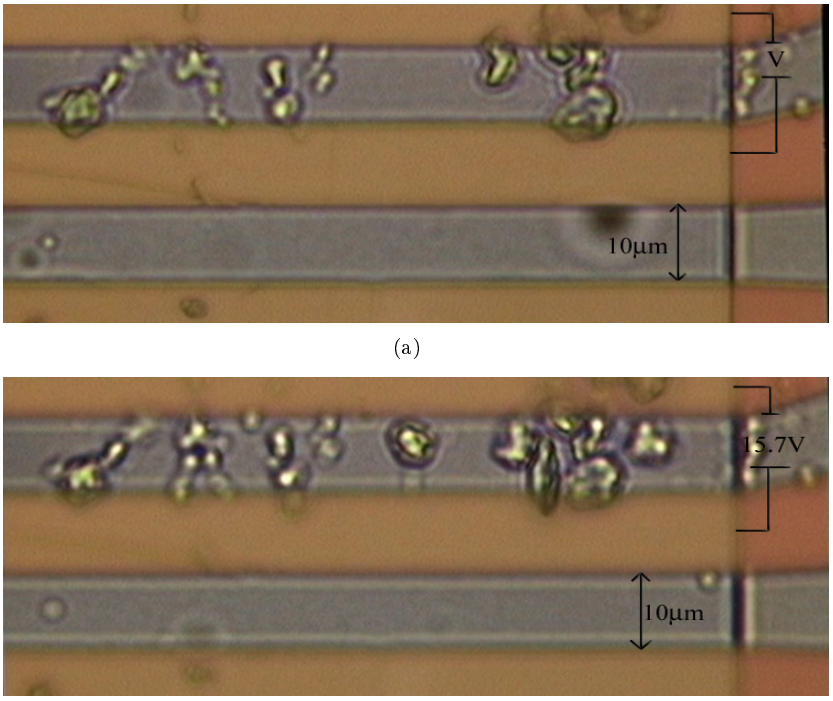

(a)

(b)

Figure 5.12: *Droplet of* $5\mu l$ *from the supernatant phase of sample* S_2*, placed over the microbands of a* $10\mu m$ *gap electrode. Picture (a) shows the particle configuration at an applied voltage of* $V \approx 15V$ *over the upper gap. There are indications of the ER-effect here. Picture (b) shows the particle configurations when* $V_{max} = 15.7V$ *has been applied over the upper gap for about one minute. This picture shows large aggregates filling the gap at the right end of the upper gap.*

There were also signs of chain formations in experiments with sample S_1, before the gap was filled by large aggregates. Fig.5.13 depicts the particle configuration after the applied voltage has increased from $0V$ to $15.8V$ and the experimental video is presented in file 5 in App.A.

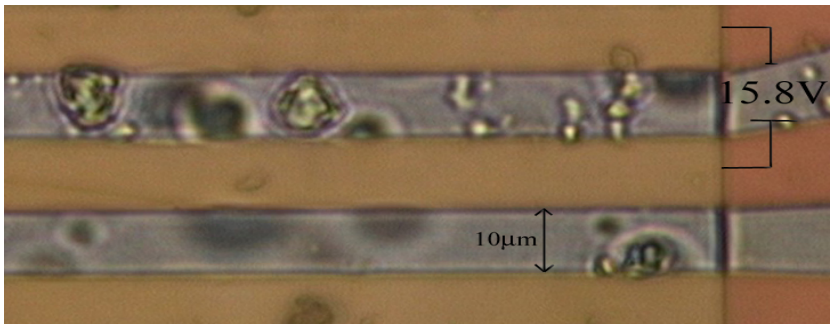

(a)

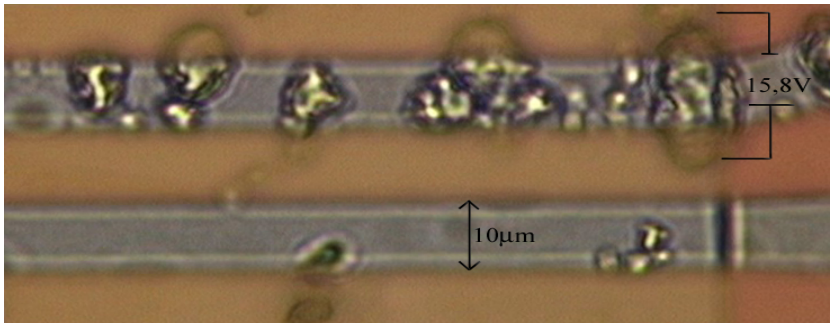

(b)

Figure 5.13: *Droplet of $5\mu l$ from the supernatant phase of sample S_1, placed over the microbands of a $10\mu m$ gap electrode. Picture (a) shows the particle configuration when a voltage of $15.8V$ was applied over the upper gap. There are indications of the ER-effect here. Picture (b) shows the particle configuration when $V_{max} = 15.8V$ was applied over the upper gap for about one minute. This picture shows that the possible chain formations were replaced by large aggregates that fill the gap.*

One minute after the video snapshot presented in Fig.5.13(a) was observed, the upper electrode gap was filled with large Laponite aggregates destroying the earlier signs of the ER-effect. This is pictured in Fig.5.13(b), and observed in the recorded video in file 5 in App.A. Like before, the increased number of particles present within the upper gap attracted other Laponite particles, including large particle aggregates. As the time increased, these large aggregates dominated over the smaller ones making it impossible to preserve chain formations.

Another sign of chain formations was observed with the S_1 sample. An increasing voltage from $0 - 10V$ was applied over the upper microband gap where a $5\mu l$ droplet from the supernatant phase of this sample was placed. At the maximum voltage, there were signs of chain formations which is shown by comparing the two pictures in Fig.5.14.

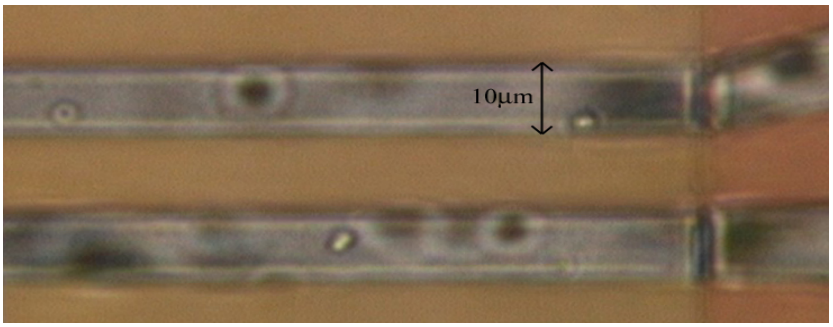

(a)

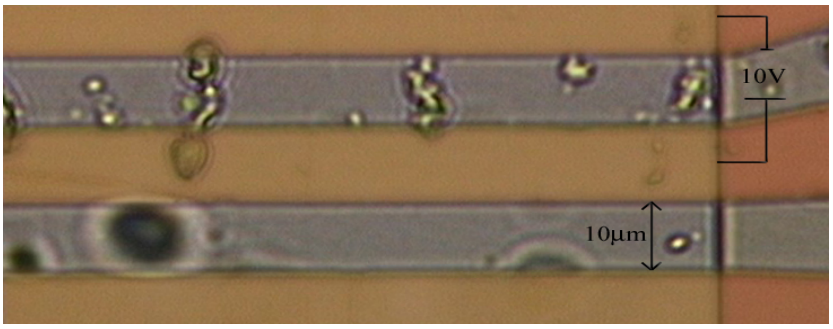

(b)

Figure 5.14: *Droplet of* $5\mu l$ *from the supernatant phase of sample* S_1*, placed over the microbands of a* $10\mu m$ *gap electrode. Picture (a) shows the particle configuration before the voltage was applied. Picture (b) shows the particle configuration after a voltage of* $10V$ *was applied. This picture indicates the presence of the ER-effect.*

Also sample S_2 showed indications of the presence of the ER-effect at an applied voltage of $10V$. This is pictured in Fig.5.15.

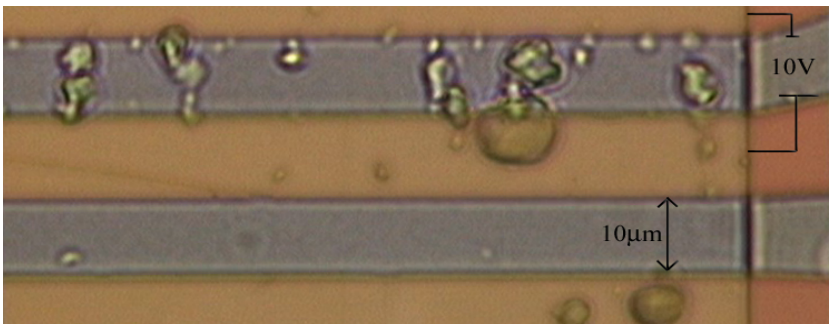

Figure 5.15: *Droplet of $5\mu l$ from the supernatant phase of sample S_2, placed over the microbands of a $10\mu m$ gap electrode. A voltage of $V_{max} = 10V$ was applied over the upper gap. There are indications of the ER-effect here.*

From the captured videos, which the pictures in this section were taken from, it was apparent that the Laponite particle behavior was quite different in silicone oil compared to its behavior in turpentine. The applied electric field accelerated the Laponite particles, but their velocity was quite low due to the high viscosity of silicone oil compared to turpentine. These parameters are listed in Table 3.1 on page 20. As a result, induced electrophoretic convection no longer had a great impact on the particle movement.

In the preliminary experiments presented in Sec.5.1 there were no signs of chain formations when using silicone oil as a solvent. For the filtrated or centrifuged samples, the results were probably negative due to a lack of particles, but in case of pure sedimentation, as was used in Sec.5.1.1, there should at least have been signs of chains or aggregates within the electric field. However, based on the experiments presented in this section, it was apparent that the response time was longer for silicone oil samples than for turpentine samples in this microscale system.

During the preliminary experiment described in Sec.5.1.1 the particle behavior was recorded by the Hitachi camera which can capture a video with a maximum duration of 13 seconds. In this case, by using the Nikon Optiphot microscope and accompanying equipment, the magnification was increased, and so did the duration of each experimental video. For the experiments presented in this section it took at least 30 seconds until the first signs of one chain could be seen. Hence, if there were chain formations within the silicone oil samples in the preliminary experiments, these were not observed because the sample was not exposed to the electric field for more than $10 - 13$ seconds.

For the experiments with turpentine samples presented in Sec.5.2.1, there were counteracting effects, such as convection and evaporation, making the chain formations unstable. In the case where silicone oil was used instead of turpentine, there were no evaporation effects present, and the convection effect was not observed to be of significant importance in regard to the particle motion. However,

there were still factors that contributed to the destruction of chain formation, and in this case, the Laponite particle size was one of them.

As can be seen by comparing the pictures in this section with the pictures in Sec.5.2.1, the Laponite aggregates were larger in silicone oil than in turpentine. This contributes to the eventual aggregation within the electric field which dominates over occasional signs of chain formations with smaller aggregates. It is therefore crucial that the Laponite aggregate size is significantly smaller than the the $10\mu m$ electrode gap.

This can be done by for example filtrating the sample before it is put in the ultrasound bath, decreasing both particle concentration and size. It might be that by shaking the sample thoroughly for a longer time, e.g. $30min$ or more, before placing it in the ultrasound bath, the Laponite particles will dissolve better than for the samples used here.

The total sample volume was very small, only $10ml$ of silicone oil was used. It might be more convenient to use a sample with a larger volume but with equal concentration. This will make it easier to use a magnet stirrer to dissolve the Laponite aggregates in silicone oil, thus one can prevent the formation of large particle aggregates. It will also increase the number of small particles present in the supernatant phase.

Since the viscosity of silicone oil samples is significantly larger than turpentine, the separation of larger particles from smaller ones by sedimentation will require a longer time. By letting the sample sediment for several days, the supernatant phase might contain smaller particles than what was present here.

Brief Summary

A brief summary of the experimental results presented in this section is given below.

- Both of the silicone oil samples, S_1 and S_2, showed signs of chain formations at applied voltages as low as $10V$. This is illustrated in Fig.5.14 on page 52 and Fig.5.15 on page 53.
- Formation of chains took longer time with silicone oil samples than for turpentine samples, probably due to the high viscosity of silicone oil compared to turpentine. Because the preliminary experiments with silicone oil were only captured for a duration of 13 seconds, there were not enough time for Laponite particles in silicone oil to assemble within the gap where the field was applied.
- In time, the possible chain formations were destroyed by incoming large aggregates filling the whole gap. This is depicted in Fig.5.12(b) on page 50 and Fig.5.13(b) on page 51. As a result, the signs of the ER-effect were only observed temporarily due to incoming large particle aggregates.
- In order to maintain a stable configuration of chains it is necessary to have a droplet that contains Laponite aggregates of smaller size than the $10\mu m$ microband gap.
- To reduce the particle size one could make a sample of greater volume and mix the ingredients with a magnet stirrer for a long time before the sample is placed in the ultrasound bath. It might also help to filter the silicone

oil sample before putting it in the ultrasound bath. This will reduce the final concentration, but also the Laponite particle size. By graining the Laponite particles before mixing them in silicone oil, the aggregate size will also be reduced. Subsequent to graining the particles, the samples must be placed in the ultrasound bath to diminish their tendency to aggregate.

5.2.3 Evaporation of Droplets

The experimental technique presented as a scientific background in Sec.2.3 on page 12 was utilized in some of the experiments presented here. With the aim to detect birefringent behavior within the electric field, i.e. anisotropic distribution of particles, the sample was observed while placed between two crossed polarizers. To detect anisotropic distribution of particles, the sample must be in a stationary state i.e. particle movement was not allowed. Hence, the sample was left to evaporate over a longer period of time, i.e. between 6 hours and 12 hours, to ensure complete evaporation and hence eliminating particle mobility.

In addition to reading the theory about the crossed polarizer technique described in Sec.2.3, it is also recommended to gain a brief theoretical background within droplet evaporation effects by reading Sec.2.4 on page 15 before the experimental results in this section are presented further.

Three different cases were investigated and compared. First, an evaporated droplet of turpentine containing modified Laponite particles and positioned on hydrophobic (non-wetting) glass was investigated with the Zeiss optical microscope to observe the particle distribution.

Second, droplets of same type, i.e. turpentine and modified Laponite, evaporated on hydrophilic (wetting) glass which resulted in a different particle distribution than what was observed on the hydrophobic substrate.

Finally, same type of droplet was placed on the $1\mu m$ gap electrode with an applied electric field of $2.0V/\mu m$ and observed with the Zeiss optical microscope. In addition, a droplet of turpentine and modified Laponite, or distilled water and modified Laponite, was placed on the $10\mu m$ gap electrode over which an electric field of about $2V/\mu m$ was applied. These droplets were observed by either the Zeiss optical microscope, or the Nikon Optiphot microscope. Pictures of the particle distributions within and around the electric field are compared to the distributions seen for droplets evaporated on hydrophobic or hydrophilic glass, without the presence of an electric field. With this, one can analyze the degree of impact evaporation effects have on the final particle distribution when a strong electric field is applied.

Results from these experiments are presented and analyzed below.

Particle Distribution on Hydrophobic Glass

A $0.1\mu l$ droplet was taken from the supernatant phase of the sample containing $0.1g$ modified Laponite dissolved in $10ml$ turpentine. It was the same sample that was used in the experiments presented in Sec.5.2.1 and referred to as T_1. The droplet was placed on hydrophobic(non-wetting) glass and left to evaporate for about 12 hours while covered with a plastic basin to protect it from pollution. After complete evaporation it was observed with the Zeiss optical microscope

while placed between crossed polarizers. Images were captured with the Q-imaging camera and had a resolution of $1197x973$ pixels. Fig.5.16 presents the dried droplet on a hydrophobic substrate.

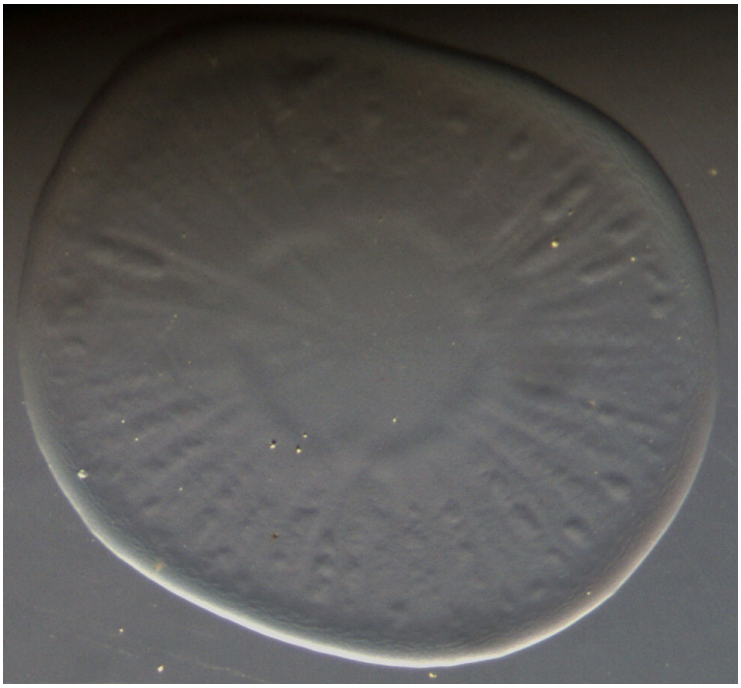

Figure 5.16: *Dried* $0.1\mu l$ *droplet of turpentine and modified Laponite on hydrophobic glass, placed between two crossed polarizers. A red region appears at the bottom right and upper left part of the droplet's edge and blue regions appear at the upper right and bottom left part of the edge. This characterizes birefringent sections due to anisotropic particle distribution at the edge.*

By examining the picture in Fig.5.16, it is apparent that in case of a hydrophobic substrate, the particles within the droplet show an anisotropic distribution at the edge of the droplet. Red and blue sections arise at the edge while the droplet is placed between crossed polarizers. As is argued in Sec.2.3, observed color patterns of samples positioned between crossed polarizers is a result of birefringence which in turn is a result of anisotropic particle distribution. Hence, the colors observed at the edge of the droplet pictured in Fig.5.16 represent two different orientational distributions.

With respect to particle orientation and density, the dried droplet on hydrophobic glass can be divided into three or four different regions as shown in Fig.5.17.

Zone 1 represents the edge of the droplet, where the particles show nematic order indicated by birefringent behavior. It is also apparent that a large portion of the particles have accumulated at the edge of the droplet while the droplet's interior includes fewer particles. This signifies the presence of the coffee-stain effect described in Sec.2.4.1 page 15. Colored regions only occurred at the edge

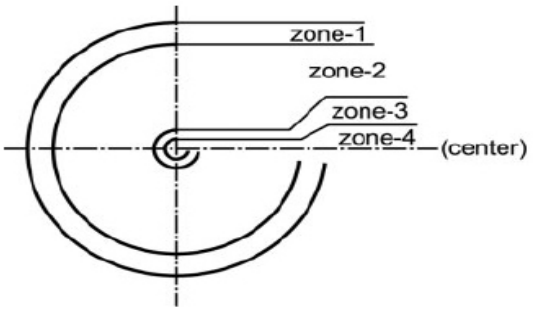

Figure 5.17: *Illustration of observed zone structure in an evaporated droplet of modified Laponite in turpentine on hydrophobic glass [48].*

where the particle concentration was higher than within zone 2, 3 and 4. The degree of observability of birefringence depends strongly on the concentration, configuration and size of the particles. Thus, the lack of birefringence at the inside of the edge was probably due to the low particle concentration compared to the concentration at the edge. Correspondingly, when nematic order is present, the observed color patterns would appear with increased intensity as the particle concentration within the region of nematic state increases.

However, not 100% of the solute was transferred to the edge. Some of the particles ended up in zone 2 which exhibits a different particle distribution with no observable birefringence. Due to rapid evaporation, slow particle motion or other factors, some of the Laponite particles were left within the inner zones. Since the particle flow toward the periphery of the droplet was directed radially, the particles left in zone 2 show a radial distribution.

The two inner zones, i.e. zone 3 and 4, were a result of the final stage of evaporation. Fig.5.18 shows the probable drying process valid in case of hydrophobic substrate. Since the evaporation process was faster at the edge, the last liquid residue was located at the inner part of the droplet. Once again, the particles were transported toward the edge of the remaining liquid area (as illustrated in Fig.5.18 (c)). Hence, after complete evaporation of the entire droplet, most of the particles in zone 3 and 4 ended up in zone 3, creating a new edge with higher particle concentration. In spite of this, there were not enough particles at the inner edge, i.e. zone 3, to cause birefringent behavior as was seen within the outer edge, represented by zone 1.

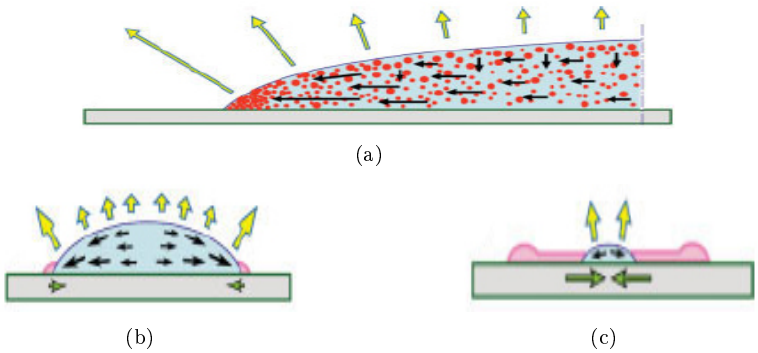

Figure 5.18: *Probable stages of the drying process for the droplet on a hydrophobic substrate [48].*

Particle Distribution on Hydrophilic Glass

A sample of $0.1g$ modified Laponite dissolved in $20ml$ turpentine was treated in an ultrasound bath for one hour and left to sediment for several hours. Three droplets with a volume of $0.1\mu l$ were taken from the supernatant phase and placed on hydrophilic(wetting) glass, i.e. a microscope slide. After over 12 hours, covered with a glass basin to protect it from pollution, the droplets were regarded as fully evaporated and subsequently examined with the Zeiss optical microscope. The Q-imaging camera was used to capture images with a resolution of $2048x1536$ pixels. With the aim to compare the particle distribution of droplets on hydrophilic glass to that on hydrophobic glass, these droplets were also placed between crossed polarizers in search of birefringence.

The difference in concentration of the two samples used for hydrophobic and hydrophilic glass may be regarded as negligible, not due to an assumption that the final concentration within the supernatant phase is similar, but because it was only focused on particle distribution, such as edge stains and radial deposits within the droplet's interior region. The droplet was expected to show similar behavior despite the possible difference in particle concentration within the supernatant phase of both samples.

Fig.5.19 presents the pictures of the three dried droplets together with a close-up at the edge to visualize the pattern resembling the coffee-stain effect.

In the case of hydrophilic(wetting) substrates, the dried droplet showed a different particle distribution compared to what was observed with a hydrophobic substrate. Here, the particle distribution was isotropic, indicated by a lack of birefringent behavior when placed between crossed polarizers. No colored regions similar to what was seen in Fig.5.16 was observed.

There is accumulation of particles at the edge of the droplets which is a characteristic sign of the coffee-stain effect, described in Sec.2.4.1. Outside the dried droplets, one can see sample residue shaped as a continuous or discontinuous ring surrounding the dried droplet and centered at the same point. Such patterns may occur when the droplet contracts during evaporation.

Besides the larger particle concentration at the droplet's edge, the particle distribution within the droplet remained isotropic and showed no signs of regions with accumulation of particles. Since the droplet was spread over a large area

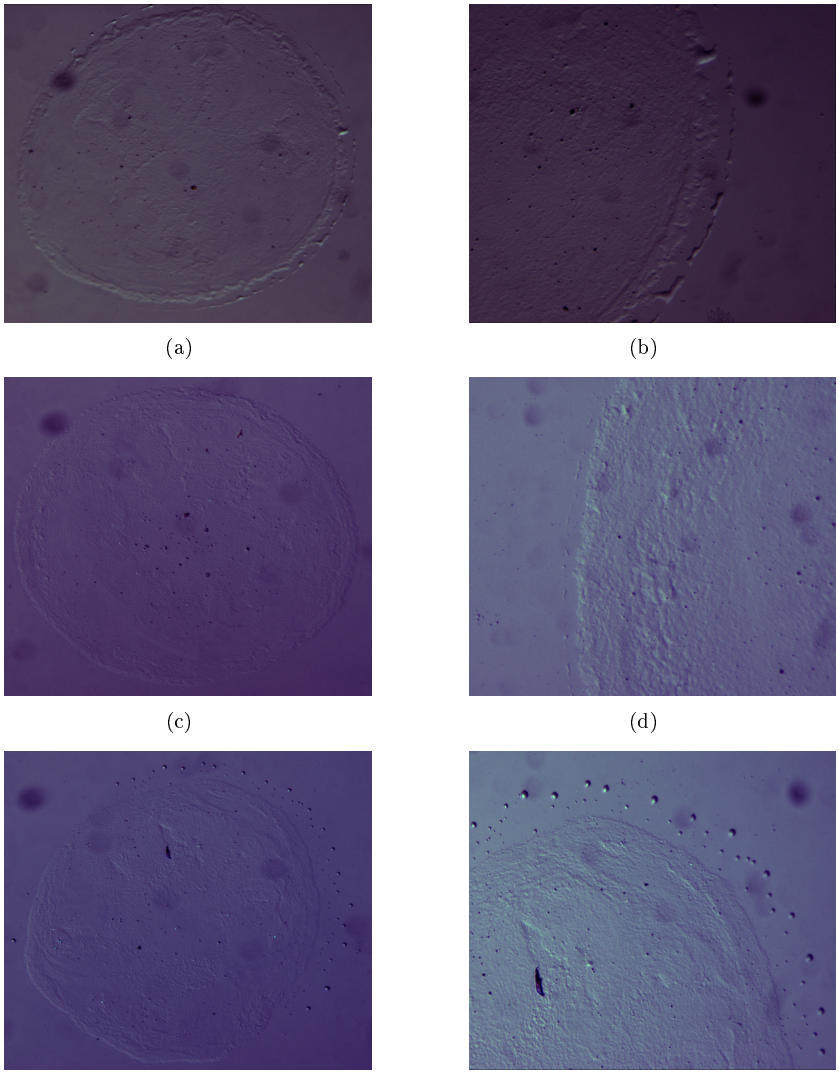

(a) (b) (c) (d) (e) (f)

Figure 5.19: *Dried* $0.1\mu l$ *droplets of modified Laponite in turpentine placed on hydrophilic glass and observed when placed between crossed polarizers. All pictures in the left column, i.e. (a), (c) and (e), are pictures of the entire droplet while those in the right column, i.e. (b), (d) and (f), show the edge of the corresponding droplet.*

compared to the hydrophobic case, the resulting free surface increased, which in turn resulted in an increased evaporation rate and a reduction in number of particles per unit area. Thus, the drying process differed from the one illustrated in Fig.5.18. It was expected that except for the edge, all of the liquid inside the droplet was fully evaporated at approximately the same time due to a large area of free surface. Hence, a more uniform particle distribution was seen at the interior of the droplet. By analyzing the final particle distribution, the evaporation process seemed to follow the steps illustrated in Fig.5.20.

Figure 5.20: *Evaporation process of droplets on hydrophilic glass [43].*

Electric Field Effects on Particle Distribution

The particle assembly with and without the presence of an electric field was compared in the experiments presented here. In addition, it was desirable to confirm the presence of the ER-effect by using crossed polarizers to detect birefringence within the electric field.

$1\mu m$ **Gap Electrode**

A sample containing $0.1g$ of modified Laponite dissolved in $20ml$ turpentine was placed in an ultrasound bath for one hour and subsequently left for sedimentation. A droplet of $0.1\mu l$ was taken from the supernatant phase and placed on the fingered microbands of the $1\mu m$ gap electrode described in Sec.4.1.1, page 23. The fingered $5+5$ microbands were used instead of the four independent addressable microbands because of a greater total area where the electric field was applied. Hence, particle configurations within the fingered microbands should be easier to observe than in the independent addressable microbands, when the magnification was at its lower limit. This was the case for the Zeiss optical microscope which was utilized in this experiment. To capture single frames, a Q-imaging camera was used together with accompanying software. The images had a resolution of $2048x1536$ pixels.

Fig.5.21 presents the captured images of the dried droplets. The particle configurations within dried droplets where no electric field has been applied (a-c) were compared to the particle configurations within dried droplets where an electric field of $2V/\mu m$ has been applied (d-f).

No birefringence was observed while the electrode was placed between crossed polarizers. Fig.5.21(d), where the electric field was applied, show bright spots outside the fingered microbands and bright microbands, as opposed to the case of no applied electric field represented by Fig.5.21(a). However, to validate the presence of birefringence, colored regions must be observable and this was absent here. The bright spots outside the microbands and the strong electric field were probably aggregates, while the microbands probably appeared bright due to optical noise.

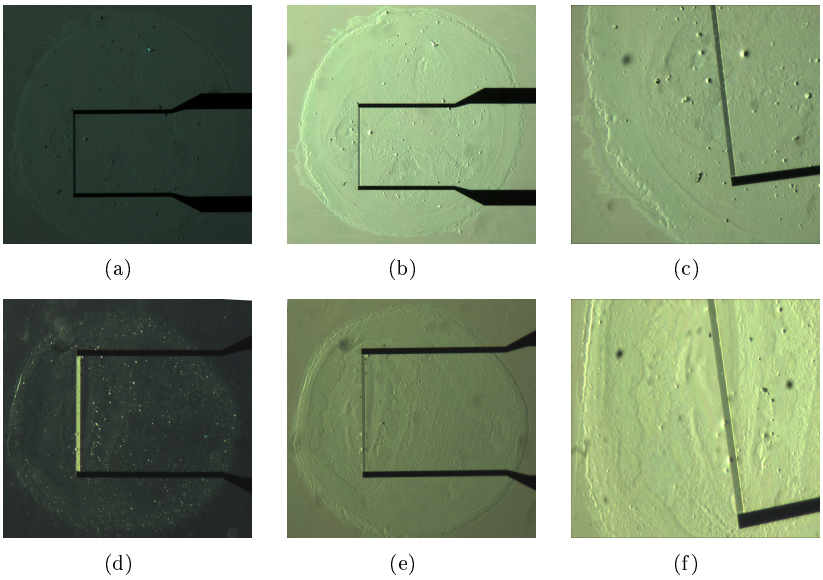

Figure 5.21: *Dried droplet on the fingered microbands of the* $1\mu m$ *gap electrode. Pictures (a) to (c) shows the particle configuration of the dried droplet when no electric field has been applied. Picture (a), (b) and (c) shows the dried droplet pictured between crossed polarizers, without polarizers and a part of the edge without polarizers, respectively. Pictures (d) to (f) show the particle configuration of the dried droplet after an electric field of* $2V/\mu m$ *has been applied. Picture (d), (e) and (f) shows the dried droplet pictured between crossed polarizers, without polarizers and a part of the edge without polarizers, respectively. There is no observable birefringence, i.e. ER-effect, here.*

Despite the lack of chain formations it appears that the particle configuration was influenced by the applied electric field. By comparing Fig.5.21(b) and (e), one can see a different topography and texture around the microbands when the electric field was applied (e) than for no applied electric field (b). Previous experiments with the $10\mu m$ gap electrode, e.g. Sec.5.1.1 and Sec.5.1.2, showed signs of induced electrophoretic convection by strong circular flows around the gap where the electric field was applied. Thus, a large portion of the particles were kept close to the electric field. The same phenomenon was probably also present here, and led to a greater particle deposition within and close to the microbands. As seen by comparing Fig.5.21(b) and (e), the large particles seem to assemble close to the microbands in case of an applied electric field, while when there was no electric field to accelerate and redistribute the particles, they seemed to assemble uniformly within the liquid surface.

In both cases, the coffee-stain effect was present, signified by accumulation of particles at the edge. This can be seen in Fig.5.21(c) and (f) which is similar to the edges formed for droplets placed on plain hydrophilic glass without microbands and electric field, as shown in Fig.5.19(b), (d) and (f). Independent of the presence of the electric field, the particles were drawn toward the edge due to evaporation. However, since the electrode had a substrate of hydrophilic glass, a lot of the particles within the droplet also ended up in the interior region of the droplet. In addition, the width of the accumulated edge was large compared to the diameter of the dried droplet.

$10\mu m$ Gap Electrode

A sample containing $0.1g$ modified Laponite dissolved in $10ml$ turpentine was used in this case. It had been placed in an ultrasound bath for at least one hour and left for sedimentation in advance. This was the same sample as was used in Sec.5.2.1 and referred to as T_1. A $0.1\mu l$ droplet was placed on the $10\mu m$ gap electrode and a voltage of either $15V$ or $20V$ was applied over the two upper microbands for approximately one hour. It was given at least 12 hours to evaporate to ensure complete evaporation before investigation. The entire electrode was covered with a plastic basin during evaporation to protect it from pollution.

The droplet was examined by using the Zeiss optical microscope together with the Q-imaging camera. The captured images had a resolution of $2048x1536$ pixels. With the aim to detect anisotropic particle configuration, the sample was examined while placed between two crossed polarizers.

Fig.5.22 presents the particle configuration, in the case of an applied electric field of $15V/10\mu m$ over the upper microband gap, as the dried droplet was placed between crossed polarizers.

The lack of aggregates or chains within the upper gap where the electric field was applied might be a result of an insufficient strength of the electric field. Hence, the same experiment was carried out with an increased applied voltage from $15V$ to $20V$. Fig.5.23 presents the resulting particle configuration as the sample was placed between crossed polarizers.

Due to the bright spots within and close to the electric field gap, depicted in this figure and lack of these in Fig.5.22 it was evident that the increased electric field had influenced the particle configuration, resulting in an increased amount of particles within the upper gap as the field was applied. However, due to a

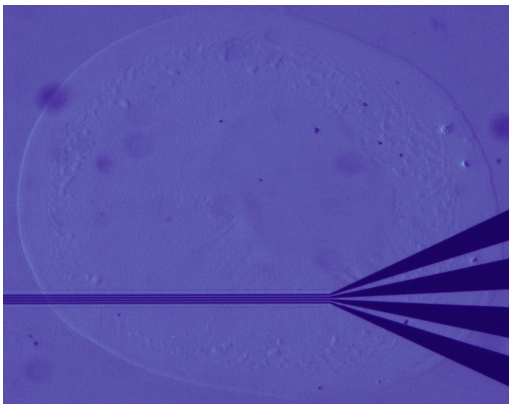

Figure 5.22: *Particle configuration of an evaporated sample of modified Laponite and turpentine exposed to a strong electric field created by an applied voltage of* $15V$ *over the upper two microbands. There is no sign of birefringence here, i.e. there is no observable ER-effect after complete evaporation in this case.*

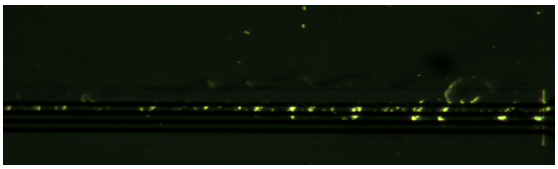

Figure 5.23: *Particle configuration of an evaporated sample of modified Laponite and turpentine exposed to a strong electric field created by an applied voltage of* $20V$ *over the upper two microbands. There is no sign of birefringence here, but the bright spots indicate agglomeration of particles within the electric field.*

lack of distinct colors, there were no signs of chain formations. Instead, only large particle aggregates, signified by bright spots, appeared within the upper microband gap.

A sample containing $0.1g$ modified Laponite dissolved in $20ml$ turpentine was placed in an ultrasound bath for at least one hour and left to sediment before this experimental session. A $0.1\mu l$ droplet was taken from the supernatant phase and placed on the $10\mu m$ gap electrode. For $30min$, a voltage of $20V$ was applied over one of the microband gaps. Subsequently, the droplet was left to evaporate for another $30min$. During evaporation, the droplet was covered with a plastic basin to protect it from pollution.

Afterward, the droplet was placed between crossed polarizers and observed through the Nikon Optiphot microscope connected to a Q-imaging camera. The captured images had a resolution of $2560x1920$ pixels.

To compare the particle distribution with and without an electric field, the same type of sample droplet was placed on the $10\mu m$ gap electrode to evaporate for about one hour with no applied electric field.

Fig.5.24 presents the observed particle distribution as these to sample droplets were placed between crossed polarizers.

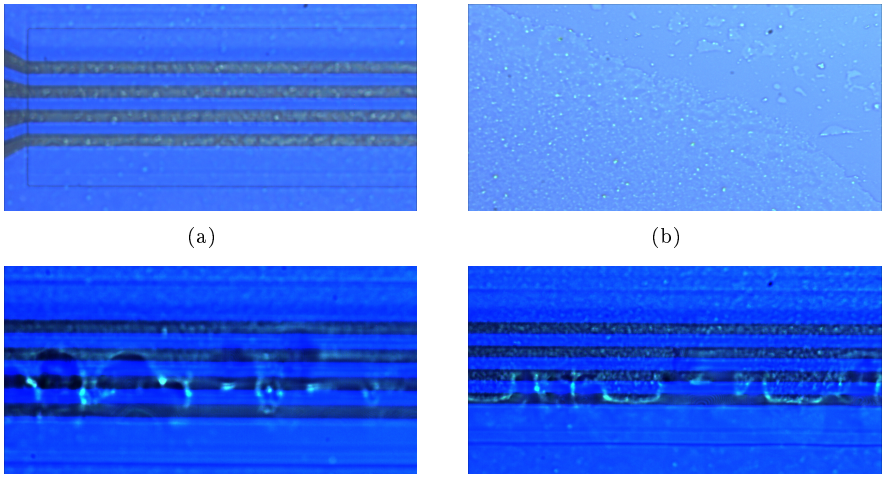

Figure 5.24: *Evaporated droplets of modified Laponite dissolved in turpentine placed on hydrophilic susbtrate are investigated when placed between crossed polarizers. Picture (a) shows the particle configuration after one hour of evaporation without exposure of an electric field and picture (b) shows the particle configuration at the edge of the droplet. Pictures (c) and (d) shows the particle configuration after one hour of evaporation when a voltage of* $20V$ *has been applied over the two lowest (black) microbands (with a spacing of* $10\mu m$*) during the first* 30 *minutes. Bright spots indicate aggregation within the electric field, but there is no observable birefringence after evaporation, i.e no ER-effect.*

These pictures show similar particle distribution as what was pictured in Fig.5.23, although the droplets observed here did not evaporate over such a

long period of time and hence, they were most likely not completely dry. Despite a lack of complete evaporation, if chain formations were present, these should be observed when the droplet was placed between crossed polarizers. Due to rapid chain formation and evaporation of liquid it would not take long before the particles became more or less immobile within the droplet. Although there might have been some liquid left that evaporated slower, it would not be enough to transport the modified Laponite particles. This was seen in several experimental videos where the droplet evaporated, e.g. see file 8 in App.A.

Birefringence was not observed here, which indicated that chain formations were not present. As observed in many experimental videos, there might be signs of chain formations within the droplet while it was still liquid, but after evaporation there were no signs of chains neither with nor without using crossed polarizers. It might be that evaporation effects, such as the coffee-stain effect which attract the particles toward the edge and away from the electric field, contributed to a destruction of temporarily formed chains.

The edge of the evaporated droplet was similar with and without the applied electric field and is depicted in Fig.5.24(b). In this picture, the particle distribution at the edge appeared similar to what was observed further away from the edge. This might be due to a large magnification which led to a limited surface area within the picture. In other words, if accumulation of particles was present at the edge, it might not have appeared within the picture. Fig.5.21 (b), (c), (e) and (f) pictures the particle distribution at the edge of the dried droplets placed on the hydrophilic $1\mu m$ gap electrode and Fig.5.22 pictures the particle distribution at the edge of a droplet placed on the hydrophilic $10\mu m$ gap electrode. In all these pictures, the edges appeared similar with and without an applied electric field. Accumulation of particles was observed by a distinct edge i.e. both the inner border and the outer border of the edge were visible. Hence, the coffee-stain effect appeared to have influenced the final particle configuration during evaporation. Most importantly, the width of the edge was large compared to the diameter of the droplet. Due to the width of the edge, one can not confirm the presence of the coffee-stain effect based on the single picture shown in Fig.5.24(b) where the magnification was large compared to the magnification in Fig.5.21 and Fig.5.22.

The electrorheological properties of two different samples containing modified Laponite dissolved in distilled water were also explored with the $10\mu m$ gap electrode. One sample contained $0.1g$ of modified Laponite dissolved in $20ml$ distilled water, and the other contained $0.2g$ modified Laponite dissolved in $20ml$ distilled water. Both samples were placed in an ultrasound bath and left to sediment in advance of each experiment. A droplet of $0.1\mu l$ was taken from the supernatant phase and placed on the $10\mu m$ gap electrode where a voltage of $20V$ was applied over the two lower microbands. The dried droplets were examined with the Nikon Optiphot microscope with a connected Q-imaging camera, while placed between crossed polarizers. The captured images had a resolution of $2560x1920$ pixels. Fig.5.25 pictures the particle configuration after one hour of evaporation, while the droplet was placed between two crossed polarizers.

Large particles was observed as bright spots in Fig.5.25(a) and did not in-

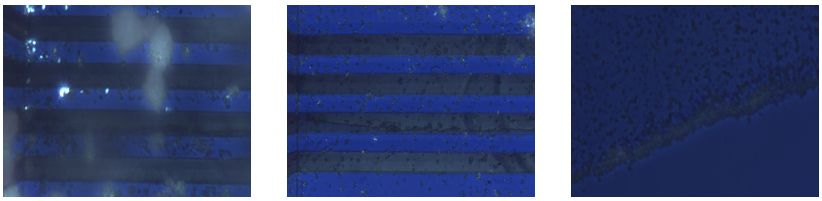

(a) (b) (c)

Figure 5.25: *Particle configuration within evaporated droplets from: (a) the sample containing* $0.2g$ *modified Laponite in* $20ml$ *distilled water, b) the sample containing* $0.1g$ *modified Laponite in* $20ml$ *distilled water. Picture (c) shows the particle configuration at the edge of the dried droplet from the sample containing* $0.1g$ *modified Laponite. A voltage of* $20V$ *has been applied over the two lower microbands. No birefringence or accumulation of particles can be seen within the lower gap, i.e. there is no observable ER-effect here. Accumulation at the edge (c) indicates the presence of the coffee-stain effect.*

dicate the presence of chain formations, especially since the field was applied over the lower gap and not the upper gap. The particle configuration at the edge of the dried droplets were equal for both types of samples. A narrow and evident edge of higher particle concentration was observed and is depicted in Fig.5.25(c). Evidently, the coffee-stain effect had a large impact on the final particle configuration. In fact, in this case the coffee-stain effect seemed to have a greater impact on the particle configuration than that from the electric field. It is known that adding small amounts of water can produce a larger ER-response [2]. However, water increases the dielectric conductivity and degrades overall performance, thus, it was expected that an ER-fluid consisting of pure water as a solvent was unable to exhibit the ER-effect. The lack of ER-effect within samples of distilled water as a solvent was therefore reasonable.

Brief Summary

A brief summary of the experimental results presented in this section is given below.

- A dried droplet of turpentine and modified Laponite placed on hydrophobic glass showed birefringence at the edge while placed between crossed polarizers. This was evident due to the red and blue sections pictured in Fig.5.16 on page 56. In addition, a large portion of the particles within the droplet settled at the edge as a result of the coffee-stain effect. Due to the radial flow of particles toward the edge of the droplet, a section of radially deposited particles occurred inside of the edge. The center of this droplet had few or no particles.

- Dried droplets of turpentine and modified Laponite placed on hydrophilic glass showed no birefringence while placed between crossed polarizers (see Fig.5.19). This was probably due to the increase in free surface of the droplets due to the hydrophilic substrate. As a result, the density of particles was reduced and potential birefringence was not observable. Particles

within the interior of the droplets were uniformly distributed and showed signs of accumulation at the edge. However, the area with higher particle concentration at the periphery of the droplet was large compared to the total surface area of the dried droplet. A ring shaped residue of dried liquid and particles was seen outside the dried droplet. This might be due to rapid contraction of the droplet during evaporation, leaving some of the solute and solvent behind.

- Dried droplets which have been exposed to an electric field showed no sign of birefringence while placed between crossed polarizers, whether the solvent was turpentine as depicted in Fig.5.23 or distilled water as depicted in Fig.5.25.

- All dried droplets on hydrophilic glass that were exposed to a strong electric field, showed particle accumulation at the edge independent of the applied electric field. The width of this edge was larger for particles dissolved in turpentine, see Fig.5.21(e), than for those in water, see Fig.5.25(c). Accumulation of particles at the edge implies that the coffee-stain effect influenced the particle configuration despite the presence of an electric field.

- Due to the lack of chain formation and thus birefringence within a dried droplet, it might be problematic to use crossed polarizers to determine the presence of the ER-effect. It was likely that evaporation effects not only temporarily destroyed chain formations while the droplet was still liquid, but also eliminated the possibility of retaining chain formations after complete evaporation.

5.2.4 Using Cover-Glass to Reduce Convection

During the experimental activities presented in the previous sections, it was evident that an evaporating solvent, such as turpentine, showed unstable chain formations. Counteracting effects from evaporation and convection led to alternating formation and destruction of chains within the electric field.

The experiments presented in this section were performed to investigate possible actions to diminish the counteracting effects. As suggested in Sec.5.2.1, placing a cover glass on top of the droplet might be helpful to reduce convection within the droplet.

A sample of $0.10g$ of modified Laponite dissolved in $20ml$ turpentine was exposed to ultrasonic treatment for at least one hour, and subsequently left to sediment. A droplet of $0.1\mu l$ was extracted from the supernatant phase and placed on the $10\mu m$ gap electrode where a voltage of $15V$ was applied. To observe the particle movements, the Nikon Optiphot microscope was utilized with a connected 3-CCD JVC camera. Recorded videos of the electrorheological response within the sample droplet covered with a cover glass are compared to the electrorheological response when cover glass was not used. The captured videos had a resolution of $720x576$ pixels. Results are presented and discussed below.

Results

Snapshots are presented from the captured videos of the liquid sample droplets with and without a cover glass on top. Fig.5.26 presents snapshots from a recorded video of the sample droplet before (a) and after (b) the voltage of $15V$ was applied over the upper gap. The video of the experiment is presented in file 6 in App.A. Here, a cover glass was not placed on the sample droplet. When comparing the particle configuration before and after the field was applied, there might be observable signs of chain formations within the upper gap. However, due to the large amount of particles within this gap, it is impossible to determine whether the particle assembly show chain formations or accumulation.

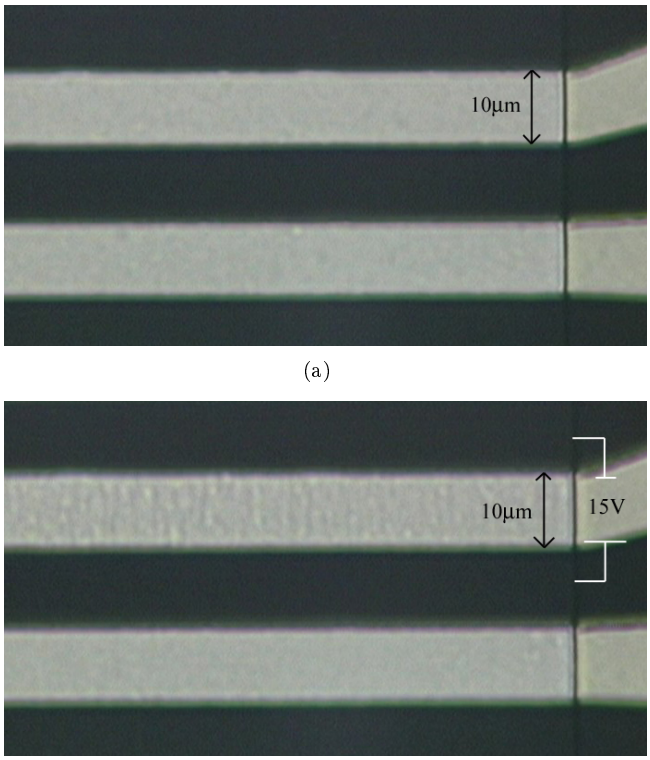

Figure 5.26: $0.1\mu l$ *droplet from the supernatant phase of the sample was placed over the microbands of a* $10\mu m$ *gap electrode. No cover glass was used here. Picture (a) shows the sample before the voltage was applied, and picture (b) shows the sample after the voltage of* $15V$ *was applied over the upper microband gap. There are indications of the ER-effect here.*

When a cover glass was placed on the same type of droplet, the ER-behavior changed. Fig.5.27 presents snapshots from a recorded video of the electrorheological response from this sample when a voltage of $15V$ was applied over the upper gap. The recorded video is presented in file 7 in App.A.

When comparing the particle configuration before and after the electric field was applied, as pictured in Fig.5.27(a) and (b), respectively, there were no

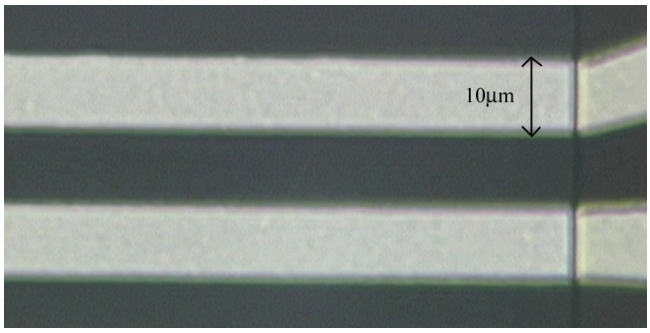

(a)

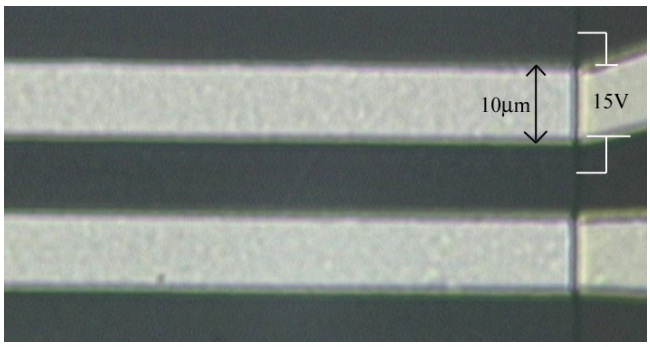

(b)

Figure 5.27: $0.1\mu l$ *droplet from the supernatant phase of sample* T_1 *was placed over the microbands of a* $10\mu m$ *gap electrode. A cover glass was placed on top of the droplet. Picture (a) shows the sample before the voltage was applied, and picture (b) shows the sample after a voltage of* $15V$ *was applied over the upper microband gap. There are no indications of the ER-effect here.*

evident signs of chain formations within the upper gap. At best, the density of particles might be higher within the upper gap than within the other gap.

By using a cover glass on top of the droplet, the droplet was squeezed between the electrode microbands and the cover glass, resulting in a two-dimensional shape of the droplet. A flattened droplet could contribute to reduce the destructive convection flows. When using a cover glass on the droplet, convection within the droplet was apparently reduced, however, also the particle mobility was significantly reduced. Hence, based on several videos with similar negative results, it was assumed that, with the present experimental system, a cover glass would not contribute to a stable ER-effect.

Brief Summary

A brief summary of the experimental results presented in this section is given below.

- In an attempt to reduce the counteracting effects from evaporation and thermal convection, the sample droplet was covered with a cover glass. A voltage of $15V$ was applied over the upper gap. This resulted in a weak accumulation of particles within the electric field, but no ER-effect was observed with the Nikon Optiphot microscope.
- The same sample was exposed to the same electric field, where no cover glass was placed on the sample droplet. Here, there was a large amount of particles within the electric field gap and their configuration resembled chain formations, but due to the large amount of particles, it was difficult to determine the presence of the ER-effect. This is depicted in Fig.5.26.
- From these examples it seemed that using a cover glass on the sample droplet does not contribute to stabilize the ER-effect.

5.2.5 Evaporation of Turpentine

Turpentine was chosen as an ER-solvent for laponite particles due to its low polarizability and low boiling temperature. After the turpentine was fully evaporated, the only remains within the electric field gap was thought to be the Laponite particles, formed as chains.

However, several experiments have shown that not all of the turpentine disappears after complete evaporation. The experiments presented here, show the remains of evaporated droplets of turpentine and illustrates the effect that such remains have on the ER-effect.

Results

A $0.1\mu l$ droplet was placed on a microscope slide and left to evaporate for several hours at ambient temperature. Afterward, it was examined with the Zeiss optical microscope connected to a Q-imaging camera. The captured images had a resolution of $2048x1536$ pixels. A picture of the dried droplet is presented in Fig.5.28.

Evidently, turpentine does not completely evaporate but leaves a thin film of residue after the liquid has disappeared. One can imagine that an evaporated

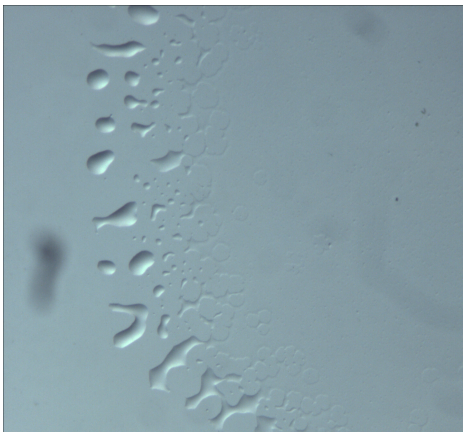

Figure 5.28: *Dried droplet of pure turpentine left a thin film of residue on the substrate.*

droplet of turpentine containing chain formations of Laponite particles will show a less well-defined structure due to the film of turpentine residue covering the particles. Hence, it was necessary to explore possible actions to remove the residual turpentine film, while keeping the chain formations. A dried droplet of turpentine was placed in a heating cabinet at a temperature close to its boiling temperature, for over 10 hours. The aim was to make the final turpentine film evaporate, but, after this heating treatment, there were no observable differences in the dried droplet.

Several movies with samples of turpentine and modified Laponite particles showed indications of chain formations while the turpentine was still liquid. However, after a lot of the liquid has evaporated, the particles became seemingly immobile and the previous chain formations were difficult to observe with optical microscopy.

A $2.5\mu l$ droplet from the supernatant phase of a sample containing $0.048g$ modified Laponite dissolved in $10ml$ turpentine was placed on a $10\mu m$ gap electrode. The sample used here was the same as the one used in Sec.5.2.1 on page 39 and termed T_2. An increasing voltage between $0V$ and $27V$ was applied over the upper gap. The Nikon Optiphot microscope was used to observe the particle motion within the electric field, and this was recorded with a connected CCD-camera. The captured videos had a resolution of $720x576$ pixels. Fig.5.29 presents snapshots from the captured movie which is presented file 8 in App.A.

These snapshots illustrate a common problem occurring with turpentine samples. When in liquid phase, turpentine and modified Laponite particles showed signs of chain formations. However, the chain formations were unstable due to induced electrophoretic convection, thermal convection and evaporation effects. Fig.5.29(a) presents the particle configuration before the turpentine droplet had evaporated. There are signs of chain formations here. After most of the liquid turpentine evaporated, the particles became immobile and it was difficult to determine the presence of chains due to a film of turpentine residue covering the particles. This is seen in Fig.5.29(b)

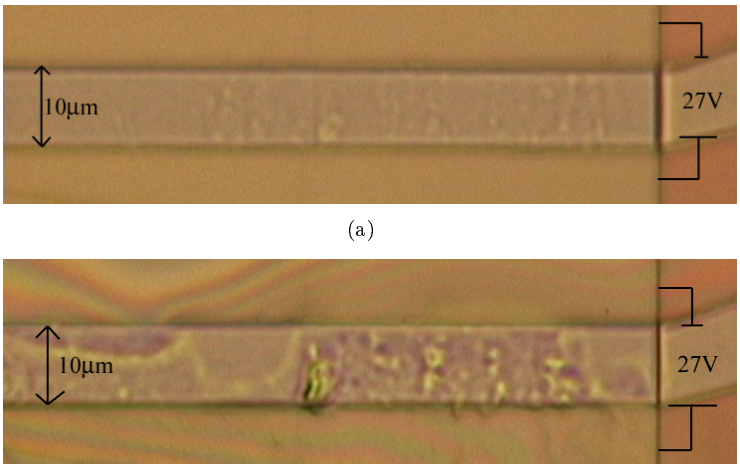

Figure 5.29: *The observability of chain formations was reduced when the turpentine has evaporated. Picture (a) shows the particle configuration while a voltage of 27V was applied. There are indications of chain formations here. Picture (b) shows the same sample after the turpentine has evaporated enough to make the particles immobile. The voltage was still applied over the gap. The previous chain formations were then covered with a thin film of turpentine residue.*

Brief Summary

A brief summary of the experimental results presented in this section is given below.

- All of the constituents in turpentine did not evaporate completely. This led to a residual thin, transparent film covering the substrate.
- Placing the evaporated turpentine droplet in a heating cabinet at a temperature close to its boiling point for several hours did not make the film evaporate completely.
- Several movies where samples of turpentine and modified Laponite particles evaporates were recorded. When the turpentine was still liquid, the sample showed indications of chain formations, but after after a while the turpentine made a transition into a gelled state where the particles became immobile. Due to the thin gelled film, chain formations were less (or not at all) observable.

Chapter 6

Discussion

For the experiments presented in this thesis, the ER-fluid mainly consisted of either Laponite RD or modified Laponite (AQAS) dissolved in silicone oil or turpentine.

During the preliminary experiments presented in Sec.5.1, it was apparent that Laponite RD did not give a satisfying ER-response within either of the solvents. Modified Laponite showed promising results when dissolved in turpentine whereas silicone oil gave no observable indications of the ER-effect independent of the type of solute. In addition, different methods for preparing samples were tested, all giving the same negative ER-response. This was most likely due to a low amount of particles within the sample droplet.

Subsequent to these preliminary experiments, more details about the ER-behavior of synthetic silicate particles were noticed. Due to the promising ER-behavior of modified Laponite particles, and lack of this for Laponite RD, only modified Laponite was used as a solid constituent in the ER-fluid for the continued experimental activities, presented in Sec.5.2. In addition, these samples were given ultrasonic treatment to reduce the average particle size.

It was evident that the evaporating solvent, turpentine, was able to allow chain formations of modified Laponite particles within the $10\mu m$ gap electrode at an applied voltage between $15V$ and $20V$. However, due to induced electrophoretic convection, thermal convection and evaporation effects, the chain formations became unstable. Chains were alternately formed and destroyed by induced electrophoretic convection, thermal convection and possibly evaporation effects. Samples, which at an early stage displayed signs of the ER-effect at an applied voltage of $15V$, required a stronger applied voltage after several ultrasonic treatments. Signs of chain formations were not observed for voltages lower than the maximum applied voltage of $27V$ when the samples had been given several ultrasonic treatments in advance. It might be that the ultrasonic treatment resulted in a decrease in average particle size which in turn altered the trigger voltage.

In addition, it was noticed that even though chain formations could be observed in droplets of turpentine and modified Laponite, it was difficult to observe the same chain formations after (most of) the liquid turpentine had evaporated. Evidently, the evaporation process of turpentine prohibited the formation of

chains to remain after complete evaporation. In this state, no chains were observed neither with, nor without, crossed polarizers. Only large aggregates were visible within the electric field gap.

In contrast to water, turpentine did not completely evaporate, but left a thin film of a gelled or solid residue on the substrate. When particles were dissolved in turpentine, the evaporated droplet of such a solution consisted of particles covered with a gelled, thin film . Due to refraction of light when transmitted through this film, it was difficult to determine the particle configuration after evaporation.

It was attempted to remove the film of turpentine residue after evaporation by placing it in a heating cabinet for several hours at a temperature close to its boiling temperature. This proved not to be helpful i.e. the film of turpentine remained on the substrate.

Turpentine has an evaporation rate of $40min$ [74] which is considered to be large. To diminish the counteracting evaporation effect, it might be helpful to use a solvent with a smaller rate of evaporation. A new evaporating solvent should in addition be non-conductive and have a large polarizability represented by a large dielectric constant.

As opposed to the preliminary experiments, ER-fluids of silicone oil and modified Laponite have shown signs of chain formations when placed on an electrode with $10\mu m$ gaps. However, the formation of chains proceeded slowly due to the high viscosity of silicone oil, and several gaps within which the particles got trapped. Since the videos of interest in the preliminary experiments had a duration of 13 seconds, there were not enough time to detect accumulation or chain formation within the electric field gap, thus it appeared that silicone oil did not allow chain formations in such small gaps. Proceeding experimental activities included captured videos of longer duration, hence it was possible to observe the slow accumulation or chain formation of modified Laponite particles in silicone oil.

One of the limiting factors in this case, was the particle size. Despite the ultrasonic treatment, the average particle size within silicone oil was significantly larger than when dissolved in turpentine. To reduce the particle size within the sample droplet, it might be helpful to make a sample of greater volume and stir it with a magnet rotator for several hours. Thus, the particles might dissolve better in silicone oil. Filtration of the sample might also be helpful.

Both silicone oil samples and turpentine samples would benefit an electrode construction of only two parallel microbands where the entire sample droplet could be placed within the electric field. In this way, all of the particles within the sample droplet would be within the electric field gap as this is applied. This was one of the problems with silicone oil samples. In addition, destruction of chains from particles outside the electric field gap would be impossible. This was one of the problems with turpentine samples. However, the main problem with such an electrode configuration is to place the entire sample within one gap with size in the order of $1\mu m$.

Pure water was also used as a solvent for modified Laponite, but no signs of the ER-effect were observed. Independent of the presence of the electric field, the dried droplets indicated the former presence of the coffee-stain effect by accumulation of particles at the edge. Since adding water in ER-fluids degrades the overall performance, these results were reasonable and represent the utter limit where the particle distribution after complete evaporation is solely controlled by evaporation effects.

A solution of turpentine and modified Laponite placed on the fingered microbands of the $1\mu m$ gap electrode, showed no signs of the ER-effect when placed between crossed polarizers. Signs of accumulation of particles at the edge were observed both with and without the electric field. Hence, the coffee-stain effect probably influenced the particle flows independent of the electric field. Apparently, the particle size of modified Laponite in turpentine was too large to form fibrillated chains within a $1\mu m$ gap electrode. Particles of smaller size is essential to form chains within such small gaps and this can either be done by minimizing the modified Laponite particle size, or by replacing the synthetic clay particles with polar colloids of smaller size. It is, however, important to keep in mind that too small particles will prevent the ER-effect because Brownian motion is expected to dominate over chain formations.

Chapter 7

Concluding Remarks

The objective of this thesis was to study the micro scale electrorheological behavior of synthetic clay particles in various solvents. In the experiments presented here, the synthetic silicates in the ER-fluid were either Laponite RD or modified Laponite, and these were dissolved in either silicon oil, turpentine or distilled water. The two latter solvents evaporate at ambient temperature. Electrodes with several microbands separated by a distance of either $1\mu m$ or $10\mu m$ were purchased and constituted the electric field environment. Two optical microscopes with different magnifications were utilized to observe the ER-behavior of the solution.

Recorded videos of liquid turpentine and modified Laponite particles placed on the $10\mu m$ gap electrode, displayed strong indications of chain formations made unstable by induced electrophoretic convection, thermal convection and evaporation effects. Placing a cover glass on top of the droplet resulted in a significant reduction in particle mobility and did not increase the stability of the ER-response. As a result, no ER-effect was observed. After complete evaporation, a thin film of turpentine residue covered the Laponite particles and no signs of chain formations were observed in this dry state. Evidently, evaporation effects temporarily destroyed chain formations and prohibited chain formations to remain after complete evaporation. Hence, no birefringence was observed while placing the dried droplet between crossed polarizers.

The ER-fluids containing silicone oil displayed particle configurations similar to chains after being exposed to the electric field for several minutes. The extended reaction time was suggested to be a result of the high viscosity of silicone oil. Eventually, the particle configuration within the electric field resembled flocculation instead of chain formations due to large particles filling the gap. Since a large portion of the Laponite particles within the silicone oil droplet were located outside the electric field gap when the field was applied, many of these never ended up within this gap and could therefore neither participate in chain formations. As a result, the probability of forming thin fibrillated chains of small particles within the entire electric field gap, was fairly reduced.

Droplets of turpentine and modified Laponite, or distilled water and modified Laponite, were placed on the fingered microbands of the $1\mu m$ gap electrode and exposed to an electric field of $2V/\mu m$. Neither of these samples showed

indications of chain formations or flocculation within the electric field. The main reason for this was probably the large particle size compared to the microband spacing of $1\mu m$.

The influence of evaporation effects on particle distribution when an electric field was applied was investigated for both types of electrodes. It was apparent that the coffee-stain effect was present both with and without the presence of the electric field. When placing a dried droplet of turpentine and modified Laponite between crossed polarizers, birefringence was observed at the edge in the form of four sections of red and blue colors due to particle self-assembly. No birefringence was observed at the edge of droplets dried on hydrophilic glass.

Pure water droplets containing modified Laponite particles were also placed on the $10\mu m$ gap and exposed to a strong electric field. The coffee-stain effect led to particle accumulation at the edge independent of the electric field, but no ER-effect was observed.

7.1 Suggestions for Future Experiments

The experiments presented in this thesis demonstrated that the ER-effect can also be observed in microscale systems, though the ER-behavior differs from what is observed in larger systems(e.g. [8]).

There are several factors that need further research in order to gain more knowledge on the ER-behavior of nano-silicate particles in microscale systems. One of the main aims for future experimental activities on this subject, could be to investigate several possibilities to make the ER-effect stable within similar microscale systems as those used here.

Turpentine might be replaced by other evaporative solvents with the aim to improve the stability of the chain formations. If turpentine proceeds as an evaporating ER-solvent, one could investigate different methods to remove the residual film of turpentine after evaporation.
The samples could also be prepared in a larger volume to increase the amount of small particles within the supernatant phase.

Instead of confirming the ER-effect by optical microscopy, one could measure the friction between two parallel conducting plates versus the applied voltage over these. If the the ER-effect is present, it will be detected by a sudden increase in viscosity which can be measured. A suggestion of experimental setup is illustrated in Fig.7.1. Between two parallel copper plates, covered with a thin layer of teflon and separated by a distance in the order of $10\mu m$, is an ER-fluid of Laponite particles dissolved in an insulating oil. A variable DC voltage is applied over the copper plates while one of the plates is shifted horizontally (in the parallel direction) with a constant velocity. When the ER-effect is induced, the viscosity of the ER-fluid will increase, which in turn will lead to an increase in friction between the copper plate and the ER-fluid. The measured friction versus applied voltage will show the presence of the ER-effect and indicate the strength of the chains.

In addition, applicable areas of such microscale systems could be investigated further. The fingered microbands on the $1\mu m$ gap electrode can be used as an inspiration for making locks with similar structure.

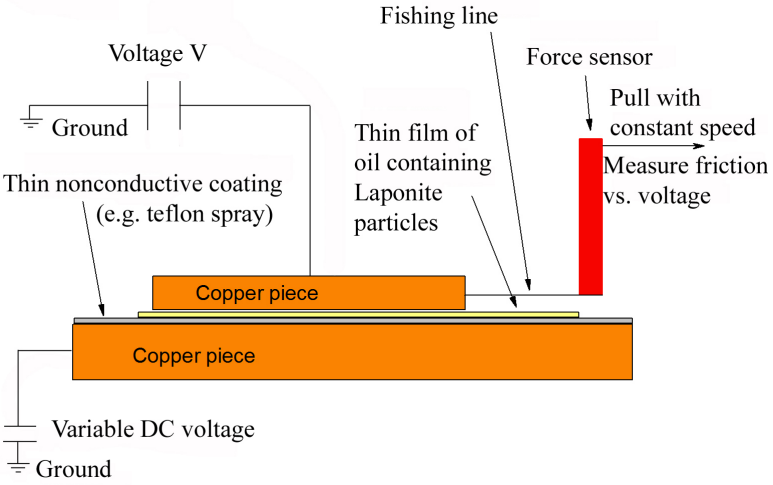

Figure 7.1: *Experimental setup to measure friction as a function of applied voltage.*

The idea is to finger together several parallel, conducting microbands as illustrated in Fig.7.2.

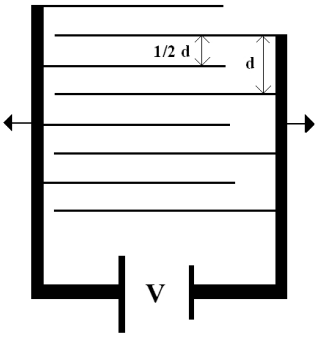

Figure 7.2: *A lock of several fingered microbands.*

The space between the fingered microbands is filled with an ER-fluid. When a voltage of sufficient strength is applied, the fibrillated chains will keep the microbans in position and thus making it difficult to move the two sides away from each other. The locked direction is denoted by the two horizontal arrows. Since the spacing, d, between the microbands is in the order of micrometers, it is not necessary to have a high-voltage supply. However, to make a strong locking system, one needs an ER-fluid that, within a very short time, can form stable chains. In addition, the microbands must have a very low roughness.

Bibliography

[1] W.M. Winslow. Induced fibration of suspensions. *Journal of Applied Physics*, 20:1137–1141, 1949.

[2] Alice P. Gast and Charles F. Zukoski. Electrorheological fluids as collodial suspensions. *Advances in Colloid and Interface Science*, 30:153–202, 1989.

[3] Tian Hao. Electrorheological fluids. *Adv. Mater.*, 13(24), December 2001.

[4] Hongru Ma, Weijia Wen, Wing Yim Tam, and Ping Sheng. Dielectric electrorheological fluids: theory and experiment. *Advances in Physics*, 52(4):343–383, 2003.

[5] Weijia Wen, Xianxiang Huang, Shihe Yang, Kunquan Lu, and Ping Sheng. The giant electrorheological effect in suspensions of nanoparticles. *Nature Materials*, 2:727–730, November 2003.

[6] Shu-Mei Chen and Chen-GuanWei. Experimental study of the rheological behavior of electrorheological fluids. *Smart Mater. Struct.*, 15:371–377, 2006.

[7] Jon Otto Fossum. Physical phenomena in clays. *Physica A*, 270:270–277, 1999.

[8] Kanak P.S Parmar. *Oil dispersions of nano-layered silicates in an external electric field: An experimental study.* PhD thesis, NTNU, 2006.

[9] Tian Hao. Electrorheological suspensions. *Advances in colloid and interface science*, 97:1–35, 2002.

[10] Weijia Wen, Xianxiang Huang, and Ping Sheng. Particle size scaling of the giant electrorheological effect. *Applied Physics Letters*, 85(2):299–301, 2004.

[11] Nicos Makris, Scott A Burton, and Douglas P Taylor. Electrorheological damper with annular ducts for seismic protection applications. *Smart Mater. Struct.*, 5:551–564, 1996.

[12] Keith Yates Design Group. Glossary. `http://www.keithyates.com/glossary.htm#anchor517411`, Last visited Dec. 18, 2006.

[13] Young-Min Han and Seung-Bok Choi. Force-feedback control of a spherical haptic device featuring an electrorheological fluid. *Smart Mater. Struct.*, 15:1438–1446, 2006.

[14] Tian Hao, Akiko Kawai, and Fumikazu Ikazaki. Mechanism of the electrorheological effect: Evidence from the conductive, dielectric and surface characteristics of water-free electrorheological fluids. *Langmuir*, 14:1256–1262, 1998.

[15] L.C. Davis. Polarization forces and conductivity effects in electrorheological fluids. *J. Appl. Phys.*, 72(4):1334–1340, 1992.

[16] J.N. Foule, P.Atten, and N. Felici. Macroscopic model of interaction between particles in an electrorheological fluid. *Journal of Electrostatics*, 33:103–112, 1994.

[17] R. Nava, M. A. Ponce, L. Rejon S. Viquez, and V. M. Castano. Response time and viscosity of electrorheological fluids. *Smart Mater. Struct.*, 6:67–75, 1997.

[18] Wolfram Research. Electrorheological fluid. `http://scienceworld.wolfram.com/physics/ElectrorheologicalFluid.html`, Last visited Dec.18, 2006.

[19] Seth Fraden Brandeis University Ujihta Dassanayake. Structure of electrorheological fluids. `http://www.elsie.brandeis.edu/er/index.html`, Last visited Dec.18, 2006.

[20] Gert Strobl. *Condensed Matter Physics: Crystals, Liquids, Liquid Crystals and Polymers*. Springer, 1 edition, 2004.

[21] HyperPhysics. Electric dipole field. `http://hyperphysics.phy-astr.gsu.edu/hbase/electric/dipole.html#c3`, Last visited March 2007.

[22] Jon Otto Fossum. Some thoughts about the future of complex fluids like clays. `http://folk.ntnu.no/fossumj/cpx/terminator_e.html`, Last visited Dec.18, 2006.

[23] University of Arkansas. Chapter 8: Electric dipoles. `http://www.uark.edu/depts/physinfo/up2/guide/mat-chp-top-electricdipolecap.pdf`, Last visited Dec.18, 2006.

[24] Rolf E. Hummel. *Understanding materials science*. Springer, 2 edition, 2004.

[25] F. Bergaya, B.K.G. Theng, and G. Lagaly. *Handbook of Clay Science*. Elsevier Ltd., 1 edition, 2006.

[26] Wikipedia. Clay minerals. `http://en.wikipedia.org/wiki/Clay_minerals#Structure`, 2007.

[27] Timothy P. Wangler, Angela K. Wylykanowitz, and George W. Scherer. Controlling stress from swelling clay. Conference Papers: `http://www.cee.princeton.edu/scherergroup/In\%20Press.html`, 2006.

[28] A. Mourchid, E. Lecolier, H. Van Damme, and P. Levitz. On viscoelastic, birefringent, and swelling properties of laponite clay suspensions: Revisited phase diagram. *Langmuir*, 14, 1998.

[29] S. A. Solin. Clays and clay intercalation compounds: Properties and physical phenomena. *Annu. Rev. Mater. Sci.*, 1997.

[30] Norma Negrete-Herrera, Jean-Luc Putaux, and Elodie Bourgeat-Lami. Synthesis of polymer/laponite nanocomposite latex particles via emulsion polymerization using silylated and cation-exchanged laponite clay platelets. *Solid State Chemistry*, 34:121–137, 2006.

[31] Jon Otto Fossum. Universal networks and processes in soft and complex matter: From nano to macro. *Dynamics of Complex Interconnected Systems: Networks and Bioprocesses*, pages 175–190, 2006.

[32] Norma Negrete-Herrera, Jean-Luc Putaux, and Elodie Bourgeat-Lami. Synthesis of polymer/laponite nanocomposite latex particles via emulsion polymerization using silylated and cation-exchanged laponite clay platelets. *Progress in Solid State Chemistry*, 34:121–137, 2006.

[33] Edward S. H. Leach, Andrew Hopkinson, Kevin Franklin, and Jeroen S. van Duijneveldt. Nonaqueous suspensions of laponite and montmorillonite. *Langmuir*, 21(9):3821–3830, 2005.

[34] Audun Bakk, Jon O. Fossum, Geraldo J. da Silva, Hans M. Adland, Arne Mikkelsen, and Arnljot Elgsæter. Viscosity and transient electric birefringence study of clay colloidal aggregation. *Physical Review E*, 65, January 2002.

[35] Case Western Reserve University. Light and polarization. `http://plc.cwru.edu/tutorial/enhanced/files/lc/light/light.htm`, Last visited May 2007.

[36] Jurgen R.Meyer-Arendt. *Introduction to Classical and Modern Optics*. Prentice-Hall, Inc., 4 edition, 1995.

[37] University of Colorado Chris Conery: Liquid Crystal Group, Department of Physics. Twisted nematic devices. `http://bly.colorado.edu/lcphysics/lcintro/tnlc.html`, 2007.

[38] Matt Young. *Optics and Lasers, including Fibers and Optical Waveguides*. Springer-Verlag New York, 4 edition, 1992.

[39] Robert Guenther. *Modern Optics*. John Wiley and Sons, 1990.

[40] C.J. Serna D. Levy and J.M. Otòn. Preparation of electro-optical active liquid crystal microdomains by the sol-gel process. *Materials Letters*, 10(9,10):470–476, February 1991.

[41] Robert D. Deegan, Olgica Bakajin, Todd F. Dupont, Greg Huber, Sidney R. Nagel, and Thomas A. Witten. Contact line deposits in an evaporating drop. *Physical Review E*, 62(1):756–765, July 2000.

[42] A.L. Yarin, J.B. Szczech, C.M. Megaridis, J. Zhang, and D.R. Gamotac. Lines of dense nanoparticle colloidal suspensions evaporating on a flat surface: Formation of non-uniform dried deposits. *Journal of Colloid and Interface Science*, 294:343–354, 2006.

[43] Chan Hee Chon, Sokwon Paik, Joseph B. Tipton Jr., and Kenneth D.Kihm. Effect on nanoparticle sizes and number densities on the evaporation and dryout characteristics for strongly pinned nanofluid droplets. *Langmuir*, 23:2953–2960, 2007.

[44] Robert D. Deegan, Olgica Bakajin, Todd F. Dupont, Greb Huber, Sidney R. Nagel, and Thomas A. Witten. Capillary flow as the cause of ring stains from dried liquid drops. *Nature*, 389:827–829, October 1997.

[45] Noushine Shahidzadeh-Bonn, Salima Rafa¨i, Aza Azouni, and Daniel Bonn. Evaporating droplets. *Journal of Fluid Mechanics*, 549:307–313, 2006.

[46] Rahat Duggal, Fazle Hussain, and Matteo Pasquali. Self-assembly of single-walled carbon nanotubes into a sheet by drop drying. *Advanced Materials*, 18:29–34, 2006.

[47] Hua Hu and Ronald G. Larson. Marangoni effect reverses coffee-ring depositions. *The Journal of Physical Chemistry*, 110(14):7090–7094, 2006.

[48] Nahoko Morii, Giyuu Kido, Hiroyuki Suzuki, and Hisayuki Morii. Annular self-assembly of dna molecular chains occurring in natural dry process of diluted solutions. *Biopolymers*, 77:163–172, 2005.

[49] Hege Sjeggestad Bjørnsen. Evaporating droplets of clay nanoparticle suspensions. Master's thesis, NTNU, 2007.

[50] L. Rejona, O. Manero, and C. Lira-Galeana. Rheological, dielectric and structural characterization of asphaltene suspensions under dc electric fields. *Fuel*, 83:471–476, 2004.

[51] Lu Kun-Quan, Lu Kun-Quan, Wang Xue-Zhao, Sun Gang, Sun Gang, and Sun Gang. Polar molecule dominated electrorheological effect. *Chinese Physics*, 15(11):2476–2480, 2006.

[52] Kevin J. Mutch, Vasileios Koutsos, and Philip J.Camp. Deposition of magnetic colloidal particles on graphite and mica surfaces driven by solvent evaporation. *Langmuir*, 22:5611–5616, 2006.

[53] division of chemical education American Chemical Society. Chemistry comes alive: Liquids. `http://jchemed.chem.wisc.edu/jcesoft/cca/CCA1/R1MAIN/CD1R3230.HTM`, 1997.

[54] Shell Chemicals. Product data(isopropyl alcohol). `http://www.shellchemicals.com/alcohols/1,1098,1089,00.html`, March 2007.

[55] Smart Measurement. Conductivity of common fluids. `http://www.smartmeasurement.com/en/wizards/flowmeter/flmtr_mag_conductivity.asp`, 2002.

[56] Efunda: Engineering Fundamentals. Properties of ethanol alcohol. `http://www.efunda.com/materials/common_matl/show_liquid.cfm?MatlName=AlcoholEthanol`, Last visited April 2007.

[57] Freestyle Reference. Temperature scale. `http://www.fsref.com/Fatal/FEA00002.SHTML`, Last visited April 2007.

[58] Donal OĹeary. Ethanol. http://www.ucc.ie/academic/chem/dolchem/html/comp/ethanol.html, Last visited April 2007.

[59] Clipper Controls. Dielectric constant reference guide. http://www.clippercontrols.com/info/dielectric_constants.html#Top, Last visited April 2007.

[60] Dr. Stephan Rudolph. Propanol (isopropanol, isopropyl alcohol). http://www.a-m.de/englisch/lexikon/propanol.htm, Last visited April 2007.

[61] California Air Resources Board Home. ethyl acetate. http://www.arb.ca.gov/db/solvents/solvent_pages/esters-HTML/ethyl_acetate.htm, Last visited April 2007.

[62] Engineering Tool Box. Boiling points of some common fluids and gases. http://www.engineeringtoolbox.com/boiling-points-fluids-gases-d_155.html, Last visited April 2007.

[63] LLC Glas-Col. Liquid and semi-solid materials: Viscosity. http://www.glascol.com/products/stirimag/ViscosityChart.html, Last visited April 2007.

[64] Computer Support Group. Specific gravity and viscosity of liquids. http://www.csgnetwork.com/sgvisc.html, Last visited April 2007.

[65] Shell Chemicals. Product data: Shellsol t. http://www.shellchemicals.com/isoparaffins/1,1098,661,00.html, May 2005.

[66] BOC Edwards. Material safety data sheet. http://www.bocedwards.com/pdf/P110-60-030-us.pdf, 2007.

[67] X. Tang, C. Wu, and H. Conrad. On the conductivity model for the electrorheological response of dielectric particles with a conducting film. *Appl. Phys.(6)*, 78, 1995.

[68] Carl-Roth. http://www.carl-roth.de, Last visited Dec.18, 2006.

[69] Inc. ABTECH scientific. Laboratory products. http://www.abtechsci.com/labproducts.html, Last visited Dec.18, 2006.

[70] Excel Technologies.Inc. Nikon - optiphot. http://www.microscopedealer.com/products/microscopes/nikon_optiphot150s.php, Last visited April 2007.

[71] Tiscali reference. Charge-coupled device. http://www.tiscali.co.uk/reference/encyclopaedia/hutchinson/m0025902.html, 2007.

[72] Al Kelly. What is a ccd camera and how does it work? http://www.ghg.net/akelly/ccdbasic.htm, 1996.

[73] See http://www.edmundoptics.com/.

[74] ALLPRO. Solvents, thinners, and diluents. http://www.allprocorp.com/ics/documents/SolventsThinnersDiluents.htm, 2007.

[75] Shell. Mineral turpentine. http://www.shellchemicals.com/chemicals/pdf/solvents/hydrocarbon/white_spirits/mineral\%20turpentine_ap_297.pdf?section=our_products, Last visited Dec.18, 2006.

[76] Rockwood Additives Ltd. Product bulletins. http://www.rockwoodadditives.com/product_bulletins.asp, Last visited Dec.18, 2006.

List of Figures

Appendix A

Videos of Experimental Results.

With this thesis follows a DVD including eight experimental videos. All electrodes shown here are IAME electrodes with a microband spacing of $10\mu m$. The voltage was applied within the first 10 seconds.

1. File: samp1V15V.avi
   Sample: $0.105g$ modified Laponite in $10ml$ turpentine.
   Applied voltage: $15V$ over the upper gap.
   Camera: 3-CCD JVC
   Signs of the ER-effect. Snapshots from this video are presented in Fig.5.5 on page 42.

2. File: samp2V15V.avi
   Sample: $0.048g$ modified Laponite in $10ml$ turpentine.
   Applied voltage: $15V$ over the upper gap.
   Camera: 3-CCD JVC
   Signs of the ER-effect. Snapshots from this video are presented in Fig.5.6 on page 43.

3. File: turp0p1V15V.avi
   Sample: $0.105g$ modified Laponite in $10ml$ turpentine.
   Applied voltage: $15V$ over the upper gap.
   Camera: 3-CCD JVC
   Induced electrophoretic convection counteract chain formation. A snapshot from this video is presented in Fig.5.9 on page 46.

4. File: silicon0p05T2.avi
   Sample: $0.05g$ modified Laponite in $10ml$ silicone oil.
   Applied voltage: From $V = 0V$ to $V_{max} = 15.7V$ over the upper gap. First signs of chain formations at $\approx 10V$.
   Camera: 3-CCD JVC
   Signs of the ER-effect. Snapshots from this video are presented in Fig.5.12 on page 50.

5. File: silicon0p1T5.avi
   Sample: $0.10g$ modified Laponite in $10ml$ silicone oil.
   Applied voltage: From $V = 0V$ to $V_{max} = 15.8V$ over the upper gap.
   Camera: 3-CCD JVC
   Signs of the ER-effect. Snapshots from this video are presented in Fig.5.13 on page 51.

6. File: turp0p1V15Vuten.avi
   Sample: $0.10g$ modified Laponite in $20ml$ turpentine.
   Applied voltage: $15V$ over the upper gap.
   Camera: 3-CCD JVC
   No cover glass over the droplet. Illumination was only from underneath the sample hence the dark microbands. The sample is placed between polarizers which are adjusted during video capture. Thus, the polarizers are occasionally crossed and results in some time intervals with darkened images. Snapshots from this video are presented in Fig.5.26 on page 68.

7. File: turp0p1V15Vmed.avi
   Sample: $0.10g$ modified Laponite in $20ml$ turpentine.
   Applied voltage: $15V$ over the upper gap.
   Camera: 3-CCD JVC
   With a cover glass over the droplet. This does not improve the ER-effect. Illumination was only from underneath the sample, hence the dark microbands. Snapshots from this video are presented in Fig.5.27 on page 69.

8. File: turp0p05TV3.avi
   Sample: $0.048g$ modified Laponite in $10ml$ turpentine.
   Applied voltage: From $V = 0V$ to $V_{max} = 27V$ over the upper gap. Signs of chains at V_{max}.
   Camera: 3-CCD JVC
   Turpentine evaporates and chain formations are no longer evident. Snapshots from this video are presented in Fig.5.29 on page 72.

Appendix B

Negative Experimental Results

Throughout the working period of this thesis, several experiments have given negative results, e.g. lack of the ER-effect. Some of these are presented here.

B.1 No Observable ER-Effect

Three of the samples described in Sec.5.1.1 showed no indications of the ER-effect. For sample specifications and preparation method I refer to Sec.5.1.1. Results are presented and discussed here.

Laponite RD dissolved in silicone oil
One example of a sample which gave no signs of the ER-effect was Laponite RD dissolved in silicone oil. By regarding Fig.B.1(a) and (b) there were clearly no indications of chain formation within the lower gap. These figures shows that there were some Laponite particles that were attracted to the electrode when the electric field was applied, but there was no significant reaction except from this. All three tests of this sample gave the same negative result.

Modified Laponite dissolved in silicone oil
Neither the sample of modified Laponite dissolved in silicone oil showed signs of the ER-effect. The result before and after the field was applied is shown in Fig.B.2. As for the silicone oil sample with Laponite RD, there was no observable reaction when applying the electric field. Aggregation of particles occurred within the electric field, but the reaction was not sudden and the configuration of the Laponite particles did not resemble chains. Compared to Fig.B.1 one can see that there was a lot more Laponite particles present in the solution in this case. Since the concentration was equal for all solutions, the increased number of particles could have occurred as a result of a lack of sedimentation or the droplet might have been taken from a phase of higher particle concentration than the supernatant phase. The particle size was also larger in this case than in Fig.B.1. This was therefore an unsuited sample because the Laponite aggregates would, at best, only fill the electrode gap and one would not be able to verify if this was aggregation or chain formation. Hence, all three tests of this sample gave no indications of the ER-effect.

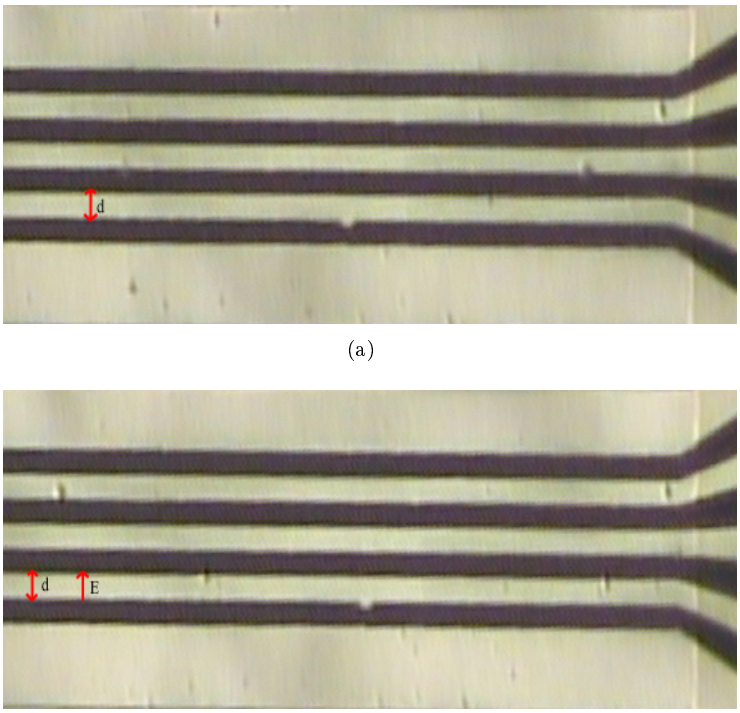

Figure B.1: *A* $0.1\mu l$ *droplet of Laponite RD and silicone oil before (a) and after (b) the electric field was applied. A DC voltage of* $20V$ *was applied over the two lowest microbands, which had a spacing of* $d = 10\mu m$*. There is no observable ER-effect here.*

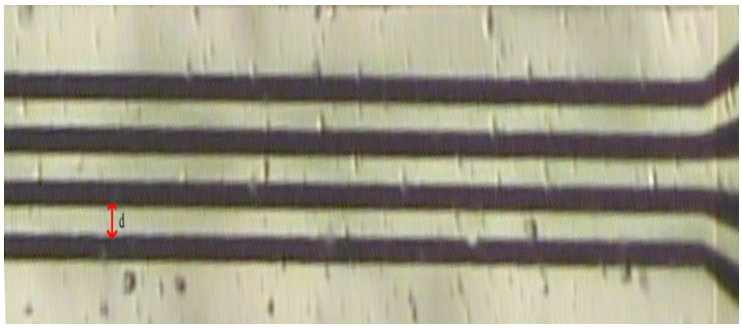

(a)

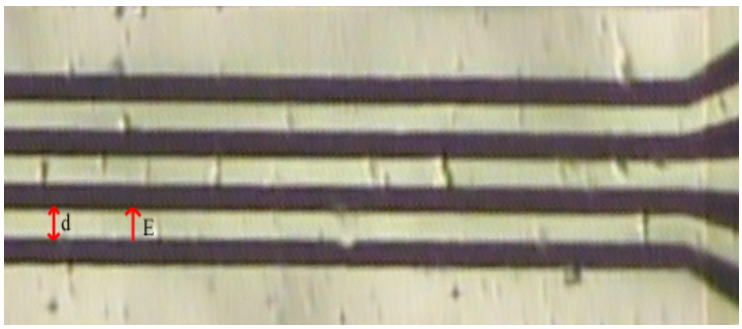

(b)

Figure B.2: $0.1\mu l$ *droplet of modified Laponite and silicone oil before (a) and after (b) the electric field was applied. A voltage of* $20V$ *was applied over the two lowest microbands, which have a spacing of* $d = 10\mu m$*. This sample gave no observable ER-effect.*

Laponite RD dissolved in turpentine
This sample also gave a negligible reaction to the applied electric field. As before, some of the Laponite particles got attached to one of the charged electrode microbands, but there was no sign of the ER-effect.

B.2 Testing Sample Preparation Techniques

Different sample preparation techniques such as centrifugation and filtration were utilized in search for an optimized sample. However, these techniques all gave a negative ER-response due to a too low concentration of particles within the supernatant phase, or too small particles to be observed with the Zeiss optical microscope. For sample specifications and preparation method I refer to Sec.5.1.3. Results are presented and discussed here.

Silicone Oil and Laponite RD
The samples were examined after centrifugation and the suspicion that none of these would show the ER-effect was confirmed. Each sample was tested twice, all with the same negative result independent of the concentration of Laponite. Occasional movement within some of the samples occurred, but seemingly independent of the electric field. To ensure that there was actually an electric field present, the contact between the electrode and the wires was tested with a multimeter. The applied voltage was registered with the multimeter, which proved that there was in fact an electric field present. As an example, two pictures are given in Fig.B.3 which shows the situation before and after the field was applied for the sample containing $0.01 g/ml$ of Laponite RD in silicone oil.

As can be seen from this figure, there was no visible change within the sample after the field was applied. The larger, dark dots are impurities on the camera lens and should be discarded. However, since there is no movement whatsoever, they play the same role as the sample particles. Even though the highest concentration was six times larger than the lowest one, there was no significant change in the amount of particles present within the sample droplet. This can be seen by comparing pictures with $0.005 g/ml$ of Laponite RD and $0.03 g/ml$ Laponite RD in silicone oil, as shown in Fig.B.4. This implied that centrifuging the samples lead to a change in the resulting concentration of Laponite particles within the supernatant phase. The speed and/or time of centrifugation might have been too high, and thus all, or most of the Laponite particles ended up in the sedimentary phase of the sample.

Same problem occurred with the filtrated samples. Independent of the initial concentration of Laponite RD, the final concentration was so low that the optical microscope could not recognize any particle movement. It might also be that the particles were too small to be observed with the Zeiss microscope.

Turpentine and Laponite RD
Two centrifuged samples with an initial concentration of $0.005 g/ml$ and $0.02 g/ml$ of Laponite RD were examined. Once again there was no observable ER-effect within the two samples when the electric field was applied. Too few particles were present within the sample. If these particles were too far away from the electrode gap, they would barely be affected by the electric field within this gap. Practically no particles could be seen within the area of which there were microbands. There might still be Laponite particles present within the elec-

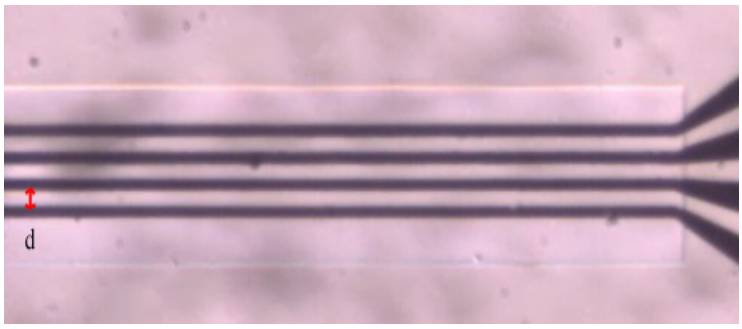

(a)

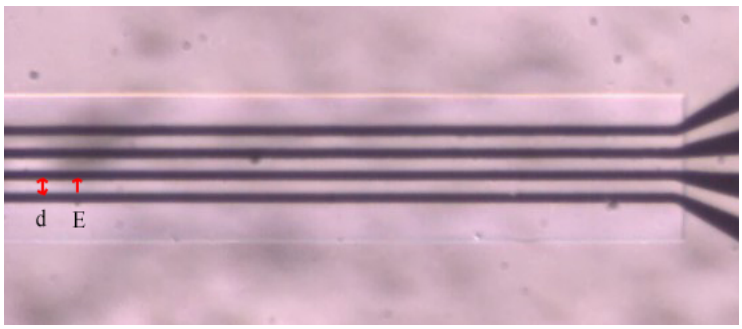

(b)

Figure B.3: *The centrifuged sample of silicone oil and Laponite RD before (a) and after (b) the electric field was applied. The voltage of* $20V$ *was applied over the two lowest microbands, which had a spacing of* $d = 10\mu m$*. There is no observable ER-effect here.*

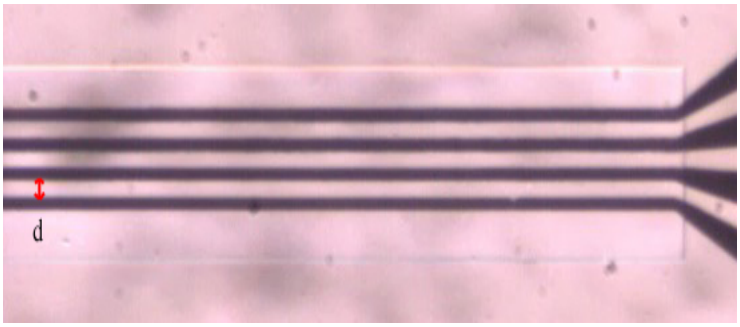

(a)

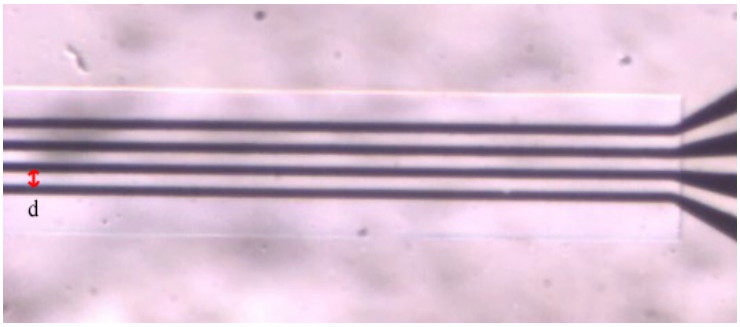

(b)

Figure B.4: *Two different concentrations of Laponite RD in silicone oil placed on the* $d = 10\mu m$ *gap electrode, after centrifugation:* $0.005g/ml(a)$ *and* $0.03g/ml(b)$*. The pictures were taken before the electric field was applied. Picture a) and b) illustrates that the resulting concentration of Laponite particles is small for both samples.*

trode gap, but with the magnification used here, they not observable and thus no results could be obtained. Same observations were made with the filtrated samples.

Turpentine and Modified Laponite

The access to the modified Laponite was limited, thus the initial sample of $0.01g/ml$ of modified Laponite dissolved in turpentine used in Sec.5.1.1 was also used here. It was first shaken thoroughly by hand and then centrifuged at a speed of $3000rpm$ in $15min$. Then, a sample droplet of $0.1\mu l$ was extracted from the supernatant phase and placed on the $10\mu m$ gap electrode.

When applying the electric field, there was no observable ER-effect, probably due to a lack of particles present close to the electrode gap where the field was applied. After the examination of the centrifuged sample, it was shaken once more before it was filtrated with a $0.2\mu m$ filter. The amount of particles within the sample was now significantly reduced and particle movement within the electric field was not observed. Fig.B.5 shows the filtrated sample after the electric field was applied. No aggregation or chain formations were observed.

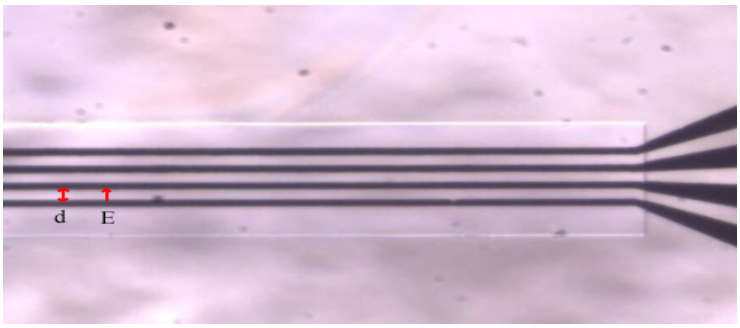

Figure B.5: *Filtrated sample with* $0.01g/ml$ *of modified Laponite in turpentine as initial solid particle concentration. This picture was taken after a voltage of* $20V$ *was applied over an electrode gap of* $d = 10\mu m$. *The voltage was applied over the two lowest microbands. There is no observable ER-effect here.*

Appendix C

Properties of Turpentine

The specifications of turpentine are taken from specifications published by SHELL [75]. The specific turpentine used in the experiments described in this thesis was not bought from Shell but it was marked as pure turpentine and hence it should fit the specifications given in this appendix. See next page.

Shell Chemicals

Data Sheet

Issued:

13-May-2005

Product Name

Mineral Turpentine

Product Code **Q7249** **Asia Pacific** **ANZ**

Product Category **White Spirits**

Description

Mineral Turpentine is a wide boiling range, medium evaporating solvent widely used in the paint industry. Mineral Turpentine conforms to Australian Standard AS 3530.

Sales Specification

Property	Unit	Min	Max	Method	
Appearance		Cl & FFSM		Visual	
Color	Saybolt	25		ASTM D156	
Density @15°C	g/mL	0.800	0.820	ASTM D4052	
Copper Corrosion			1	ASTM D130	
Distillation, IBP	°C	145	155	ASTM D86	
Distillation, 10%v	°C	150	160	ASTM D86	
Distillation, 50%v	°C	160	170	ASTM D86	
Distillation, 95%v	°C	180	190	ASTM D86	
Distillation, FBP	°C		200	ASTM D86	
Flash Point (Abel)	°C	31		IP 170	
Aniline Point	°C	20	25	ASTM D611	(4)
Aniline Point (85-95%v fraction)	°C		36	ASTM D611	(4)

(1) Guaranteed, (2) Typical, (3) Report Only, (4) Guaranteed spec with typical result

Typical Properties

Property	Unit	Method	Value
Color	Saybolt	ASTM D156	+29
Odor	-	-	Marketable
Density @15°C	kg/L	ASTM D4052	0.814
Copper Corrosion (3hr @100°C)	-	ASTM D130	1
Non Volatile Matter	mg/100mL	ASTM D1353	4
Distillation, IBP	°C	ASTM D86	149
Distillation, 10%v	°C	ASTM D86	154
Distillation, 50%v	°C	ASTM D86	165
Distillation, 95%v	°C	ASTM D86	185
Distillation, FBP	°C	ASTM D86	195
Flash Point	°C	IP 170	35
Aniline Point (M=Mixed)	°C	ASTM D611	23
Aniline Point (85-95%v fraction)	°C	ASTM D611	27
Electrical Conductivity @23°C	pS/m	ASTM D2624	400

Test Methods

Copies of copyrighted test methods can be obtained from the issuing organisations:

American Society for Testing and Materials (ASTM) : www.astm.org
Energy Institute (IP) : www.energyinst.org.uk
Deutsches Institut für Normung (DIN) : www.din.de

Shell Method Series (SMS) methods are issued by Shell International Chemicals B.V., Shell Research and Technology Centre, Amsterdam, The Netherlands. Copies of SMS can be obtained through your local Shell Chemicals company.

For routine quality control analyses, local test methods may be applied that are different from those mentioned in this datasheet. Such methods have been validated and can be obtained through your local Shell Chemicals company.

Quality

Mineral Turpentine does not contain detectable quantities of polycyclic aromatics, heavy metals or chlorinated compounds.

Storage and Handling

Provided proper storage and handling precautions are taken we would expect Mineral Turpentine to be technically stable for at least 12 months. For detailed advice on Storage and Handling please refer to the Material Safety Data Sheet on www.shell.com/che

Hazard Information

For detailed Hazard Information please refer to the Material Safety Data Sheet on www.shell.com/chemicals.

Appendix D

Properties of Laponite RD

The specifications for Laponite RD are reproduced from specifications published by Rockwood [76]. See next page.

SOUTHERN CLAY PRODUCTS / A SUBSIDIARY OF ROCKWOOD SPECIALTIES, INC.

PRODUCT BULLETIN/Laponite®

Southern Clay Products, Inc.
1212 Church Street
Gonzales, TX 78629
Phone: 800-324-2891
Fax: 830-672-1903
www.scprod.com

Laponite RD

The Clear Leader

Description

LAPONITE RD is a synthetic layered silicate. It is insoluble in water but hydrates and swells to give clear and colorless colloidal dispersions. At concentrations of 2% or greater in water, highly thixotropic gels can be produced.

Application

Used for imparting a shear sensitive structure to a wide range of waterborne formulations. These include household and industrial surface coatings, cleansers, ceramic glazes agrochemical, oilfield and horticultural products.

Typical Characteristic

Appearance free flowing white powder
Bulk Density 1000 kg/m3
Surface Area (BET) 370 m2/g
pH (2% suspension) 9.8

Chemical Composition	(dry basis)
SiO2	59.5%
MgO	27.5%
Li2O	0.8%
Na2O	2.8%
Loss on Ignition	8.2%

General Specifications

		Rockwood QA Test Code
Gel strength	22g min	ELP-L-1H
Sieve Analysis	2% Max >250 microns	ELP-L-6A
Free Moisture	10% Max	ELP-L-5A

Specifications can be agreed to meet individual requirements.

Storage

Laponite is hygroscopic and should be stored under dry conditions.

For additional information or technical assistance contact Southern Clay Products, Inc. toll free at 800-324-2891.